

Supporting Information

Stereodivergent, chemoenzymatic synthesis of azaphilone natural products

Joshua B. Pyser,^{1,2‡} Summer A. Baker Dockrey,^{1,2‡} Attabey Rodríguez Benítez,^{2,3‡} Leo A. Joyce,⁴
Ren A. Wiscons,¹ Janet L. Smith,^{2,3,5} Alison R. H. Narayan^{1,2,3*}

‡These authors contributed equally to this work.

¹*Department of Chemistry, University of Michigan, Ann Arbor, Michigan 48109*

²*Life Sciences Institute, University of Michigan, Ann Arbor, Michigan 48109*

³*Program in Chemical Biology, University of Michigan, Ann Arbor, Michigan 48109*

⁴*Department of Analytical Chemistry Merck & Co., Inc., Rahway, New Jersey 07065*

⁵*Department of Biological Chemistry, University of Michigan, Ann Arbor, Michigan 48109*

*To whom correspondence should be addressed. Email: arhardin@umich.edu

Table of Contents

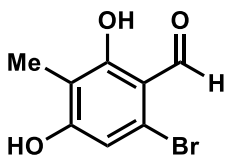
Part I. Substrate Synthesis	S3-9
Part II. Plasmids and Proteins	S10-15
Part III. Generation of AfoD Y118F variant	S16-17
Part IV. Sequence Similarity Network (SSN) of Flavin-Dependent Monooxygenases	S18-19
Part V. FDMO Sequence Alignment	S20-21
Part VI. Biocatalytic Reactions	S22-23
Part VII. Substrate Calibration Curves	S24-25
Part VIII. UPLC Traces of Biotransformations	S26-33
Part IX. Determination of Enantiomeric Excess	S34-40
Part X. NMR Spectra of Compounds	S41-56
Part XI. Single-Crystal Structure Determination	S57-58
Part XII. Circular Dichroism Spectroscopy of Azaphilones 17, 24, and 28	S59-74
Part XIII. Bibliography	S75-76

Part I. Substrate Synthesis

All reagents were used as received unless otherwise noted. Reactions were carried out under a nitrogen atmosphere using standard Schlenk techniques unless otherwise noted. Solvents were degassed and dried over aluminum columns on an MBraun solvent system (Innovative Technology, inc., Model PS-00-3). Reactions were monitored by thin layer chromatography using Millipore 60 F₂₅₄ precoated silica TLC plates (0.25 mm) that were visualized using UV, *p*-anisaldehyde, CAM, DNP, or bromocresol stain. Flash column chromatography was performed using Machery-Nagel 60 μ m (230-400 mesh) silica gel. All compounds purified by column chromatography were sufficiently pure for use in further experiments unless otherwise indicated. ¹H and ¹³C NMR spectra were obtained in CDCl₃ at rt (25 °C), unless otherwise noted, on Varian 400 MHz or Varian 600 MHz spectrometers. Chemical shifts of ¹H NMR spectra were recorded in parts per million (ppm) on the δ scale. High resolution electrospray mass spectra were obtained on an Agilent HPLC-TOF at the University of Michigan Life Sciences Institute.

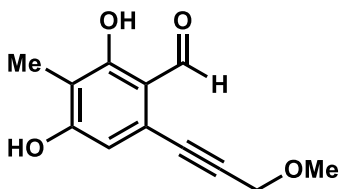
List of reagents prepared or purified:

2-Iodoxybenzoic Acid (IBX) was synthesized according to the procedure described by Sputore *et al.*¹ **Trifluoroacetic acid** and **acetic anhydride** were distilled prior to use.



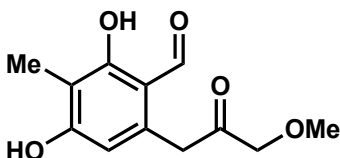
6-Bromo-2,4-dihydroxy-3-methylbenzaldehyde (S1)

Prepared as previously reported by Baker Dockrey *et al.*²



2,4-Dihydroxy-6-(3-methoxyprop-1-yn-1-yl)-3-methylbenzaldehyde (S2)

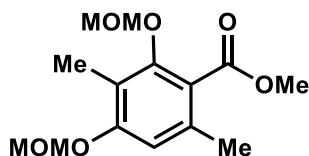
Aryl bromide **S1** (150 mg, 0.65 mmol), PdCl₂(PPh₃)₂ (23 mg, 0.033 mmol, 0.050 equiv), CuI (12 mg, 0.065 mmol, 0.10 equiv) was stirred in 4.8 mL of anhydrous DMF in a flame-dried round bottom flask equipped with a stir bar. Et₃N (0.30 mL, 2.2 mmol, 3.3 equiv) was added and the mixture was sparged with N₂ for 15 min before methyl propargyl ether (0.11 mL, 1.3 mmol, 2.0 equiv) was added. The resulting mixture was heated to 60 °C for 14 h. The reaction mixture was cooled to rt, diluted with water (2.0 mL), and acidified with 1 M HCl (4.0 mL). The mixture was extracted with EtOAc (3 x 10 mL) and the combined organic layers were washed with water and brine, dried over anhydrous Na₂SO₄, filtered, and concentrated under reduced pressure to afford a dark brown solid. Purification on silica gel (10-20% EtOAc in hexanes) afforded 135 mg (94% yield) of **S2** as a tan solid. ¹H NMR (400 MHz, CD₃OD) δ 10.04 (s, 1H), 6.47 (s, 1H), 4.33 (s, 2H), 3.41 (s, 3H), 1.98 (s, 3H). All spectra obtained were consistent with literature values.³



2,4-dihydroxy-6-(3-methoxy-2-oxopropyl)-3-methylbenzaldehyde (S3)

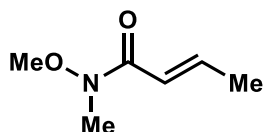
To a mixture of **S2** (20 mg, 0.091 mmol, 1.0 equiv) and Au(OAc)₃ (1.7 mg, 0.0046 mmol, 0.050 equiv) in DCE (1.0 mL) was added TFA (0.091 mL, 1.2 mmol, 13 equiv) in a flame-dried vial under N₂. The resulting mixture

was stirred for 1 h at rt before 10 mL of 20% H₂O/MeCN was added. The mixture was stirred for 12 h at rt before it was diluted with water (1.0 mL) and extracted with EtOAc (3 x 5.0 mL). The combined organic layers were washed with brine, dried over Na₂SO₄, and concentrated under reduced pressure to afford a dark brown solid. Purification on silica gel (80% EtOAc in hexanes) afforded 20 mg (92% yield) of **S3** as a light tan solid. ¹H NMR (400 MHz, CD₃OD) δ 9.82 (s, 1H), 6.23 (s, 1H), 4.18 (s, 2H), 4.02 (s, 2H), 3.39 (s, 3H), 2.00 (s, 3H); ¹³C NMR (150 MHz, CD₃OD) δ 205.8, 193.4, 163.7, 163.0, 137.0, 112.3, 110.2, 110.1, 76.4, 58.1, 41.0, 5.9; HR-ESI-MS: *m/z* calculated for C₁₂H₁₅O₅ [M+H]⁺: 239.2465, found: 239.2465; IR (thin film): 2921, 2827, 1721, 1614, 1503 cm⁻¹; MP: 127-129 °C.



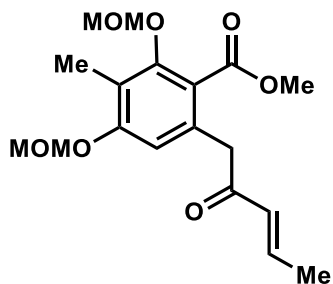
Methyl 2,4-bis(methoxymethoxy)-3,6-dimethylbenzoate (**S4**)

Methyl atratate (13 g, 66 mmol, 1.0 equiv) in THF (650 mL) was cooled to 0 °C and NaH (60%, 7.9 g, 200 mmol, 3.0 equiv) was added portionwise. MOMCl⁴ (15 mL, 200 mmol, 3.0 equiv) was slowly added to the resulting mixture. The solution was warmed to rt and stirred for 5 h before it was cooled to 0 °C and quenched with NH₄Cl (500 mL, saturated aq.). The layers were separated, and the aqueous layer was extracted with EtOAc (3 x 500 mL). The combined organic layers were washed with NaHCO₃, dried over Na₂SO₄ and concentrated under reduced pressure to afford a yellow oil. Purification on silica gel (0-20% EtOAc in hexanes) afforded 15 g of the ester as a colorless oil (90% yield). ¹H NMR (300 MHz, CDCl₃): δ 6.72 (s, 1H), 5.19 (s, 2H), 4.96 (s, 2H), 3.89 (s, 3H), 3.54 (s, 3H), 3.47 (s, 3H), 2.28 (s, 3H), 2.15 (s, 3H). All spectra obtained were consistent with literature values.⁵



(*E*)-*N*-methoxy-*N*-methylbut-2-enamide (**S5**)

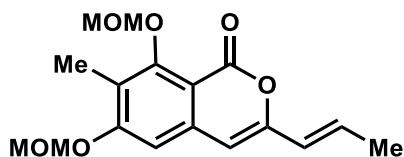
Crotonic acid (10 g, 120 mmol, 1.0 equiv) was dissolved in oxalyl chloride (12 mL, 140 mmol, 1.2 equiv) and stirred at 70 °C for 1 h. The resulting acyl chloride was distilled at 124 °C, then added to a solution of *N,N*-dimethylhydroxylamine hydrochloride (10 g, 100 mmol, 0.90 equiv) in DCM (190 mL). The mixture was cooled to 0 °C before pyridine (21 mL, 260 mmol, 2.2 equiv) was added slowly. The mixture was stirred at 0 °C for 30 min, then allowed to warm to rt for 30 min before it was diluted with 1 M HCl (150 mL) and extracted Et₂O (3 x 150 mL). The combined organic layers were washed with brine (300 mL), dried over MgSO₄, and concentrated to afford a red oil. Purification on silica gel (60-80% Et₂O in hexanes) afforded 12 g (82% yield) of the title compound as a pale yellow oil. ¹H NMR (400 MHz, CDCl₃) δ 6.98 (m, 1H), 6.41 (d, *J* = 15.4 Hz, 1H), 3.69 (s, 3H), 3.23 (s, 3H), 1.90 (d, *J* = 8.6 Hz, 3H). All spectra obtained were consistent with literature values.⁶



Methyl (*E*)-2,4-bis(methoxymethoxy)-3-methyl-6-(2-oxopent-3-en-1-yl)benzoate (**S6**)

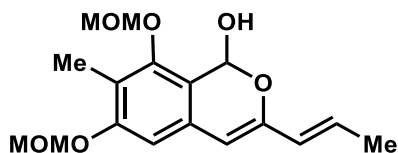
Diisopropylamine (9.1 mL, 65 mmol, 1.1 equiv) in THF (300 mL) was stirred at -78 °C. *n*-BuLi (2.5 M in hexane, 26 mL, 65 mmol, 1.1 equiv) was slowly added. The resulting mixture was warmed to 0 °C and stirred for 15 min before it was cooled to -78 °C and a solution of ester **S5** (15 g, 20 mmol, 1.0 equiv) in THF (50 mL) was added. The resulting mixture was stirred at -78 °C for 15 min before a solution cooled to -78 °C of amide **S6** (9.2 g, 71

mmol, 1.2 equiv) in THF (25 mL) was added by cannula. The mixture was stirred for 1 h at -78 °C and was then acidified with 1 M HCl (aq. 100 mL). The layers were separated, and the aqueous layer was extracted with EtOAc (3 x 400 mL). The combined organic layers were washed with brine (400 mL), dried over Na₂SO₄, and concentrated under reduced pressure to afford a yellow oil. Purification on silica gel (5-15% EtOAc in hexanes) afforded 4.5 g of an inseparable mixture of the title compound and remaining amide **S5**. This mixture was carried forward without further purification.



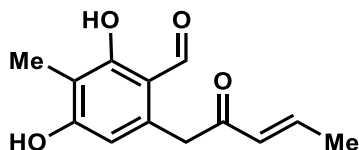
(E)-6,8-bis(methoxymethoxy)-7-methyl-3-(prop-1-en-1-yl)-1H-isochromen-1-one (S7)

NaH (170 mg, 4.50 mmol, 1.05 equiv, 60%, dispersion in mineral oil) was stirred in THF (290 mL) at -20 °C. Enone **S7** (1.5 g, 4.3 mmol, 1.0 equiv) in THF (50 mL) was slowly added to the suspension. *t*-BuOH (10 µL) was added and the solution was stirred for 1 h at 20 °C. The reaction was cooled to 0 °C and quenched with EtOAc (30 mL), followed by addition of a saturated aqueous solution of NH₄Cl (40 mL). The mixture was then allowed to warm to rt. The layers were separated, and the aqueous layer extracted with EtOAc (3 x 200 mL). The combined organic layers were washed with brine (400 mL), dried over Na₂SO₄, and concentrated under reduced pressure to afford a white solid. Purification on silica gel (0-20% EtOAc in hexanes) afforded 1.3 g of the lactone **S8** as a white crystalline solid (22% yield over 2 steps). ¹H NMR (400 MHz, CDCl₃): δ 6.78 (s, 1H), 6.59 (m, 1H), 6.12 (s, 1H), 5.99 (dt, J = 15.7, 1.7 Hz, 1H), 5.28 (s, 2H), 5.16 (s, 2H), 3.64 (s, 3H), 3.49 (s, 3H), 2.27 (s, 3H), 1.89 (d, J = 6.9 Hz, 3H); ¹³C NMR (150 MHz, CDCl₃) δ 161.0, 159.2, 158.9, 152.2, 139.1, 131.6, 122.9, 122.3, 107.4, 105.1, 103.7, 101.6, 94.2, 57.7, 56.4, 18.3, 9.9; **HR-ESI-MS**: *m/z* calculated for C₁₇H₂₁O₆ [M+H]⁺: 321.1333, found: 321.1335; **IR** (thin film): 2934, 2832, 1715, 1658, 1598 cm⁻¹; **MP**: 124-126 °C.



(E)-6,8-bis(methoxymethoxy)-7-methyl-3-(prop-1-en-1-yl)-1H-isochromen-1-ol (S8)

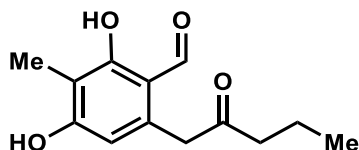
Lactone **S7** (1.0 g, 2.6 mmol, 1.0 equiv) in THF (13 mL) was stirred at -78 °C. DIBALH (0.48 mL, 2.7 mmol, 1.1 equiv) was added dropwise via syringe. The resulting solution was allowed to stir at -78 °C for 30 min, and then the reaction was quenched by the addition of EtOAc (1.0 mL) and Rochelle's salt (saturated, 4.0 mL). The resulting mixture was stirred for 1 h at rt. The crude mixture was extracted with EtOAc (3 x 50 mL), and the combined organic layers were washed brine (20 mL), dried over Na₂SO₄, and concentrated under reduced pressure. Purification on silica gel (0-20% EtOAc in hexanes) afforded 730 mg of the lactol **S8** as a colorless oil (89% yield). ¹H NMR (400 MHz, CDCl₃): δ 6.63 (s, 1H), 6.56 (d, J = 5.8 Hz, 1H), 6.33 (m, 1H), 5.97 (dd, J = 15.3, 2.1 Hz, 1H), 5.78 (s, 1H), 5.16 (s, 2H), 5.01 (s, 2H), 3.60 (s, 3H), 3.45 (s, 3H), 2.15 (s, 3H), 1.84 (m, 3H); ¹³C NMR (100 MHz, CDCl₃) δ 156.7, 153.0, 148.7, 129.1, 128.3, 126.0, 119.0, 116.4, 105.8, 102.0, 99.9, 94.4, 89.0, 57.5, 56.0, 18.2, 9.9; **HR-ESI-MS**: *m/z* calculated for C₁₇H₂₃O₆ [M+H]⁺: 323.1489, found: 323.1489; **IR** (thin film): 3357, 2930, 2823, 1604, 1447 cm⁻¹; **MP**: 62-65 °C.



(E)-2,4-dihydroxy-3-methyl-6-(2-oxopent-3-en-1-yl)benzaldehyde (19)

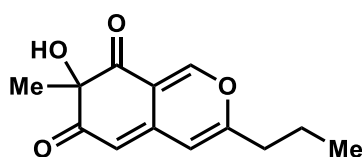
Lactol **S8** (300 mg, 0.933 mmol) in MeCN and water (7:1, 0.04 M) was stirred at rt. LiBF₄ (630 mg, 6.7 mmol, 7.2 equiv) was added and the resulting mixture was stirred at 70 °C for 3 h. The reaction mixture was cooled to rt and quenched by the addition of water (15 mL). The mixture was diluted with EtOAc (30 mL) and the layers were

separated. The aqueous layer was extracted with EtOAc (3 x 30 mL) and the combined organic layers were washed brine (40 mL), dried over Na₂SO₄, and concentrated under reduced pressure. Purification on silica gel (10-40% EtOAc in hexanes) afforded 200 mg (90% yield) of the title compound as a tan crystalline solid. **¹H NMR** (600 MHz, CD₃OD) δ 9.77 (s, 1H), 7.06 (m, 1H), 6.25 (d, J = 1.8 Hz, 1H), 6.22 (s, 1H), 4.12 (s, 2H), 2.00 (s, 3H), 1.92 (d, J = 5.2 Hz, 3H); **¹³C NMR** (150 MHz, CD₃OD) δ 197.5, 193.4, 163.7, 163.0, 144.8, 138.0, 130.3, 112.3, 110.3, 109.9, 42.5, 17.0, 5.8; **HR-ESI-MS**: *m/z* calculated for C₁₃H₁₅O₄ [M+H]⁺: 235.0965, found: 235.0947; **IR** (thin film): 3231, 2928, 2824, 2409, 1614 cm⁻¹; **MP**: 139-142 °C.



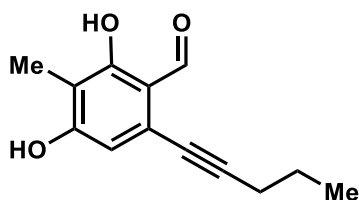
2,4-Dihydroxy-3-methyl-6-(2-oxopentyl)benzaldehyde (S9)

Prepared as previously reported by Baker Dockrey *et al.*²



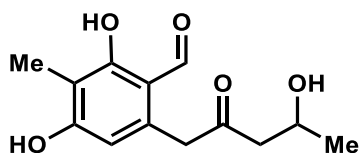
7-hydroxy-7-methyl-3-propyl-6H-isochromene-6,8(7H)-dione (S10)

Prepared as previously reported by Baker Dockrey *et al.*²



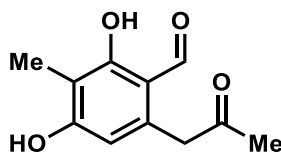
2,4-Dihydroxy-3-methyl-6-(pent-1-yn-1-yl)benzaldehyde (S11)

Prepared as previously reported by Baker Dockrey *et al.*²



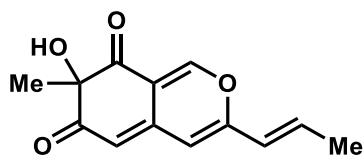
2,4-Dihydroxy-6-(4-hydroxy-2-oxopentyl)-3-methylbenzaldehyde (S12)

Prepared as previously reported by Baker Dockrey *et al.*²



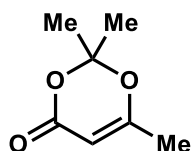
2,4-dihydroxy-3-methyl-6-(2-oxopropyl)benzaldehyde (21)

Prepared as previously reported by Baker Dockrey *et al.*²



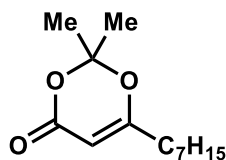
(E)-7-hydroxy-7-methyl-3-(prop-1-en-1-yl)-6H-isochromene-6,8(7H)-dione (18)

19 (20 mg, 0.085 mmol, 1.0 equiv) and Au(OAc)₃ (1.7 mg, 0.0043 mmol, 0.05 equiv) in DCE (0.94 mL) were added to a flame-dried vial. The mixture was stirred at rt for 30 min before IBX (28 mg, 0.10 mmol, 1.1 equiv), TBAI (19 mg, 0.051 mmol, 0.60 equiv), and TFA (0.094 mL, 10% total volume) were added. The mixture was stirred for an additional 40 min before the reaction was quenched with 5 drops of a saturated Na₂S₂O₃ solution. The mixture was filtered through a plug of celite, which was washed with DCM, before the solution was concentrated under reduced pressure. Purification by preparative TLC with 2.5% MeOH in DCM yielded 4.7 mg **18** (22% yield) of the title compound as an orange oil. ¹H NMR (400 MHz, CDCl₃) δ 7.90 (s, 1H), 6.59 (m, 1H), 6.10 (s, 1H), 6.01 (d, J = 15.6 Hz, 1H), 5.58 (s, 1H), 1.94 (d, J = 7.0 Hz, 3H), 1.55 (s, 3H). All spectra obtained were consistent with reported values.⁷



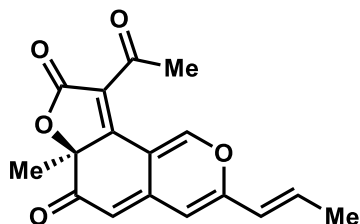
2,2,6-trimethyl-4H-1,3-dioxin-4-one (20)

Prepared as reported previously by Fuse *et al.*⁸ 1.04 g (73% yield) of the title compound was obtained as a yellow oil. ¹H NMR (400 MHz, CDCl₃) δ 5.24 (s, 1H), 1.98 (s, 3H), 1.68 (s, 6H). All spectra obtained were consistent with literature values.⁸



6-heptyl-2,2-dimethyl-4H-1,3-dioxin-4-one (23)

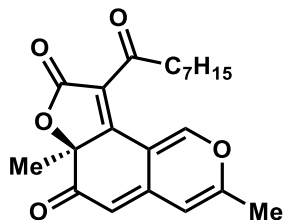
Prepared as reported previously by Franck and coworkers.⁵ 356 mg (26% yield over 3 steps) of the title compound was obtained as a yellow oil and taken on crude without further purification.



trichoflectin (17)

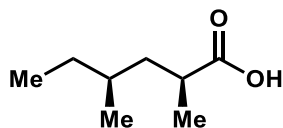
To a solution of **18** (5.5 mg, 0.023 mmol, 1.0 equiv) and dioxinone **20** (5 mg, 0.035 mmol, 1.5 equiv) in toluene (0.64 mL) in a flame dried vial under N₂ was added mol sieves. The mixture was stirred at rt for 10 min and then heated to 110 °C. After 1 h, Et₃N (0.0064 mL, 0.046 mmol, 2.0 equiv) was added. The mixture was stirred for an additional hour at 110 °C before it was cooled to room temperature and quenched with 1 M HCl (1.0 mL). The mixture was extracted with EtOAc (3 x 2.0 mL). The organic layers were combined, washed with brine, dried over Na₂SO₄, and concentrated under reduced pressure. Purification by preparative HPLC yielded 7.2 mg of **17** (>99% yield) as a yellow oil. ¹H NMR (600 MHz, CDCl₃) δ 8.82 (s, 1H), 6.63 (m, 1H), 6.06 (s, 1H), 6.01 (d, J = 13.8 Hz, 1H), 5.35 (d, J = 1.2 Hz, 1H), 2.60 (s, 3H), 1.95 (d, J = 5.2 Hz, 3H), 1.69 (s, 3H); ¹³C NMR (150 MHz, CDCl₃) δ 194.5, 190.0, 168.2, 165.6, 155.2, 153.1, 144.0, 136.3, 123.3, 122.3, 110.9, 107.5, 105.8, 87.6, 30.1,

29.7, 26.3, 18.7; **HR-ESI-MS**: m/z calculated for $C_{17}H_{15}O_5$ $[M+H]^+$: 299.0914, found: 299.0922; **IR** (thin film): 2921, 2827, 1721, 1614, 1503 cm^{-1} ; $[\alpha]_D^{+34}$ (c 0.1, $CHCl_3$). All spectra obtained were consistent with literature values.⁹



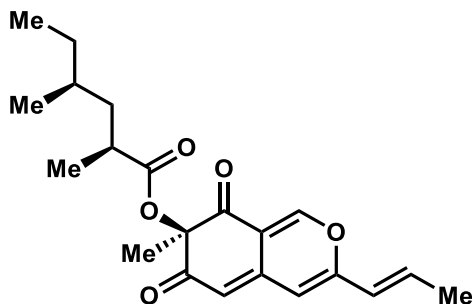
deflectin-1a (**24**)

To a solution of **22** (4.0 mg, 0.019 mmol, 1.0 equiv) and dioxinone **23** (6.6 mg, 0.029 mmol, 1.5 equiv) in toluene (0.55 mL) in a flame dried vial under N_2 was added mol sieves. The mixture was stirred at rt for 10 min and then was heated to 110 °C. After 1 h, Et_3N (53 μ L, 0.038 mmol, 2.0 equiv) was added. The mixture was stirred for an additional hour at 110 °C before it was cooled to room temperature and quenched with 1 M HCl (1.0 mL). The mixture was extracted with EtOAc (3 x 2.0 mL) and the combined organic layers were washed with (5.0 mL), dried over Na_2SO_4 , and concentrated under reduced pressure. Purification on silica gel (20% EtOAc in hexanes) yielded 5.9 mg of **24** (87% yield) as a yellow oil. **1H NMR** (599 MHz, $CDCl_3$) δ 8.77 (s, 1H), 6.08 (s, 1H), 5.28 (s, 1H), 3.16 (m, 1H), 2.83 (m, 1H), 2.20 (s, 3H), 1.68 (s, 3H), 1.62 (m, 2H), 1.55 (s, 3H), 1.27 (m, 8H), 0.87 (m, 3H); **^{13}C NMR** (151 MHz, $CDCl_3$) δ 197.3, 190.3, 168.1, 165.2, 158.7, 153.3, 144.1, 123.6, 111.1, 108.4, 104.9, 87.6, 42.1, 31.6, 29.0, 29.0, 26.2, 23.4, 22.6, 19.4, 14.1; **HR-ESI-MS**: m/z calculated for $C_{21}H_{25}O_5$ $[M+H]^+$: 357.1697, found: 357.1754; **IR** (thin film): 2924, 1763, 1684, 1642 1540 cm^{-1} ; $[\alpha]_D^{+88}$ (c 0.1, EtOAc). All spectra obtained were consistent with literature values.¹⁰



(**2S,4S**)-2,4-dimethylhexanoic acid (**S13**)

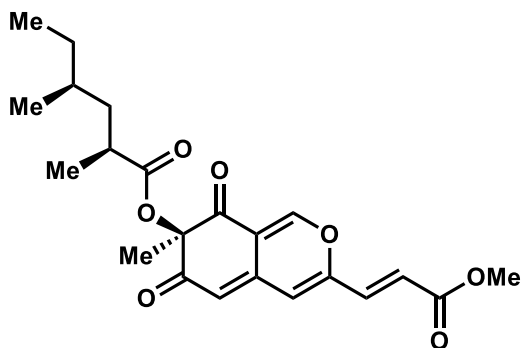
Prepared as reported previously by Myers *et al.*¹¹ 278 mg (32% yield over 3 steps) of the title compound was obtained as a white crystalline solid. **1H NMR** (599 MHz, $CDCl_3$) δ 2.56 (m, 1H), 1.72 (m, 1H), 1.39 (m, 1H), 1.32 (m, 1H), 1.17 (d, J = 7.0 Hz, 3H), 1.13 (m, 2H), 0.88 (d, J = 6.6 Hz, 3H), 0.86 (t, J = 7.4 Hz, 3H). All spectra obtained were consistent with literature values.¹¹



(**R**)-7-methyl-6,8-dioxo-3-((**E**)-prop-1-en-1-yl)-7,8-dihydro-6H-isochromen-7-yl (**2S,4S**)-2,4-dimethylhexanoate (**26**)

To a solution of carboxylic acid **S13** (4.5 mg, 0.031 mmol, 1.1 equiv) in THF (0.2 mL) was added 2,4,6-trichlorobenzoyl chloride (0.0048 mL, 0.031 mmol, 1.1 equiv) and Et_3N (0.0043 mL, 0.031 mmol, 1.1 equiv). The mixture was stirred at rt for 30 min before it was filtered through celite and concentrated. The resulting clear oil was dissolved in toluene (0.8 mL) and added to **18** (6.5 mg, 0.028 mmol, 1 equiv) and DMAP (10.3 mg, 0.084 mmol, 3 equiv). This mixture was stirred at 110 °C for 1 h before it was cooled to rt, acidified with a half-saturated

solution of NH_4Cl (1 mL), and extracted with EtOAc. The organic layers were washed with brine, dried over Na_2SO_4 , and concentrated under reduced pressure. Purification on silica gel (10-30% EtOAc in hexanes) provided 5 mg (50% yield) of the title compound as an orange oil. $^1\text{H NMR}$ (400 MHz, CDCl_3) δ 7.88 (s, 1H), 6.55 (m, 1H), 6.07 (s, 1H), 6.00 (d, $J = 15.0$ Hz, 1H), 5.57 (s, 1H), 2.70 (m, 1H), 1.93 (d, $J = 6.9$ Hz, 3H), 1.77 (m, 1H), 1.53 (s, 3H), 1.34 (m, 2H), 1.19 (d, $J = 6.9$ Hz, 3H), 1.13 (m, 2H), 0.89 (m, 6H). $^{13}\text{C NMR}$ (151 MHz, CDCl_3) δ 193.2, 192.7, 176.3, 155.3, 153.4, 142.6, 135.3, 122.4, 114.9, 108.5, 107.8, 83.8, 40.8, 36.2, 31.8, 29.4, 22.1, 19.1, 18.6, 17.6, 11.1; **HR-ESI-MS**: m/z calculated for $\text{C}_{21}\text{H}_{27}\text{O}_5$ $[\text{M}+\text{H}]^+$: 359.1853, found: 359.1858; **IR** (thin film): 2925, 2853, 1717, 1634, 1453 cm^{-1} .



(R)-3-((E)-3-methoxy-3-oxoprop-1-en-1-yl)-7-methyl-6,8-dioxo-7,8-dihydro-6H-isochromen-7-yl (2S,4S)-2,4-dimethylhexanoate (28)

To a solution of **26** (5.5 mg, 0.015 mmol, 1 equiv) and methyl acrylate (5.4 μL , 0.060 mmol, 4.0 equiv) in degassed DCM (0.6 mL) was added a solution of Grubbs Catalyst 2nd generation (2.5 mg, 0.0030 mmol, 0.20 equiv) in degassed DCM (0.5 mL). The mixture was stirred at 45 $^\circ\text{C}$ for 4 h before it was cooled to rt and concentrated. Purification on silica gel (10-35% EtOAc in hexanes) afforded 2.6 mg (48% yield) of the title compound as a yellow glass. $^1\text{H NMR}$ (400 MHz, CDCl_3) δ 7.88 (s, 1H), 7.13 (d, $J = 15.6$ Hz, 1H), 6.52 (d, $J = 15.6$ Hz, 1H), 6.45 (s, 1H), 5.69 (s, 1H), 3.82 (s, 3H), 2.69 (m, 1H), 1.75 (m, 1H), 1.53 (s, 3H), 1.29 (m, 2H), 1.19 (d, $J = 6.8$ Hz, 3H), 1.13 (m, 2H), 0.89 (m, 6H). $^{13}\text{C NMR}$ (201 MHz, CDCl_3) δ 192.8, 192.5, 165.8, 153.2, 153.1, 152.7, 140.7, 133.5, 124.0, 115.8, 114.9, 110.5, 83.8, 52.3, 40.8, 36.2, 31.8, 29.5, 21.9, 19.1, 17.6, 11.1; **HR-ESI-MS**: m/z calculated for $\text{C}_{22}\text{H}_{27}\text{O}_6$: 403.1751, found: 403.1728; **IR** (thin film): 2926, 2853, 1718, 1630, 1454 cm^{-1} . $[\alpha]_D -12.2$ $^\circ$ (c 0.1, CHCl_3). All spectra obtained were consistent with literature values.¹²

Part II. Plasmids and Proteins

Plasmids: The plasmid encoding *azaH* (G3XMC2.1), in a modified pET28 vector to afford protein with both C- and N-terminal 6 x His-tags, was a generous gift from Professor Yi Tang at the University of California, Los Angeles.¹⁹ The plasmid encoding *afuD* was synthesized by GeneArt and cloned into a pET21a vector. The plasmids encoding for *fdm1-7* were synthesized by Twist Bioscience and cloned into a pET28a vector.

Non-optimized *azaH* Sequence

```
ATGAGTACAGACTCGATCGAAGTTGCCATTATAGGCGCCGGGATCACGGGAATCACCCCTGGCCCTGGGCCTCCTGTCTCGC
GGCATTCCCCTCCGCGTCTACGAGCGAGCCCCGCGACTTTCACGAAATTGGAGCCGGTATCGGTTTCACCCCCAACGCCGAA
TGGGCGATGAAAGTCGTCGACCCGCGCATTCAAGCTGCTTTCAAACGCGTCGCTACCCCAATGCCTCCGACTGGTTCCAG
TGGGTGGACGGATTCAACGAGTCCGGTACCGACCCGCGCGAGACCGAGGAACAGCTACTCTTCAAGATCTACCTCGGCGAG
CGTGGATTTGAGGGCTGCCACCGTGCCGACTTCCCTAGGTGAGCTGGCACGTCTACTACCGGAAGGTGTGGTGACATTCCAG
AAGGCGCTGGATAACCGTGGAGCCTGCAGCAGATAATAGCCTCGGCCAGCTTCTTCGATTCCAAGATGGCACGACAGCTACC
GCCCACGCGGTGATCGGCTGCGATGGCATTCCGGTCGCGCGTTCGTCAGATCCTCCTAGGTGAAGACCATCCGACAGCATCA
GCCCATTACAGTCATAAATATGCAGCACGCGGCCTTATTCCCATGGACCGCGCCCCGGGAGGCGCTGGGCGAAGATAAAGTG
GCGACACGCTTCATGCATCTCGGTCCGGATGCCCATGCCCTGACCTTCCCCGTTAGCCATGGGTCCCTTGTTGAACGTCGTC
GCCTTCGTCACGGACCCTAACCCCTTGGCCATATGCTGATCGCTGGACGGCGCAGGGGGCCCAAGAAAGACGTGACGGCTGCC
TTTTCCCCTTTGGTCCGACCATGCGCACCATAATTGACCTCTTGCCTGATCCTATTGATCAATGGGCCGTTTTTTGATACA
TACGACCATCCCCAAATACGTATTCCCGGGGAGCTGTCTGTATAGCAGGGGATGCTGCTCATGCCGCGGCTCCGCATCAC
GGTGCAGGTGCAGGTTGTGGTGTGGAAGACGCGGCTGTGCTGTGCGCTGTGCTTCATATGGCTGCGAAAAAAGTTAACACC
GCAAAAACCTGGTTCTGAGGGGAAAGCCGCTCTTATCACGGCCGCATTCGAAACCTATGATTCCGGTTTGTGCGGAGCGTGCG
CAGTGGCTGGTGGAAAGTAGTCGCGTTATCGGTAATCTGTATGAGTGGCAGGATAAGGAGGTAGGGTCCGGATGCTTCCAGG
TGCCACGATGAGGTGTATTGGCGCTCTCATCGCATTTGGGACTATGATATTGATGCGATGATGAGAGAGACAGCTGAGGTG
TTTGAGGCGCAGGTAGCTGGGGTGGCGAGAAAT
```

AzaH Protein Sequence

```
MSTDSIEVAIIIGAGITGITLALGLLSRGI PVRVYERARDFHEIGAGIGFTPNAEWAMKVVDPRIQA AFKRVATPNASDWFQ
WVDGFNESGTDPRETEEQLLFKIYLG ERFEGCHRADFLGELARLLPEGVVTFQKALD TVEPAADNSLGQLLRFQDGT TAT
AHAVIGCDGIRSRVRQILLGEDHPTASAHYSHKYAARGLI PMDRAREALGEDKVATRFMHLGPD AHALTFPVSHGSL LNVV
AFVTDPNPWPYADRWTAQGPKKDVTA AFSRFGPTMRTIIDLPLPIDQWAVFD TYDHPNTYSRGAVCIAGDAAHAA APHH
GAGAGCGVEDAAVLCV LHM AAKVNTAKTGSEGKAALITAA FETYDSVCRERAQWLVESSRVI GN LCHDE VYWRSHRIWD
YDIDAMMRETA EVFEAQVAGVARN
```

Codon-Optimized *afuD* Sequence

```
ATGAGTACAGACTCGATCGAAGTTGCCATTATAGGCGCCGGGATCACGGGAATCACCCCTGGCCCTGGGCCTCCTGTCTCGC
GGCATTCCCCTCCGCGTCTACGAGCGAGCCCCGCGACTTTCACGAAATTGGAGCCGGTATCGGTTTCACCCCCAACGCCGAA
TGGGCGATGAAAGTCGTCGACCCGCGCATTCAAGCTGCTTTCAAACGCGTCGCTACCCCAATGCCTCCGACTGGTTCCAG
TGGGTGGACGGATTCAACGAGTCCGGTACCGACCCGCGCGAGACCGAGGAACAGCTACTCTTCAAGATCTACCTCGGCGAG
CGTGGATTTGAGGGCTGCCACCGTGCCGACTTCCCTAGGTGAGCTGGCACGTCTACTACCGGAAGGTGTGGTGACATTCCAG
AAGGCGCTGGATAACCGTGGAGCCTGCAGCAGATAATAGCCTCGGCCAGCTTCTTCGATTCCAAGATGGCACGACAGCTACC
GCCCACGCGGTGATCGGCTGCGATGGCATTCCGGTCGCGCGTTCGTCAGATCCTCCTAGGTGAAGACCATCCGACAGCATCA
GCCCATTACAGTCATAAATATGCAGCACGCGGCCTTATTCCCATGGACCGCGCCCCGGGAGGCGCTGGGCGAAGATAAAGTG
GCGACACGCTTCATGCATCTCGGTCCGGATGCCCATGCCCTGACCTTCCCCGTTAGCCATGGGTCCCTTGTTGAACGTCGTC
GCCTTCGTCACGGACCCTAACCCCTTGGCCATATGCTGATCGCTGGACGGCGCAGGGGGCCCAAGAAAGACGTGACGGCTGCC
TTTTCCCCTTTGGTCCGACCATGCGCACCATAATTGACCTCTTGCCTGATCCTATTGATCAATGGGCCGTTTTTTGATACA
TACGACCATCCCCAAATACGTATTCCCGGGGAGCTGTCTGTATAGCAGGGGATGCTGCTCATGCCGCGGCTCCGCATCAC
GGTGCAGGTGCAGGTTGTGGTGTGGAAGACGCGGCTGTGCTGTGCGCTGTGCTTCATATGGCTGCGAAAAAAGTTAACACC
GCAAAAACCTGGTTCTGAGGGGAAAGCCGCTCTTATCACGGCCGCATTCGAAACCTATGATTCCGGTTTGTGCGGAGCGTGCG
CAGTGGCTGGTGGAAAGTAGTCGCGTTATCGGTAATCTGTATGAGTGGCAGGATAAGGAGGTAGGGTCCGGATGCTTCCAGG
```

TGCCACGATGAGGTGTATTGGCGCTCTCATCGCATTGGGACTATGATATTGATGCGATGATGAGAGAGACAGCTGAGGTG
TTTGAGGCGCAGGTAGCTGGGGTGGCGAGAAAT

AfoD Protein Sequence

MADHEQEPEPLSIAIIGGGIIGLMTALGLLHRNIGKVTIYERASAWPDIGAAFAFTGIARECMQRLDPAILSALSQVQRN
PHDKVRYWDGFHPKSKEEAQDPEKSVLFEIEEKNMAYWACLGRVFAEMARLLPERVVRFGKRLVAYEDGGDQKVLRFD
GEVEEADIVIACDGVHSTARRVLLGAEHPAANARYSRKAVYRALVPMPAIDALGTEKAHVQIAHCGPDAHIVSFPVNNQ
IYNVFLFTHDSNEWTGHTMTVPSSKEEILSAVENWGPHEKELASLFPEQLSKYAIQADHPLPYAAGRVALAGDAHA
SSPFHGAGACMGVEDALVLAELLEKVNQNGSAFKEKKSNIELALKTYSVRIERSQWLKSSREMGDLIEWRYEDIGDGVK
CKAEWERRSRVIWDFDVQGMVDQAREAYERAVVKV

Codon-Optimized *fdm1* Sequence

ATGCCGAGCTATAACAAAGATACCGAAAGCGTGGAAGTGGCGGTGATTGGCGGCGGCATTGTGGCCTGGTGCTGGCGGC
GGCCTGACCCGCCAGATTAAAGTGAAAGTGTATGAACAGAGCCAGGGCTTTCGCGATATTGGCGCGGCATTGGCTTT
AACGGCGCGGCGAAAGCGTGCATGCAGATGATTGATCCGGCGTGATTACCGCGCTGCATCGCGCGGCGGCGTGGCGGT
AGCGCGCGGATGAAGATGATCCGCATGATTATCTGCGCTGGATTGATGGCTTTGATCGCGGCAACGTGCAGCATCTGCAT
GATCAGAACTGTATTGCAAAGTGGATGCGGGCTATAAAAGCATTGAAGGCACCCGCCGCGATCGCTTTCTGGAAGA
GCGAAAGATCTGCCGGAAGGCATGGTGGAAATTTAAAAACGCCTGCGCACCGTGGAAGAAGGCGGCGATGATTGCAA
CAGCTGCATTTTGAAGATGGCACCATTGCGGAAGCGGATGCGCGCTGCGATGGCATTAAAAGCCGCATTCGCGAAAT
CTGAGCGAAGCGAGCGTGGCGAGCAAACCGAGCTATACCCATGTGAACTTTTATAGCAGCCTGATTCCGATGAACAA
GTGGATATTCTGGGCAAATTTAAAGCGAGCGTGTTCATAACCATATTGGCCCCGGCGCGAACCTGCTGCATTATCC
GCGAACGGCACCCCTGTGCAACGTGAGCGCGTTTGTGCATGATGCGAACGAATGGCCGGCGGAAAAAGCCCCACC
GGCTTTCGCAACATATTCAGGAAAACTGGTGGGCTGGAGCCCGTGGTGCGCGCCTGATTGATCTGTTTCCGATA
CTGCCGGTGTGGGCGGTGTTTGTGATCTGTGGGAACATCCGATGCCGTATTATAACCGCGCCGCATTTGCGTGG
GCGGCGCATGCGAGCAGCCCGCATCATGGCGCGGGCGCGGCATGGGCATTGAAGATGCGCTGTGCTGAGCGTGTG
GATGAAGTGAAGCAGCAGCATTTCGCTGGAAGGCGCGAGCCCGCGATGCGATTCCGGTGGCGTTTTCAGGTGTAT
ATTTCGCCGCCCGCAGCCAGTGGCTGGTGAACAGCAGCCCGCCGTGTGCGATCTGCAGCAGCATCATGATTGGGCG
CCGGCGAACTGGTGAAGCGGAAACCTGCTTTGAAGAAATTACCGATCGCACCTATAAAATTTGAACTTTGATAG
GGCATGATTAAGAAAGCATTGAAAAATATGGCCGCGCGATTAACAGCCTGCGCCGCAACGGCCTGGCGACCAAC
TGCAAAGGCAACGGCCATATGAACGGCGTGCAGCG

Codon-Optimized *fdm2* Sequence

ATGGCGAGCACCGAACCGCAGGCGGATAGCGTGGATGTGGTGATTGTGGGCGGCGGCATTATTGGCCTGGTGCTGACCGTG
GGCCTGCTGCGCGTGGGCGTGAAAGTGAAAGTGTATGAACAGGCGCAGGGCTTTCGCGAAATTGGCGCGGCATTGCGT
ACCGCGAACCGGATTCGCTGCATGAACCTGATTGATCCGGCGATTCCGGTGGCGCTGCGCAGCAGCGGCAGCGTGGCG
AGCAACGGCGGCGATGAAGATCCGAACGATTATCTGCGCTGGATTGATGGCTATGATCGCCAGCGCGATGATCCGAGC
CAGCAGCTGTTTTTAACTGAACGCGGGCTATCGCGGCTTTGAAGGCTGCCGCCGCGATCAGTTTCTGGAAGCGCTGGT
AAAGTGATTCCGCCGGGCGTGAATTGAACTGAAAAACGCCTGGAAACCGTGCATGATAACGGCAGCGAAAACAACTGCT
CTGACCTTTTCAGGATGGCACCACCGCGGAAGCGGATGCGGTGATTGGCTGCGATGGCGTGAAAAGCACCTGCGCCG
ATGTTTGGCGATGATCATCCGGCGAGCCCGCCGCGCTATAGCCATTGCGTGGCGTATCGCACCTGATTCCGATGGATA
GCGGTGAGCGCGCTGGGCGCGTATAAAGCGACCAACCAGCATAACCATGTGGGCCGAAACGCGAACATTCTGCATTAT
GTGGCGAACACACCATGATTAACGCGGTGGCGTTTATTCGCGATCCGAACGAATGGACCGATGAAAAACCGTGGCGG
GGCACCCGCGATGATGTGAAAGCGGCGGTGCGCGGCTGGAGCCAGCCGGTGTGAACTGGTGGATTGCTTTCCGGATA
CTGAGCAAATGGGGCATTTTTGATCTGTGGGAATTTCCGGTGCCGAGCTATAACGTGGGCCGCTGAGCCTGGCGGGCG
GCGGCGCATGCGAGCAGCCCGCATCATGGCGCGGGCGCGTGCATGGGCATTGAAGATGCGCTGTGCTGACCACCCTGAT
GAACAGGTGGTGGTGAAGCGCAGAAAAGCCGGGCGATAAAGGCCGCGCGCTGATTGCGGCGCTGGATACTATAGCGCG
GTGCGCCAGACCCCGCAGCCAGTGGTGGTGAACAGCAGCCCGCCGTGTGCGATCTGCATCAGCAGCAGGAATGGGCGG
GCGACCAAACCTGATTAAGCGCAGACCTGCTTTGAAGAAGTGAAGATCGCAGCCTGAAAATTTGGCATTGTTGATTAT
CGCATGGTGCAGGATAGCCTGCAGGGCTATAAAGCGCGCCGCGCGCCGATTAAACGGCGGACCAAGATAAAAACTGTAT

Codon-Optimized *fdm3* Sequence

ATGATTGAAGCGCGCGGATTGAAGTGGCGATTATTGGCGGCGGCATTACCGGCCTGACCCTGGCGCTGGGCTGCAGAAA
CGCAACACCAACTTTCATATTTATGAACGCGCGCAGAGCCTGCGCGAAATTGGCGCGGCATTGGCTTTACCCCGAACCG
GAACGCGGATGCTGGCGCTGGATCCGCGCATTATGAAGCGTTTAAAGCGTGGCGAGCAAAAACGCGAGCGATTGGTTT

CAGTGGGTGGATGGCTTTAGCGGCGTGAACAACGATAAAGATAACCGTGAAAGAAGATCTGCTGTTAACATGTATCTGGGC
GAACGCGGCTTTGAAGGCTGCCATCGCGCGCAGTTTCTGAAAGAACTGGTGAACCATCTGCCGAGGGCTGCGTGACCTTT
GGCGCGTGCCTGGATAACCATTATTGATCAGGGCGAAAACGAACGCATTCTGCTGAAATTTATAACGGCACCATTGCGGAA
GCGGATCTGGTGAATTGGCTGCGATGGCATTTCGACGCCGCGTGCGCCAGCTGATTCTGGGCGAAAACAACCCGGCGAGCTAT
CCGGCGTATAACCATAAAAAAGCGTATCGCGGCCTGATTCCGATGGAAAAAGCGCTGCCGGCGCTGGGCGAAAAGCAAAGTG
AACACCCGCCTGATGCATCTGGGCCCGGATGCGCATACCCTGACCTTTCCGGTGGCGGGCGGCAAACCTGATGAACGTGGTG
GCGTTTTGTGACCGATCCGGGCGAATGGCCGTATACCGAAAAACTGAGCGCGCCGGCGGAAAAAAAAGCGCGATTGAAGGC
TTTAGCAAATTTGGCGGCGCGGTGCGCACCATTATGAACCTGCTGCCGGAAGATCTGGATGAATGGGCGATTTTTGATAACC
TATGATCATCCGGCGAGCACCTATTATCATGGCCGCATTTGCATTGCGGGCGATGCGGGCGATGCGAGCAGCCCGCATCAT
GGCGCGGGCGCGGGCGCGGGCATTGAAGATGTGACCGTGTGGCGACCGTGAAGTGGCGCAGACCACCCTGCTGGAA
AGCCCGGATAAAAAGCCGCGAGCGGCGTGTGAACGCGGCGCTGGCGACCTATAACGCGGTGCGCCTGGAACGCGAGCCAGTGG
CTGGTGGAAAGCAGCCGCAATTCTGGGCGAAATTTATGAATGGCAGTATAAACCGACCGCCGCGATAAAAAAAAATGCGAA
GAAGAAGTGTATTGGCGCAGCCATAAAATTTGGGATTATGATATTGGCCAGATGCTGCAGGAAACCACCGAATATTATAAA
CAGCGCGTGGGCGCG

Codon-Optimized *fdmo4* Sequence

ATGGATACCAACAAAATTTGAAATTGCGATTATTGGCGCGGGCATTACCGGCATTACCCTGGCGCTGGGCCTGCTGAGCCGC
GGCATTCCGCCGCGCGATTTCATGAAATTGGCGCGGGCATTGGCTTTACCCCGAACCGCGAATGGGCGATGAAAAGTGGTG
GATCCGCGCATTTCATGCGGCGTTTTAAACGCGTGGCGACCCCGAACGCGAGCGATTGGTTTTAGTGGGTGGATGCGTTTTAAC
GAAACCGCGAACCGCGCTTTGAAGGCTGCCATCGCGCGCAGCTGCTGGGCGAACTGGCGCGCCTGCTGCCGGAAGGCATT
GTGACCTTTTATAAAGCGCTGGATAACCCTGGAACCGGCGGCGGATAACCGCCTGGGCCAGCTGCTGCGCTTTTCAAGATGGC
ACCACCGTGACCGCGCATGCGGTGATTGGCTGCGATGGCATTTCGACCCGCGTGCGCCAGATTCTGTTTTGGCGAAGATCAT
CCGGCGGCGAGCGCGCATTATAGCCATAAATATGCGGCGCGCGGCCCTGATTCCGATGGATCGCGCGCGCGAAGCGCTGGGC
GATGCGAAAGTGGCGACCCGCTTTATGCATCTGGGCCCGGATGCGCATGCGCTGACCTTTCCGATTGCGCATGGCAGCCTG
CTGAACGTGGTGGCGTTTTGTGACCGATCCGAACCCGTGGCCGTATGCGGATCGCTGGACCGCGCAGCGCAACGAAACCGAT
GTGGCGGCGGCGTTTTAGCCGCTTTGGCCCCACCATGCGCACCATTATTGATCTGCTGCCGGATCCGATTGATCAGTGGGCG
GTGTTTTGATACCTATGATCATCCGCCGAACACCTATAGCCGCGGCCCGGTGTGCATTGCGGGCGATGCGGCGCATGCGGCG
GCGCCGCATCATGGCGCGGGCGCGGGCTGCGCGGTGGAAGATGTGGCGGTGCTGTGCGCGGTGCTGGATCTGGCGGCGAAA
CGCGTGGATGCGACCAAATGCGATCCGAAAGGCAAAGCGGCGCTGATTACCACCGCTTTGAAACCTATGATGCGGTGCGC
CGCGAACGCGCGCAGTGGCTGGTGGAAACCAGCCGCATTATTGGCAACTTTTTATGAATGGCAGGATAACGAAGTGGGCCCG
GATGCGAGCATTGTCATGATGAAGTGTATTGGCGCAGCCATCGCATTGTTGGGATTATGATATTGATACCATGATGCGCGAA
ACCGCGAAAGTGTGTTGAAGTGC GCGTGGCGGAACTGACCAAAAAC

Codon-Optimized *fdmo5* Sequence

ATGGCGAGCAACAACAAAACCACCAACCCGAGCATTGAAGTGGCGGTGGTGGGCGGCGGCGTATTGGCGTGATGACCGCG
CTGGGCCTGATTTCGCCGCGGCATTAAAGTGACCATTATGAACGCAGCAGCAACTGGCATGAAATTAGCGCGGGCTTTGCG
TTTACCGGCGTGGCGCGGAATGCATGCAGCGCCTGGATCCGGGCATTCTGGATGTCTGAGCCGCATTAGCCAGAAAACC
GATCCGAACGATAGCAGCACCACCTATTGGAACGCGTATCATCCGCAGACCAAACAGGATGCGGAAGATGAAAGCACCAGC
CTGCTGTTTTAGCTGCCGGGCAACAACTGGCGTTTTGGGGCTGCGTGCAGCCAGTTTTCTGCTGGGCATGGTGGCGCTG
CTGCCGGATGATGTGGCGCGCTTTGGCAAACAGCTGGTGGCTATGATGATGGCGATGCGAACGATAAAGTGGTGGTGCAT
TTTTGCGGATGGCAGCACCGCGGAAGCGGATGTGGTGTGGGCTGCGATGGCATTTCATAGCACCACCCGAAAACCTGCTG
GGCGCGCATCATCCGGCGACCCGCCGAGCTATAACCATAACCGTGGCGTATCGCACCATGGTGGCGATTGATGCGGGCATT
GCGGCGCTGGGCGAAGATAAAGCGCGCCGCGCGTGCATGCATTGCGGCCCGAACGCGAACATGATGAGCTATCCGGTGTG
AACGGCACCCCTGCTGAACGTGGCGTTTTTTTTGCGCATGAAAGCAGCGAATTTCCGGATCCGGAAAAAATGACCGCGCCGGGC
ACCCGCGAAGAACTGGAACGCGTGGTGGTGGGCTGGGGCCGCATCTGGTGGAACTGACCAAACTGTTTTCCGGATAACATG
GTGAAATGGGGCATTTTTTGATATGGATGAAAACCCGGCGCCGACCTATGCGCGCGGCTGCGTGTGCTGGCGGGCGATGCG
GCGCATGCGAGCAGCCCGTTTTAGGGCGTGGGCGCGTGCATTGGCGTGGAAAGATGCGCTGGTGTGCGAAGCGCTGGCG
ACCGTGCAGGCGGGCGGCAACAGCGGCGAGCGATGATGGCAACCATAACCATAGCCAGCGCGAAGTGAACAGGCGCTG
CAGGCGTATAGCCAGGCGCGCATTGATCGCGGCCAGTGGGTGGTGGCGAGCAGCCGCGAACTGGGCCAGATTTATCAGTGG
CGCTATGGCCCCAGCCGGCCGCGATGCGGAACGCGAAGTGAACGCGCGAGCCGACCCGTGTGGGATTATGAT
GTGGATAAAAATTGTGACCGAAATTCGCGCGGTGGTGGCG

Codon-Optimized *fdmo6* Sequence

ATGACCCTGGCGGATCGCGCGCCGCTGGATGTGGCGATTATTGGCGGCGGCATTATTGGCATTATGACCGCGCTGGGCCTG
CTGCATCGCGGCTTTTCGCGTGACCGTGTATGAACGCGCGGCGAGCTGGCCGAAATTTGGCGCGGCTTTTCGCTTTACCGGC
GTGGCGCGCCAGTGCATGGAACGCCTGGATCCGCGCGTGTGAAAGCCTGGCGCGCTGGCGCAGCGCAGCCCGCATGAA
AAAGTGCCTATTGGGATGGCTTTTCATCCGCGCACCAAGAAGCGGCGCAGGAAGAAAGCGCGGTGCTGTTTGAAATTCTG
GAAAAACATATGGCGTATTGGGCGTGCATTTCGCGGCCATTTTCTGCTGGATATGGCGGCGCAGCTGCCGGATGGCGTGGT
CAGTTTGGCAAACGCCTGGTGGATTATAACGATGATGAAGCGAACGAAAAAGTGGTGTGTGCTTTGCGGATGGCAGCACC
GCGGAAAGCGATGTGGTGTATTGCGTGCATGGCATTTCATAGCGCGACCCGCAAAGTGTGTGCTGGGCGTGGATCATCCGGCG
GCGAACGCGAGCTATAGCCGCAAAGCATGTATCGCGCGATGGTGCCGATGGCGGATGCGGTGAGCGCGCTGGGCACCGAA
AAAGCGCATGTGCAGATTGCGCATCTGGGCCCGGATGCGCATGTGGTGTGAGCTTTCCGGTGAACAACGGCCAGGTGTATAAC
GTGTTTCTGTTTCTGCATGATCCGAACGAATGGGATCATGGCCATACCATGACCGTCCGAGCAGCCGCGAGCGAAGTGATG
GATGCGATTTCAGGGCTGGGGCCCGCATATTAAAGAAATTGTGAGCTGCTTTCCGAAACCGTGTGAGCAAATATGCGATTTTT
GATCAGGCGGATAACCCGCTGCCGTATTATGCGAGCGGCCGCGTGTGCCTGGCGGGCGATGCGGCGCATGCGAGCAGCCCG
TTTCATGGCGCGGGCGCGTGCATGGGCGTGAAGATGCGCTGGTGTGCGGAACTGCTGGGCGTGGTGGATGCGGGCCCG
GTGGCGGCGCGCCAGCGCAACATTAAGCGGCGCTGCAGACCTATAGCAGCGTGCGCATTGAACGCAGCCAGTGGCTGGT
CAGAGCAGCCGCGATATGGGCGATCTGTATGAATGGCGCTATCCGCCGACCGGCGAAGATGGCGCGAAATGCAAAGCGGAA
TTTGAACGCCGAGCAAAGTGATTTGGGATTTTGTATGTGGATGGCATGGTGGCGGGCGCGAAAAAAAATATGAACATAGC
ATGGAAGCG

Codon-Optimized *fdmo7* Sequence

ATGGAAGCGCCGAAACAACCATCCGAACGGCATTAACTGATTAACGGCCATAAAGCGAAAAGCCTGGAAGTGGCGATTGTG
GGCGGCGGCTGACCGGCTGGCGCTGGCGGTGGGCTGCTGCGCCGAACATTAACCTTACCATTTATGAACGCGCGGCG
AGCTTTGGCGAACTGGGCGTGGGCATTCATTTTACCCCGAACGCGGAACGCGCGATGGAAGCGCTGGATCCGCGCGTGTG
CAGAGCTATGTGGATGTGGCGACCAACGCGGAAGCGGCTTTCTGAGCTTTGTGGATGGCGCGAGCGGCGATGATGGCCTG
CTGTTTTCAGCTGCGCATGGGCAAAGGCTATAAAGCGGCGCGCCGCTGCGATTTTGTGAGCCAGCTGGTGAACATATTCCG
CAGGAACGCGTGCAGCATCTGAAATGGCTGCAGAGCGTGAAGAAGATGGCGAAGGCCGCGCGGTGCTGACCTTTTCGCGAT
GGCAGCACCGCGGAAGCGGATGTGGTGGTGGGCTGCGATGGCATTTCGAGCCAGGTGCGCAGCGCGATGTTTGGCAGCGGC
CCGAGCGCGCCGCGCGCAGTATGCGCATCAGCTGGCGTTTTCGCGGCTGGTGGCGATGGCGAAAGTGAAGAAGCGCTG
GGCAGCGGCAAAACCAGCCGCGGATTTGGCTATCTGGGCCCGGGCGGCTTTGTGCTGAGCGTGGCGTGGCGGGCATTAA
ATGATGCATCTGGAAGTGTGTTGTGATGGATCCGCTGGATTGGAGCGATACCCGCGCAAAAGCGAAAAGGCAACGATGAA
GATGATGTGAAACGCTATGTGCTGCCGGCGACCCGCGCGGAAGCGGAAAAAGCGTTTACCGAATTTAACCCGACCGTGC
AGCCTGATTAGCCTGCTGCCGAAACCTGGGCAAATGGGCGATTTTGTATATGCTGGATAGCCCGGCGCCGAGCTATGCG
CTGGGCCGATGTGCCTGGCGGGCGATGCGGCGCATGCGAGCACCCGAACCAGGGCGGCGGCGGGCGCGGGCATTGAA
GATAGCCTGGTGTGCGGAAATTTCTGGCGGCGCTGGCGGATCGCGAAAACAGCGGCGCGCCGTTGGGCTGAGCGAAATT
AGCGAAGGCTGAAAGTGTATAGCGAAGCGCGCTATGAACGCGCGCAGTGGCTGGTGCAGAGCAGCCGCCGCGTGGCGCAG
CTGTTTACCCGCAAAAGCGCGGAACAGGAAGAACCATTAGCCGCGAAATTTCTGGAACGCAGCCATCAGCTGTGGGATCAT
GATGTGGATGCGATGGTGGCGGATGCGCTGGGCAAACCTGAAAGCGAACTGAGCGAAAAAAA

Protein overexpression and purification: Plasmids containing the genes of interest were transformed using standard heat-shock protocols into chemically competent *E. coli* into BL21(DE3) cells. Overexpression of AfoD was achieved in 500 mL 4% glycerol (v/v) Terrific Broth (TB) in 2.8 L flasks. 500 mL portions of media were inoculated with 5 mL overnight culture prepared from a single colony in Luria Broth (LB) and 100 µg/mL ampicillin (Gold Biotechnology). Cultures were grown at 37 °C and 250 rpm until the optical density at 600 nm reached 0.8. The cultures were then cooled to 18 °C for 1 h and protein expression was induced with 0.1 mM isopropyl-β-D-1-thiogalactopyranoside (IPTG, Gold Biotechnology). Expression continued at 20 °C overnight (approx. 18 h) at 200 rpm. The typical yield for one 500 mL culture was ~15 g cell pellet. Overexpression of AzaH followed the same protocol as described above, except 1 L cultures were grown in 2.8 L flasks and kanamycin was used at 50 µg/mL (Gold Biotechnology) in place of ampicillin. The typical yield for one 1 L culture was ~30 g cell pellet.

General purification procedure: 25-30 g of cell pellet was resuspended in 100 mL of lysis buffer containing 50 mM Tris HCl pH 7.4, 300 mM NaCl, 10 mM imidazole, and 10% glycerol. Protease inhibitors were added to lysis

buffer of AzaH only and consisted of 1 mM phenylmethane sulfonyl fluoride (v), 0.1 mg/mL benzamidine HCl, 0.5 mg/mL leupeptin, and 0.5 mg/mL pepstatin. Approximately 1 mg/mL lysozyme was added to resuspended cells that were then incubated on a rocker at 4 °C for 30 min. Cells were lysed by passing the total cell lysate through an Avestin pressure homogenizer at 15000 psi. The total lysate was centrifuged at 40,000 x g for 30 min and the supernatant was filtered through a 0.45 µm filter. The crude cell lysate was loaded onto a 5 mL HisTrap HP column (General Electric) on an ÄKTA Pure FPLC system (General Electric) at a flow rate of 2.5 mL/min. Buffer A = the lysis buffer listed above, and Buffer B = 50 mM Tris HCl pH 7.4, 300 mM NaCl, 10% glycerol, and 400 mM imidazole. The column was washed with 25 mM imidazole (6.3% Buffer B) for 6 CV and eluted in a gradient to 100% Buffer B over 8 CV. Fractions containing AfoD or AzaH were visibly yellow and pooled for desalting on a PD10 desalting column. Average yields: 100 mg from 1 L AfoD, 20 mg from 1 L AzaH. Molecular weights including 6xHis-tags for each protein were estimated by the ProtParam tool on the ExPASy server to be 49.0 kDa for AfoD and 47.6 kDa for AzaH. These molecular weights are consistent with the mass of proteins bands observed by SDS-PAGE analysis (Figure S1). The purified proteins were aliquoted into 0.6 mL tubes and frozen in liquid nitrogen before long-term storage at -80 °C.

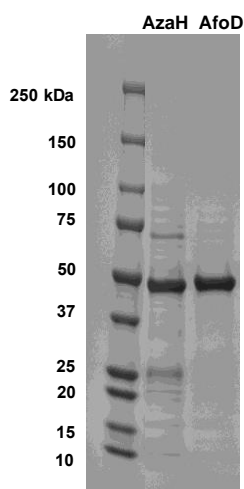


Figure S1. Purified AzaH and AfoD. Approximately 5 µL of 1.25 µM each protein was loaded onto an MiniPROTEAN TGX Precast 4-15% SDS-PAGE gel (Bio-Rad). The gel was stained with Quick Coomassie stain (Anatrace) and visualized with the Azure Gel Imaging System. The relative apparent masses are consistent with the predicted estimates.

Determination of flavin incorporation and extinction coefficients: Samples of each protein were diluted to 10 µM in 1 mL using dialysis buffer for UV-vis analysis using a disposable poly(methyl 2-methylpropenoate) cuvette. The absorbance spectrum for each protein was taken from 300 nm to 700 nm in 2 nm increments (blue traces in Figure S2). A 20 µL aliquot of fresh 10% sodium dodecyl sulfate (w/v) was added to each 1 mL solution and mixed. Samples were incubated at room temperature for 10 min before reading the absorbance spectra again under the same conditions (red traces in Figure S2). The absorbance at 450 nm for the denatured enzymes and the extinction coefficient of free FAD ($11300 \text{ M}^{-1} \text{ cm}^{-1}$) was used to calculate the concentration of FAD in each protein sample using Beer's law. The typical FAD incorporation was 82% for AzaH, 81% for AfoD. Extinction coefficients were calculated using the concentrations of free flavin obtained and the absorbance at 450 nm of the native enzymes. At 450 nm, the extinction coefficients of the proteins are $17490 \text{ M}^{-1} \text{ cm}^{-1}$ for AzaH, $6,870 \text{ M}^{-1} \text{ cm}^{-1}$ for AfoD.

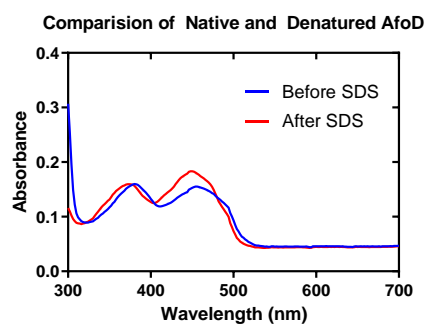
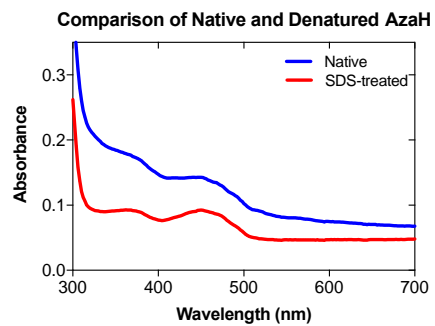


Figure S2. Native enzyme absorbance spectra compared to denatured enzyme absorbance spectra exposing free FAD to solution.

Part III. Generation of AfoD Y118F variant

General Considerations

E. coli cloning strains DH5 α (Invitrogen) were used for DNA propagation. Phusion HF polymerase was purchased from New England BioLabs. All primers were purchased from Integrated DNA Technologies (IDT) ddH₂O was sourced from a MilliQ Biocel water purification unit from Millipore.

Site-directed mutagenesis

Table S1. Primer Sequences

Variant	Plasmid ID	Oligo sequence
AfoD Y118F	AfoD_Y118F_P1	GAAAAGAACATGGCATT TTTGGGCATGTC

The AfoD(Y118F) substitution was generated by site-directed mutagenesis on pET151-afod(WT). 25 μ L PCR reaction mixture contained 5 μ L of 5X Phusion HF buffer, 1 ng/ μ L WT parent plasmid, 0.5 μ M of primer, 200 μ M dNTPs, 0.5 U μ L⁻¹ Phusion HF. Amplification was accomplished with the following PCR protocol: 95 °C for 0:30 s, (95 °C 0:30 95 °C for 0:30 s (-0.5 °C/cycle), 72 °C 0:30/kb) for 12 cycles, (95 °C for 0:30 s, 65 °C for 0:30 s, 72 °C 0:30/kb) for 20 cycles with a final extension of 72 °C for 10:00 min. This was followed by a 10 μ L digestion containing 1 μ L of NEB CutSmart buffer, 8 μ L of PCR mixture and 20 units of DpnI. The reaction was incubated at 37 °C for 3 h and transformed into chemically competent E. coli DH5 α cells.

Protein Expression and Purification

Protein overexpression: AfoD(Y118F) plasmid was transformed into E. coli strain BL21(DE3). 500 mL of Terrific Broth (TB) containing 100 μ g mL⁻¹ ampicillin was inoculated with 5 mL overnight culture prepared from a single colony in Luria Broth (LB) and 100 μ g mL⁻¹ ampicillin. The culture was grown at 37 °C and 250 rpm for 4 h. The culture was then cooled to 20 °C for 1 h at 200 rpm, and protein expression was induced with 0.1 mM isopropyl- β -D-1-thiogalactopyranoside (IPTG) and expressed at 20 °C for 18 h at 200 rpm. After overnight expression, cultures were centrifuged at 13,881 x g for 30 min. Cell pellets from overexpression were stored at -80 °C for long-term storage.

General purification procedure: Cell pellets from overexpression were resuspended in 40 mL of lysis buffer (50 mM Tris:HCl pH 7.8, 300 NaCl, 10 mM imidazole, and 10% (v/v) glycerol) with 0.1 mg mL⁻¹ lysozyme, 0.05 mg mL⁻¹ DNase, and 0.1 mM flavin adenine dinucleotide (FAD), incubated on a rocker at 4 °C for 45 min, and lysed by sonication. Insoluble material was removed by centrifugation (46,413 x g for 30 min). The cell pellet was resuspended in 40 mL lysis buffer (50 mM Tris:HCl pH 7.8, 300 NaCl, 10 mM imidazole, 10% (v/v) glycerol) with 0.1 mg mL⁻¹ lysozyme, 0.05 mg mL⁻¹ DNase, and 0.1 mM FAD, incubated on a rocker at 4 °C for 45 min, lysed by sonication and cleared by centrifugation (46,413 x g for 30 min). The supernatant was incubated with Ni-NTA on a rocker for 2 h at 4 °C, followed by purification by gravity using a 25-50 mM gradient with increments of 5 mM imidazole. Protein was eluted with 100% elution buffer (50 mM Tris:HCl pH 7.8, 300 mM NaCl, 400 mM imidazole, 10% (v/v) glycerol). Concentrated protein was desalted over a PD-10 desalting column (GE Healthcare). The protein was concentrated further using a 30 kDa centrifugal concentrator at 4,000 x g, 4 °C. Concentrated protein was divided into 100 μ L aliquots, frozen in liquid nitrogen and stored at -80 °C.

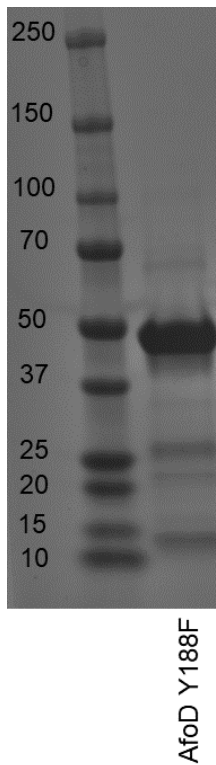


Figure S3. AfoD(Y118F) SDS-PAGE gel. The gel was stained with Quick Coomassie stain (Anatrace) and visualized with the Azure Gel Imaging System

Part IV. Sequence Similarity Network (SSN) (SSN)

Figure S4. SSN of flavin-dependent monooxygenases created using web tools originating from the Enzyme Function Initiative (EFI).¹⁴⁻¹⁶

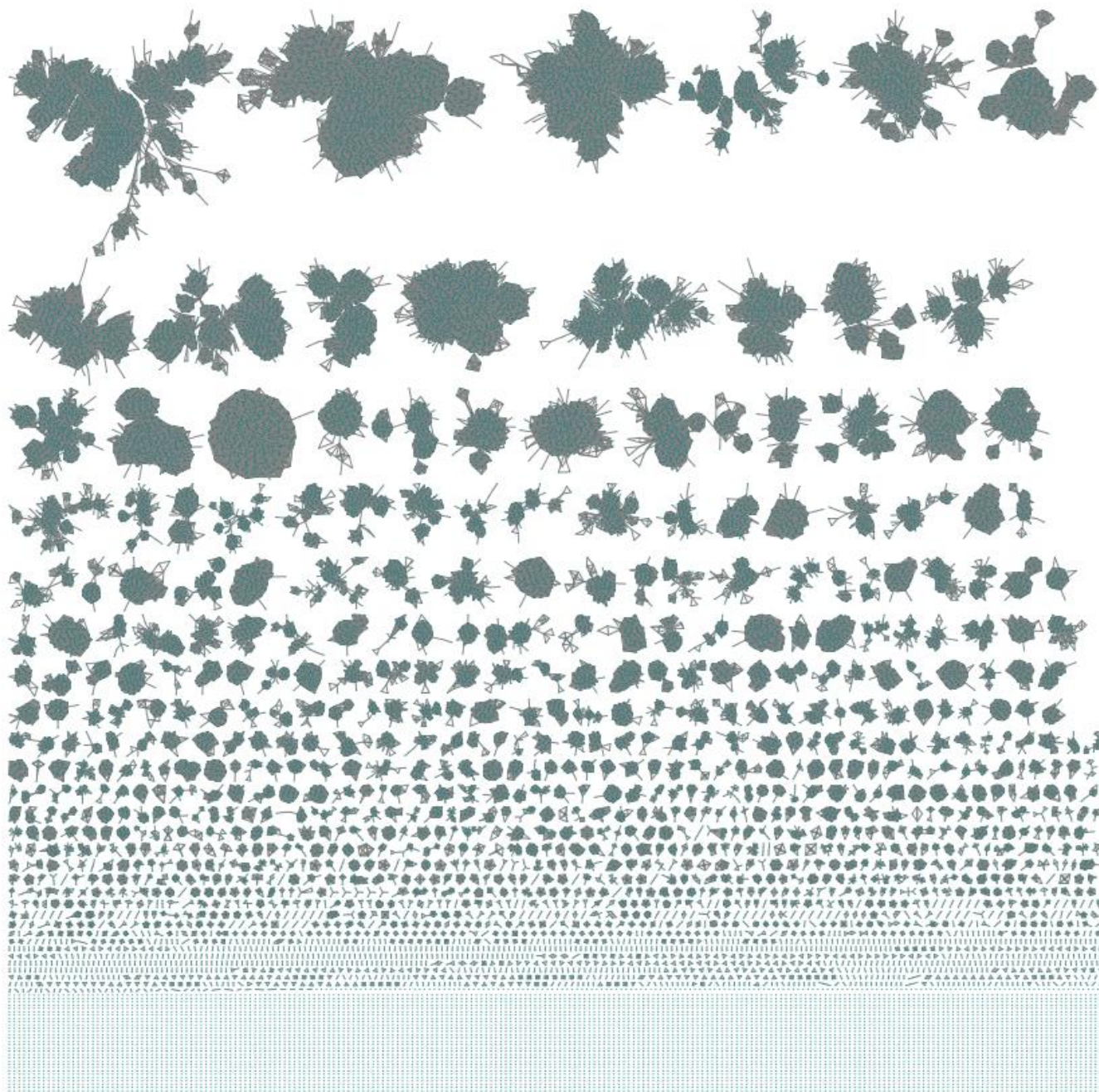
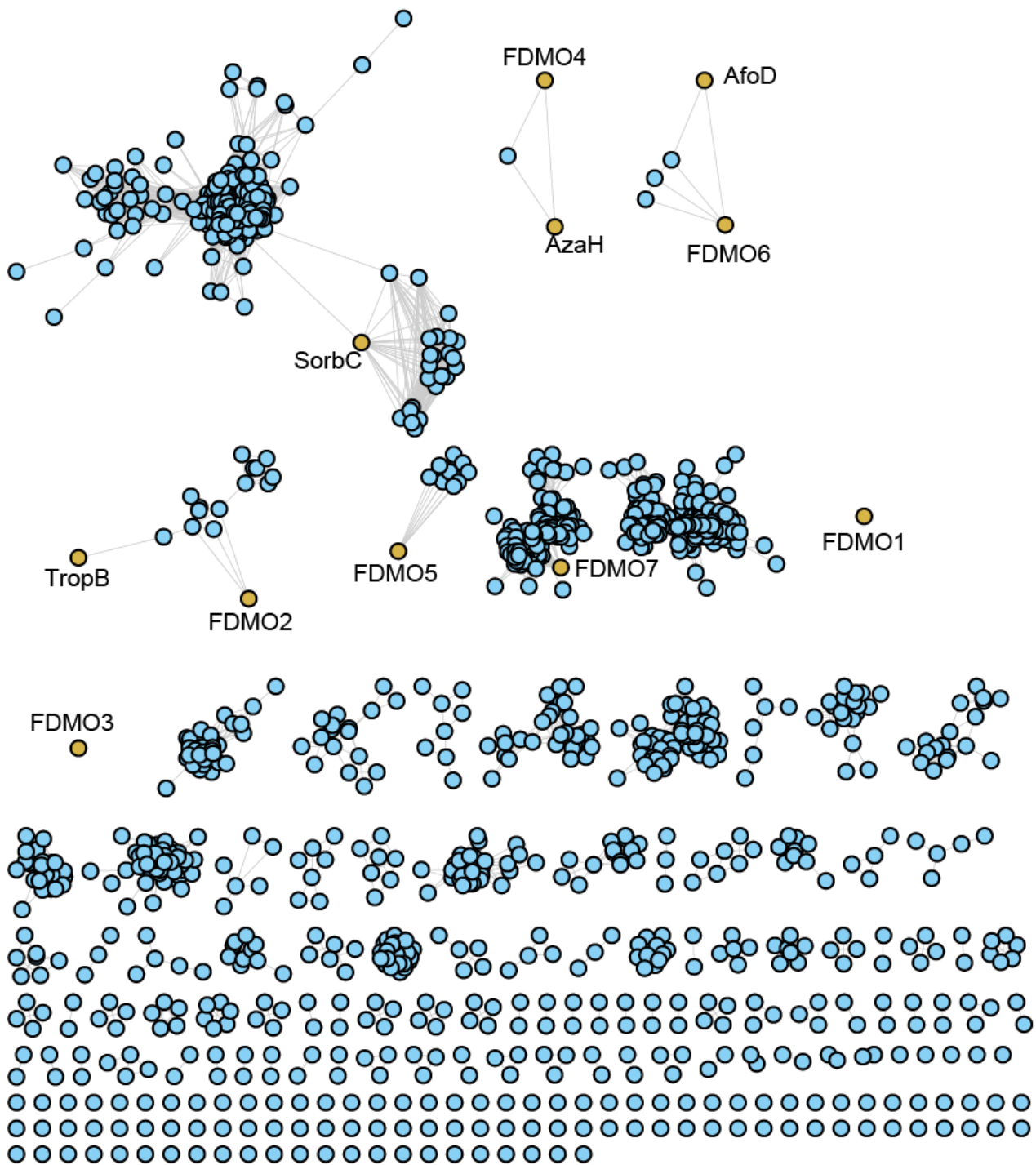


Figure S5. Sequence similarity network with E value of 150.¹⁴⁻¹⁶



Part V. FDMO Sequence Alignment

AfoD Cluster Alignment



Figure S6. AfoD cluster sequence alignment with other sequences within its cluster Y118 and F237 are highlighted. Alignment is colored by conservation.

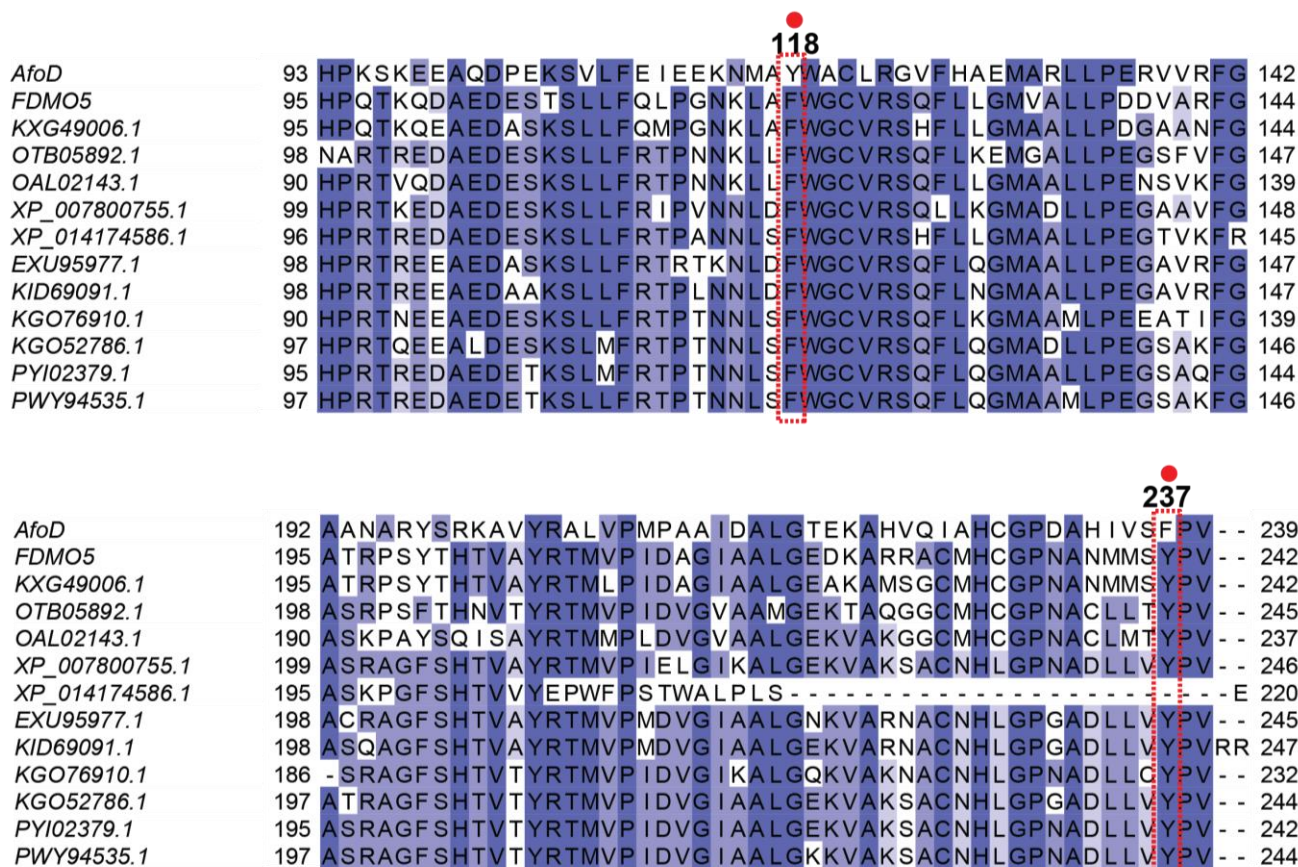


Figure S7. FDMO5 cluster sequence alignment with other sequences within its cluster Y118 and F237 are highlighted (From AfoD). Alignment is colored by conservation.

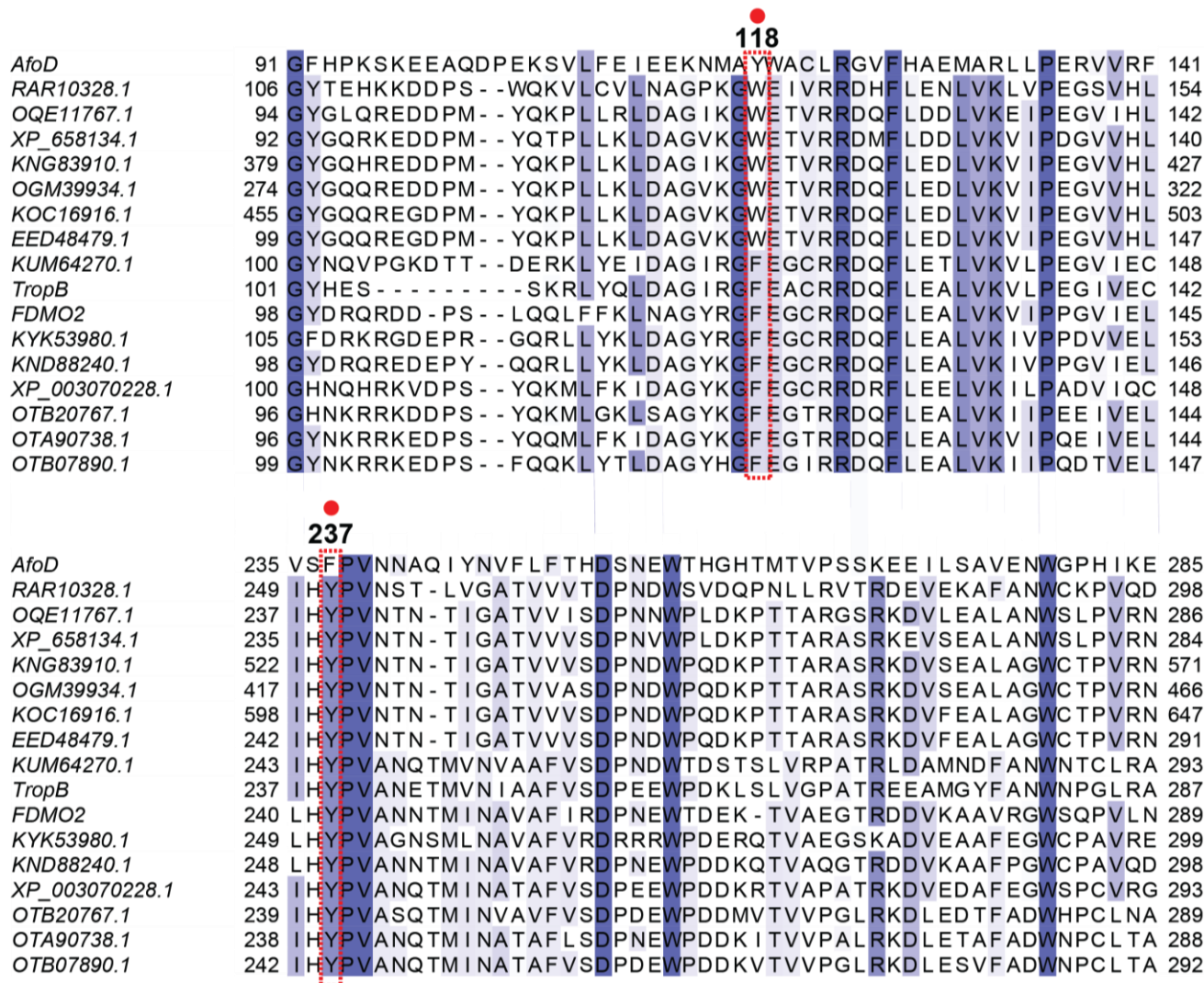
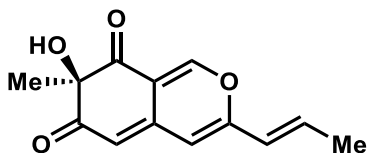


Figure S8. TropB cluster sequence alignment with other sequences within its cluster Y118 and F237 are highlighted (From *AfoD*). Alignment is colored by conservation.

Part VI. Biocatalytic Reactions

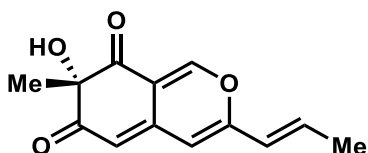
Stock solutions: Stock solutions of each substrate (50 mM) were prepared by dissolving the substrate in DMSO (analytical grade). Stock solutions of NADP⁺ (100 mM) and glucose-6-phosphate (G6P, 500mM) were stored at -20 °C. Aliquots of each flavin-dependent enzyme and glucose-6-phosphate dehydrogenase (G6PDH, 100 U/mL) were stored at -80 °C. Analytical-scale reactions: Each reaction contained 25 μ L 100 mM potassium phosphate buffer, pH 8.0, 2.5 mM substrate (2.5 μ L of a 50 mM stock solution in DMSO), 5-20 μ M flavin-dependent monooxygenase, 5 mM G6P (0.5 μ L, 500 mM), 1 mM NADP⁺ (0.5 μ L, 100 mM), 1 U/mL G6P-DH (0.5 μ L, 100 U/mL), and Milli-Q water to a final volume of 50 μ L. The reaction was carried out at 30 °C for 1 h and quenched by addition of 75 μ L acetonitrile with 25 mM pentamethylbenzene as an internal standard. Precipitated biomolecules were pelleted by centrifugation (16,000 x g, 12 min). The supernatant was analyzed by UPLC-DAD and conversion obtained by comparison to calibration curves of each substrate. The subsequent liquid chromatography PDA spectrometry (UPLC) analysis was performed on a Waters Aquity H-Class UPLC-PDA using a Phenomenex Kinetex 1.7 μ m C18, 2.1x150 mm column under the following conditions: Method A: mobile phase (A = deionized water + 0.1% formic acid, B = acetonitrile + 0.1% formic acid), 5% to 100% B over 1.5 min, 100% B for 1.0 min; flow rate, 0.5 mL/min; Method B: mobile phase (A = deionized water + 0.1% formic acid, B = acetonitrile + 0.1% formic acid), 5% to 100% B over 2 min, 100% B for 1 min; flow rate, 0.5 mL/min. Based on calibration curves of the starting materials, the percent conversion of the substrate to dearomatized product was calculated with AUC_{substrate}/AUC_{internal standard} at 270 nm. All reactions were performed and analyzed in triplicate.

General procedure for *in vitro* preparative-scale reactions: Preparative-scale enzymatic reactions were conducted on 20 mg of each substrate under the following conditions: 5-20 μ M flavin-dependent monooxygenase, 2.5 mM substrate, 1 mM NADP⁺, 1 U/mL G6PDH, and 5 mM G6P for NADPH generation in reaction buffer (50 mM potassium phosphate buffer, pH 8.0). The reaction mixture was added to a 50 mL Erlenmeyer flask and incubated at 30 °C with 100 rpm shaking. After 2 h, a 50 μ L aliquot was removed and processed in an identical manner to the analytical-scale reactions described above to determine substrate conversion. The remaining reaction mixture was diluted with acetone (2 x total reaction volume). Precipitated biomolecules were pelleted by centrifugation (4,000 x g, 12 min). Isolation procedure: The supernatant was concentrated under reduced pressure to a final volume of approximately 2 mL. The resulting mixture was filtered through a 0.22 μ m filter and purified by preparative HPLC using a Phenomenex Kinetex 5 μ m C18, 150 x 21.2 mm column under the following conditions: mobile phase A = deionized water + 0.1% formic acid and B = acetonitrile + 0.1% formic acid; method = 5% to 100% B over 13 min, 100% B for 4 min; flow rate, 15 mL/min.



(*R,E*)-7-hydroxy-7-methyl-3-(prop-1-en-1-yl)-6H-isochromene-6,8(7H)-dione ((*R*)-18)

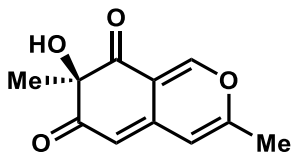
The title compound was synthesized using AzaH according to the general procedure for milligram-scale *in vitro* enzymatic oxidative dearomatization and isolated using the general isolation method. Purification by preparative HPLC afforded 9.6 mg (96% yield) of the title compound as a yellow oil. ¹H NMR (400 MHz, CDCl₃) δ 7.89 (s, 1H), 6.59 (m, 1H), 6.10 (s, 1H), 6.01 (d, J = 15.6 Hz, 1H), 5.57 (s, 1H), 2.62 (s, 2H), 1.94 (d, J = 7.0 Hz, 3H), 1.55 (s, 3H). All spectra obtained were consistent with reported values.⁷



(*S,E*)-7-hydroxy-7-methyl-3-(prop-1-en-1-yl)-6H-isochromene-6,8(7H)-dione ((*S*)-18)

The title compound was synthesized using AfoD according to the general procedure for milligram-scale *in vitro* enzymatic oxidative dearomatization and isolated using the general isolation method. Purification by preparative

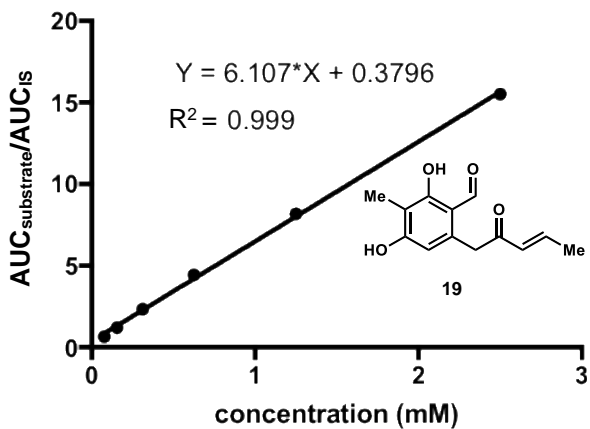
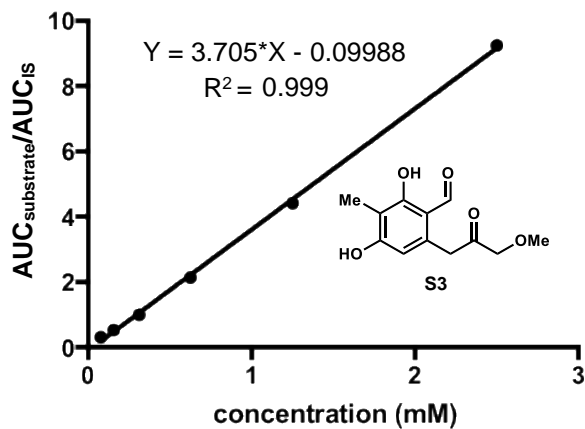
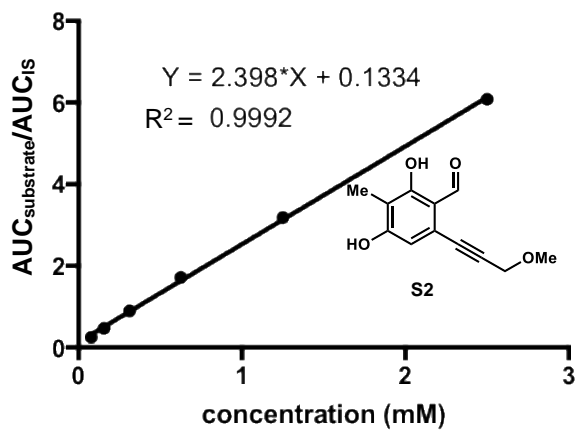
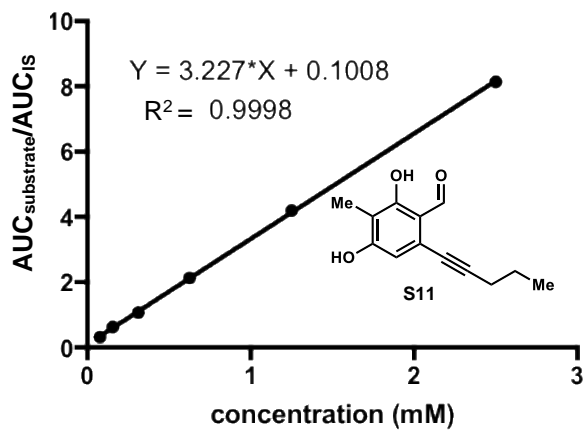
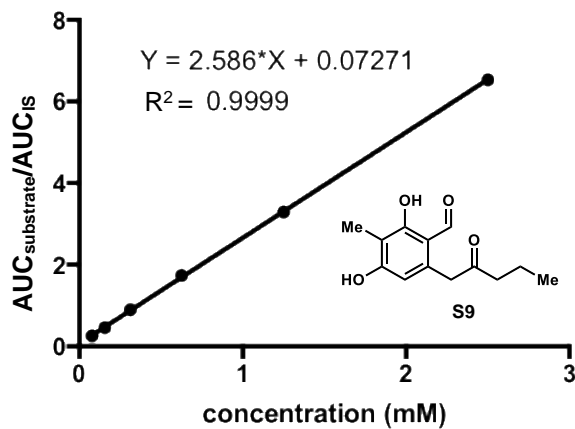
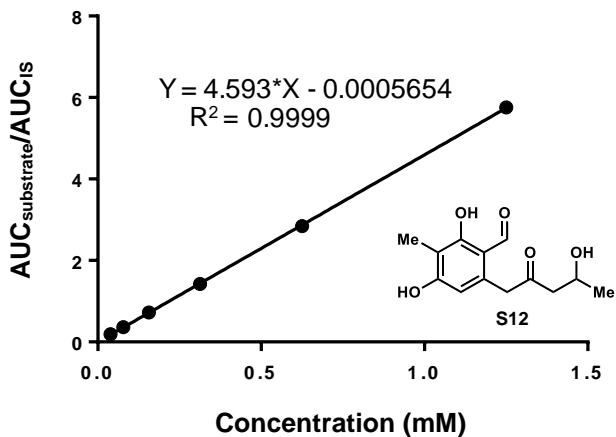
HPLC afforded 4 mg (83% yield) of the title compound as a yellow oil. $^1\text{H NMR}$ (400 MHz, CDCl_3) δ 7.89 (s, 1H), 6.59 (m, 1H), 6.10 (s, 1H), 6.01 (d, $J = 15.6$ Hz, 1H), 5.57 (s, 1H), 2.62 (s, 2H), 1.94 (d, $J = 7.0$ Hz, 3H), 1.55 (s, 3H). All spectra obtained were consistent with reported values.⁷

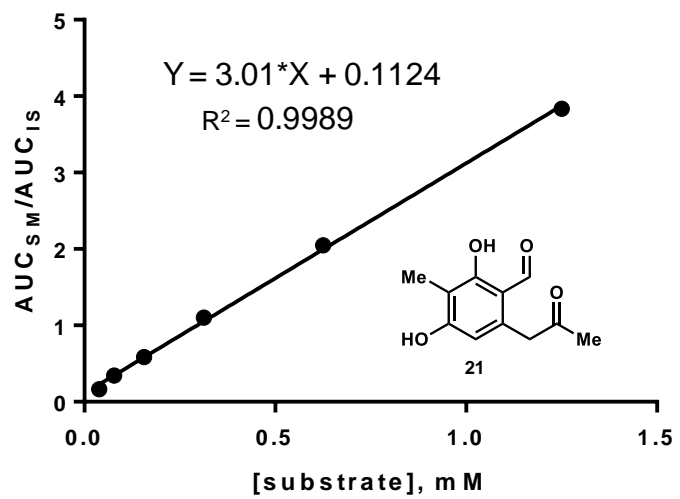


(R)-7-hydroxy-3,7-dimethyl-6H-isochromene-6,8(7H)-dione (22)

The title compound was synthesized using AzaH according to the general procedure for milligram-scale *in vitro* enzymatic oxidative dearomatization and isolated using the general isolation method. Purification by preparative HPLC afforded 9.5 mg (95% yield) of the title compound as a yellow oil. $^1\text{H NMR}$ (400 MHz, CDCl_3) δ 7.88 (s, 1H), 7.26 (s, 2H), 6.13 (s, 1H), 5.51 (s, 1H), 2.20 (s, 3H), 1.55 (s, 3H). All spectra obtained were consistent with reported values.¹³

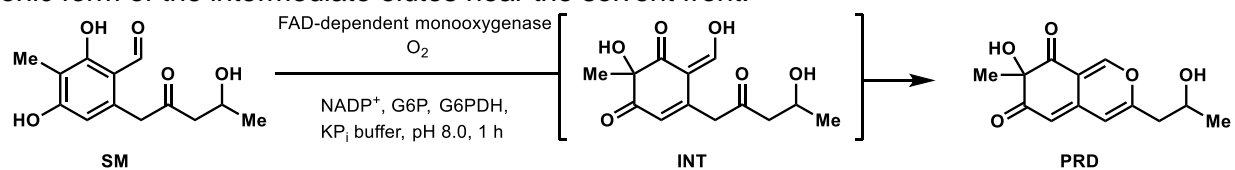
Part VII. Substrate Calibration Curves



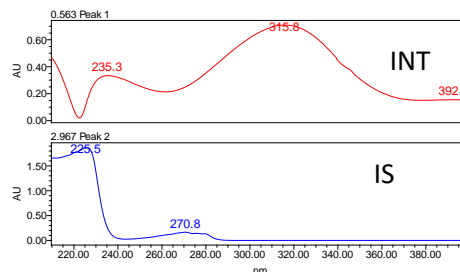
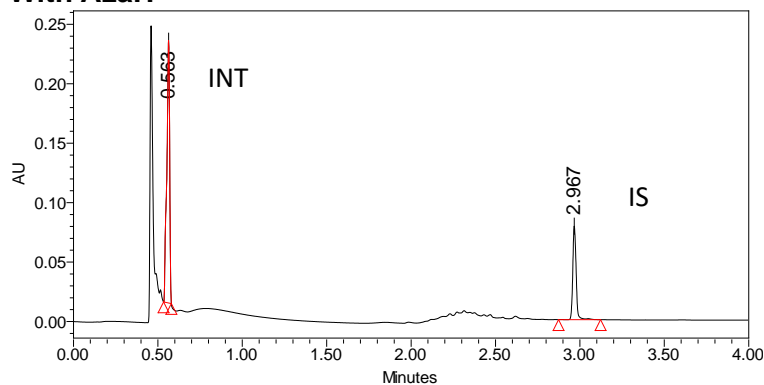


Part VIII. UPLC Traces of Biotransformations

Figure S9. Oxidative dearomatization of **S12** by AfoD and AzaH. PDA traces of enzymatic reaction and control reaction. (Table 1, entry 2). SM = starting material, INT = intermediate, PRD = product, IS = internal standard. The anionic form of the intermediate elutes near the solvent front.

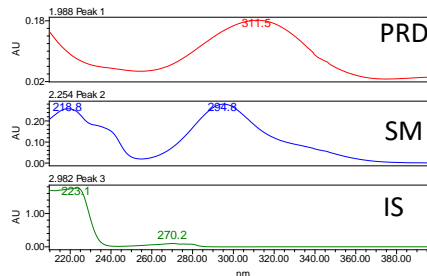
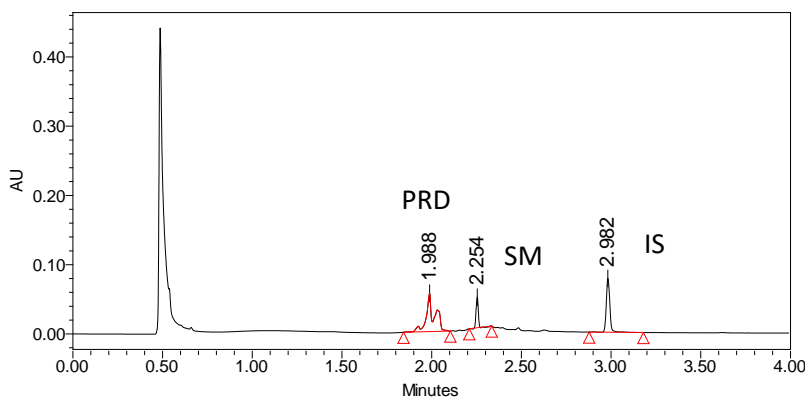


With AzaH



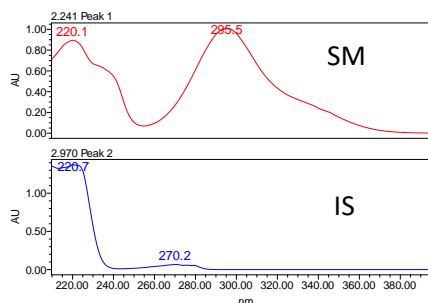
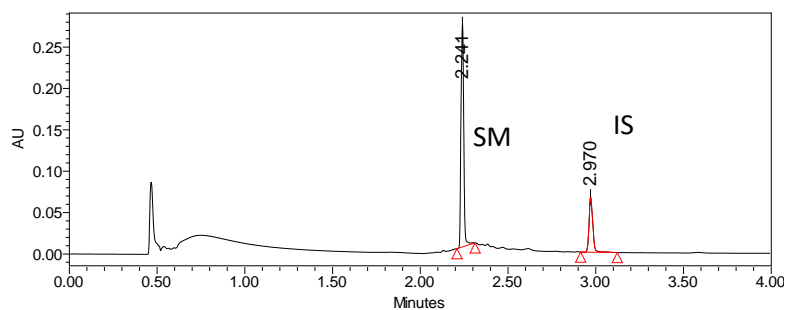
	Retention Time	Area	% Area	Height
1	0.563	258810	70.42	220721
2	2.967	108693	29.58	78693

With AfoD



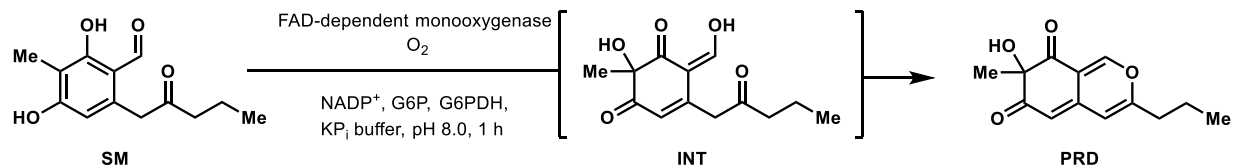
	Retention Time	Area	% Area	Height
1	1.988	174634	54.03	55311
2	2.254	41199	12.75	44106
3	2.982	107399	33.23	77715

NEC

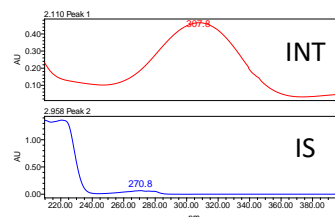
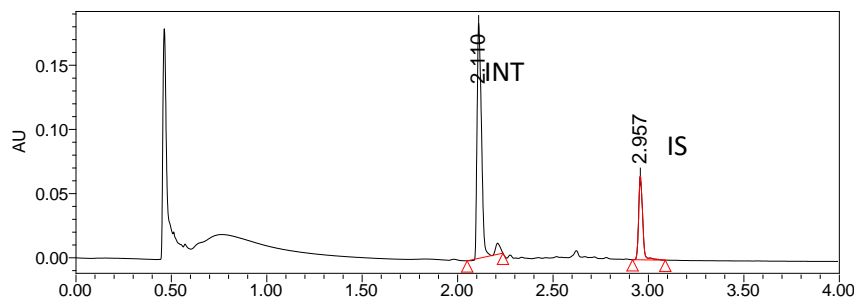


	Retention Time	Area	% Area	Height
1	2.241	292664	74.92	268642
2	2.970	97969	25.08	66721

Figure S10. Oxidative dearomatization of **S9** by AfoD and AzaH. PDA traces of enzymatic reaction and control reaction (Table 1, entry 1).

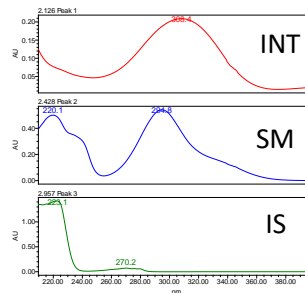
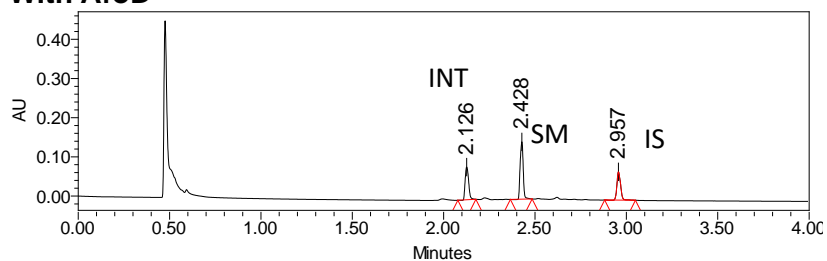


With AzaH



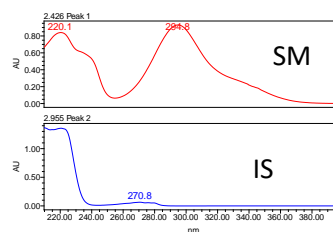
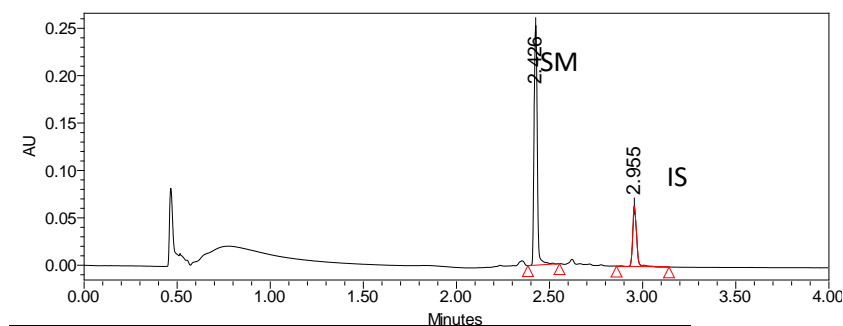
	Retention Time	Area	% Area	Height
1	2.110	305704	76.28	183131
2	2.957	95087	23.72	65154

With AfoD



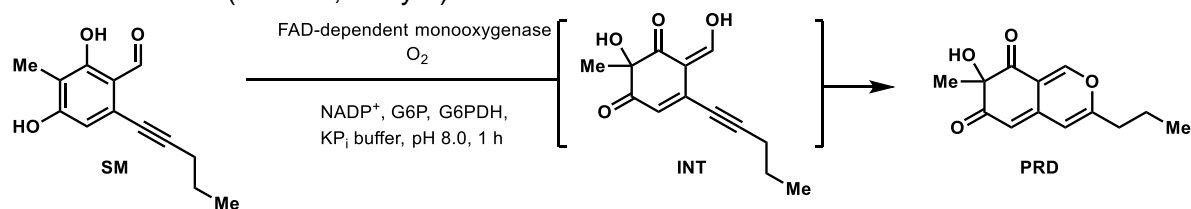
	Retention Time	Area	% Area	Height
1	2.126	111917	29.11	83638
2	2.428	171664	44.65	146387
3	2.957	100880	26.24	72085

NEC

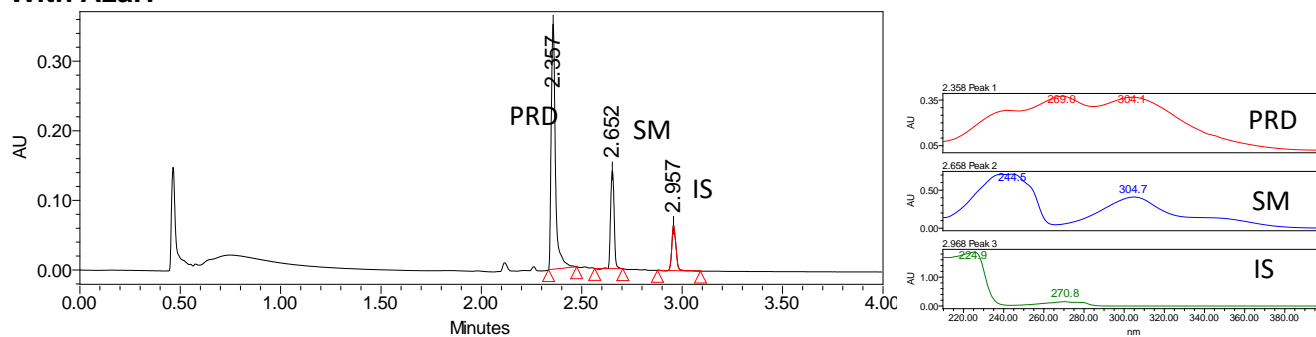


	Retention Time	Area	% Area	Height
1	2.426	301558	76.61	252996
2	2.955	92051	23.39	63755

Figure S11. Oxidative dearomatization of **S11** by AfoD and AzaH. PDA traces of enzymatic reaction and control reaction. (Table 1, entry 3).

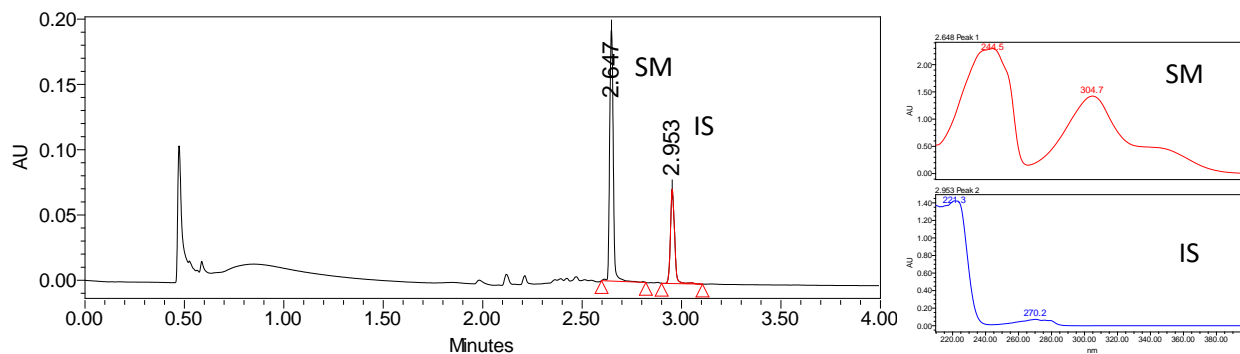


With AzaH



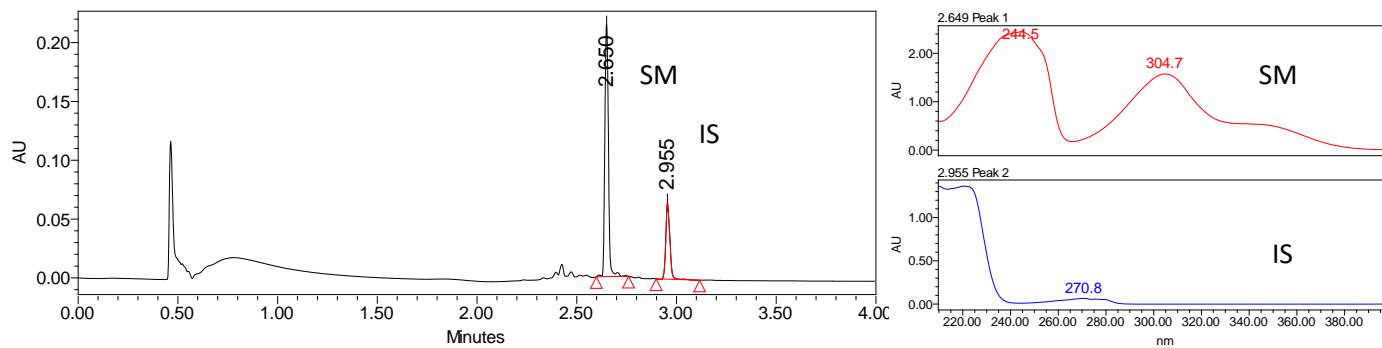
	Retention Time	Area	% Area	Height
1	2.357	517469	65.70	351986
2	2.652	176051	22.35	140720
3	2.957	94126	11.95	65187

With AfoD



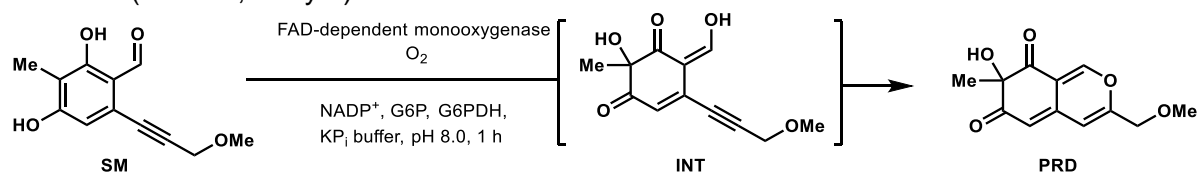
	Retention Time	Area	% Area	Height
1	2.647	240563	69.66	192549
2	2.953	104788	30.34	72317

NEC

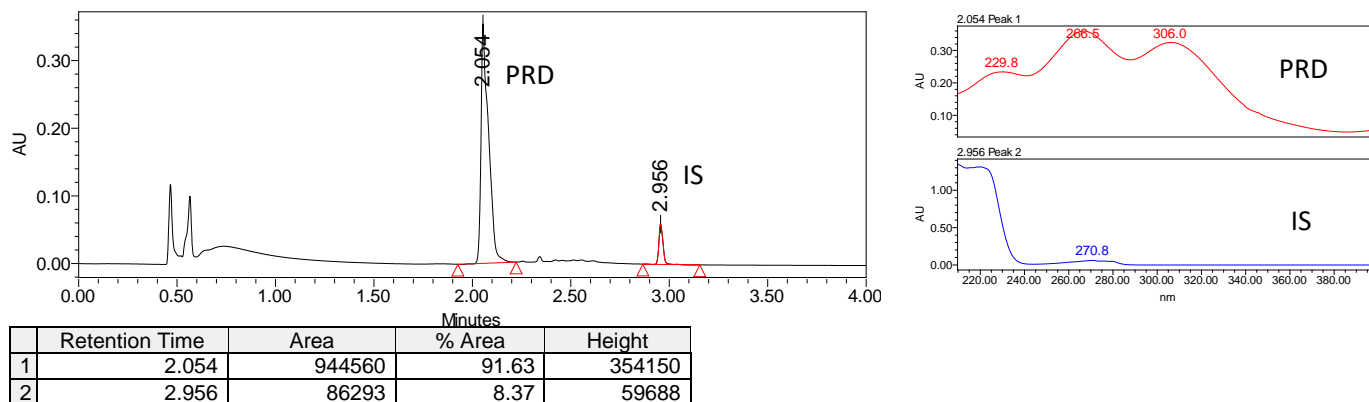


	Retention Time	Area	% Area	Height
1	2.650	266100	74.22	214826
2	2.955	92442	25.78	64989

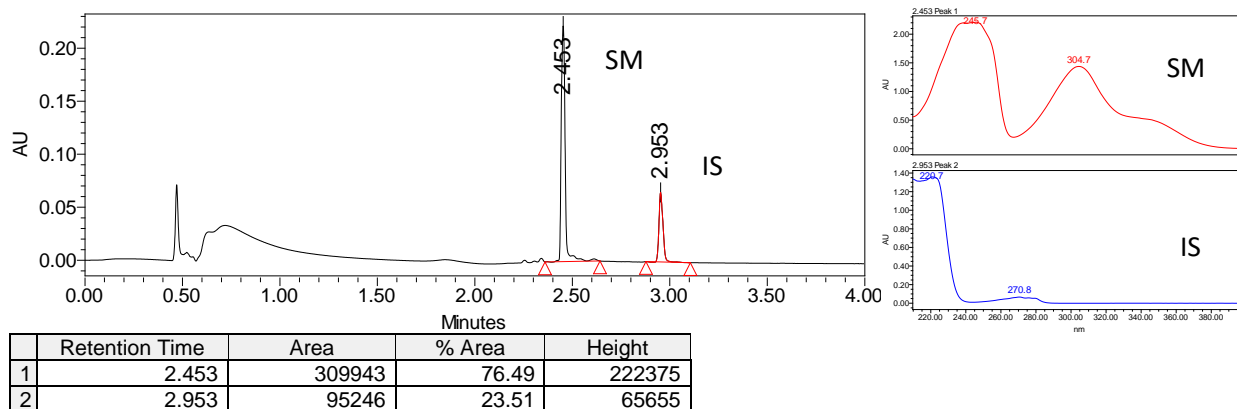
Figure S12. Oxidative dearomatization of **S2** by AfoD and AzaH. PDA traces of enzymatic reaction and control reaction. (Table 1, entry 4).



With AzaH



With AfoD



NEC

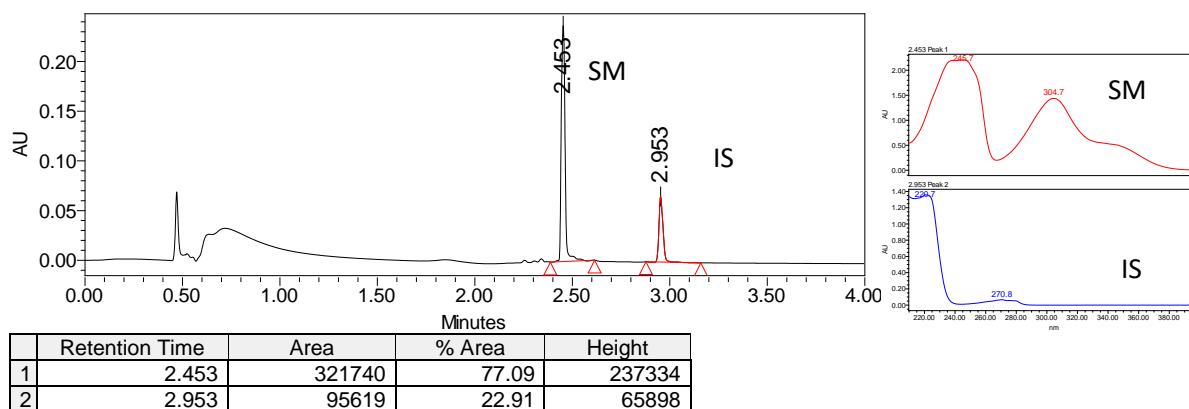
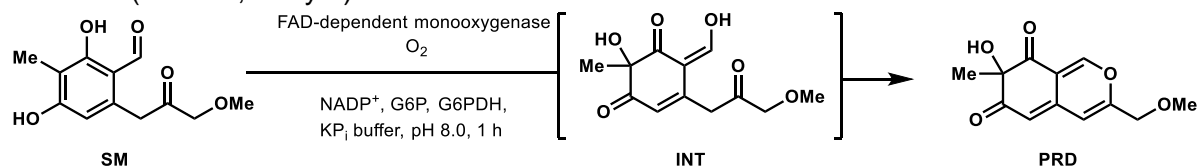
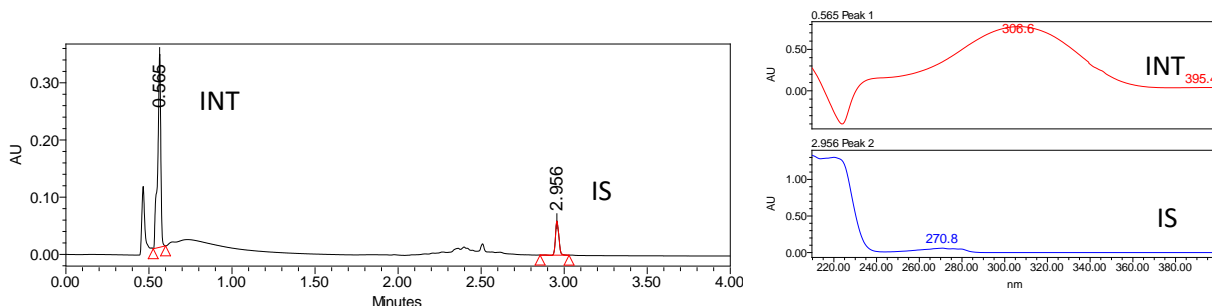


Figure S13. Oxidative dearomatization of **S3** by AfoD and AzaH. PDA traces of enzymatic reaction and control reaction. (Table 1, entry 5).

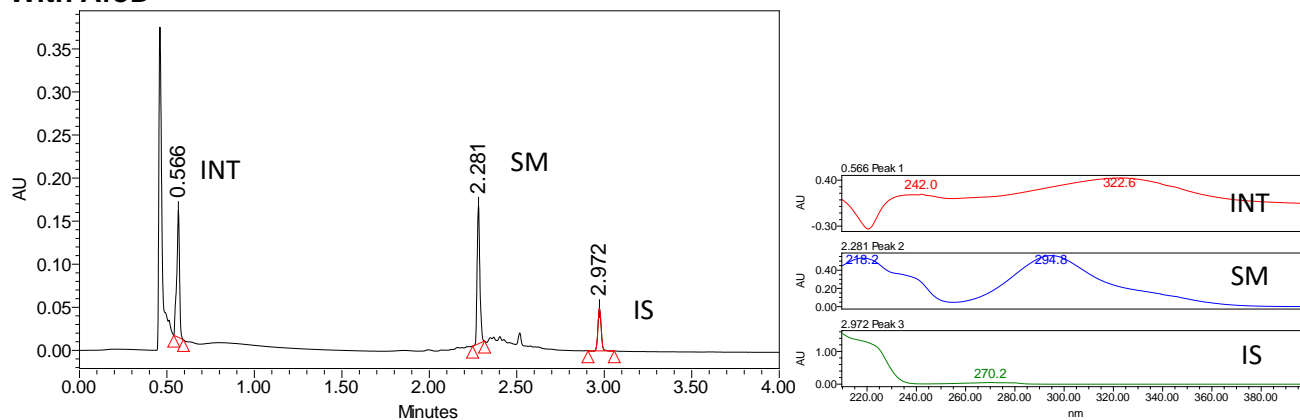


With AzaH



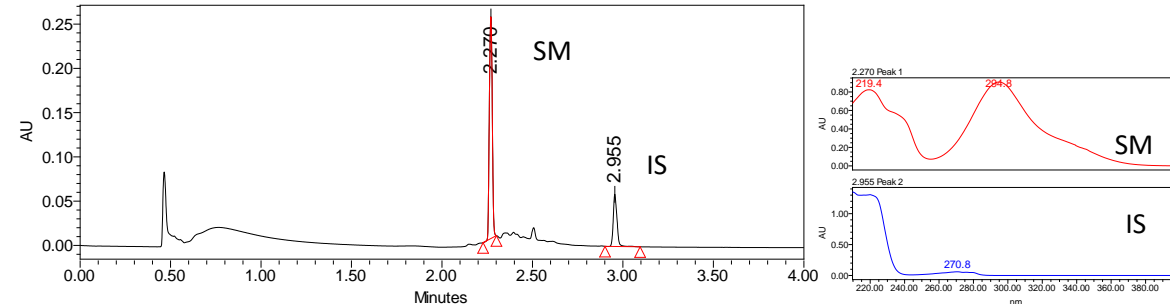
	Retention Time	Area	% Area	Height
1	0.565	434990	83.72	338239
2	2.956	84593	16.28	59668

With AfoD



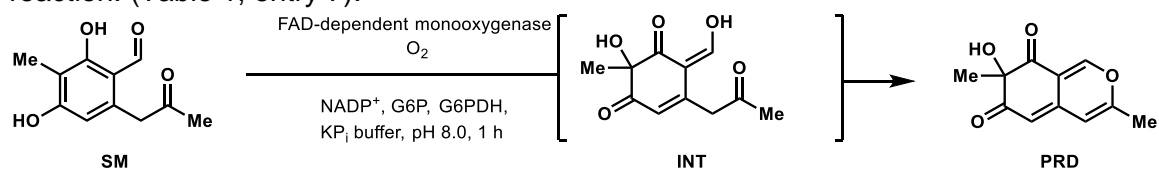
	Retention Time	Area	% Area	Height
1	0.572	113995	30.42	89263
2	2.271	157150	41.94	133701
3	2.953	103585	27.64	72398

NEC

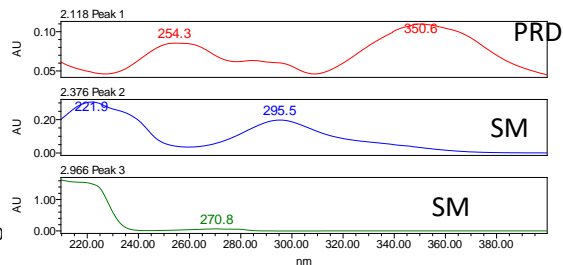
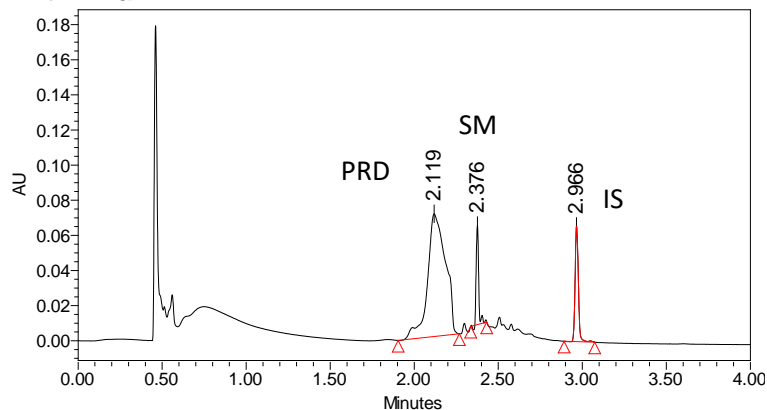


	Retention Time	Area	% Area	Height
1	2.270	284197	77.11	250475
2	2.955	84347	22.89	58999

Figure S14. Oxidative dearomatization of **21** by AfoD and AzaH. PDA traces of enzymatic reaction and control reaction. (Table 1, entry 7).

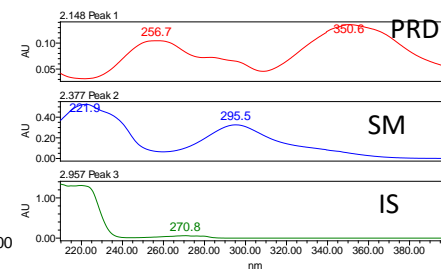
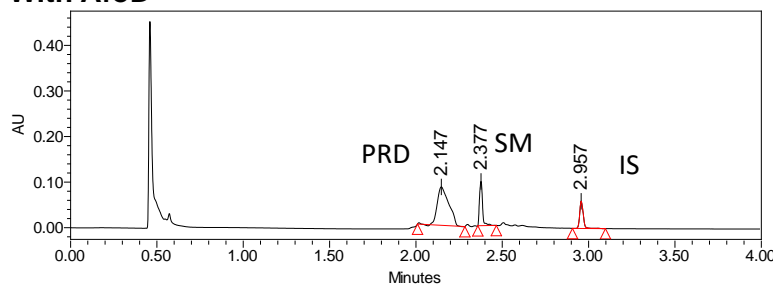


With AzaH



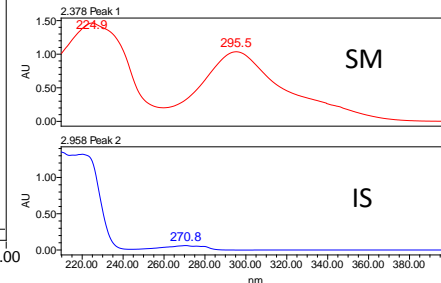
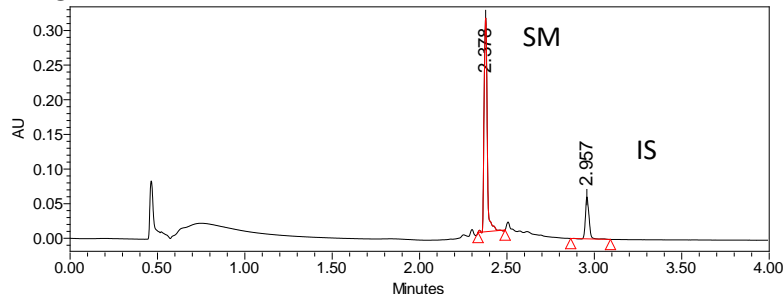
	Retention Time	Area	% Area	Height
1	2.119	519413	77.67	69861
2	2.376	60100	8.99	56370
3	2.966	89232	13.34	65670

With AfoD



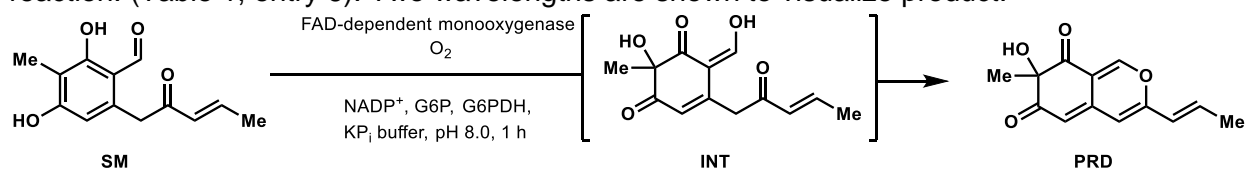
	Retention Time	Area	% Area	Height
1	2.147	398043	65.96	84339
2	2.377	119827	19.86	97170
3	2.957	85588	14.18	59788

NEC

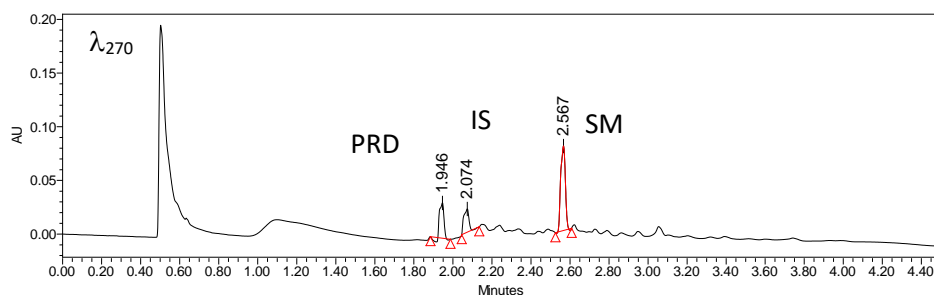
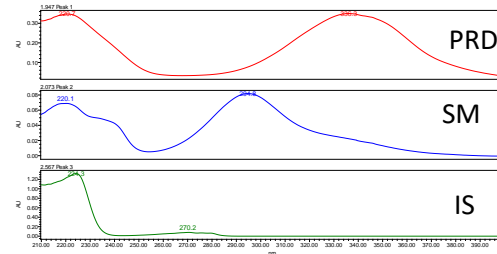
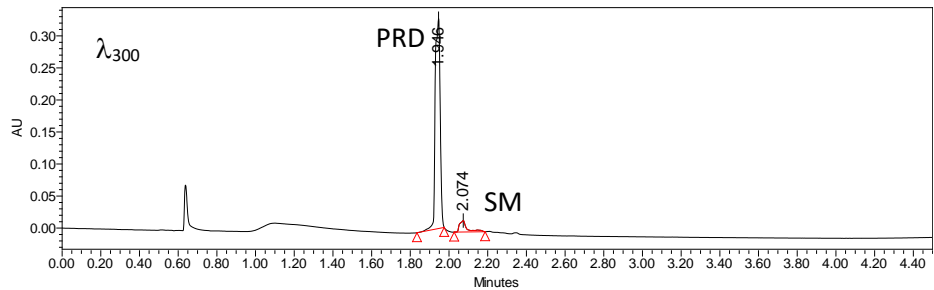


	Retention Time	Area	% Area	Height
1	2.378	383633	81.55	308926
2	2.957	86811	18.45	60584

Figure S15. Oxidative dearomatization of **19** by AfoD and AzaH. PDA traces of enzymatic reaction and control reaction. (Table 1, entry 6). Two wavelengths are shown to visualize product.

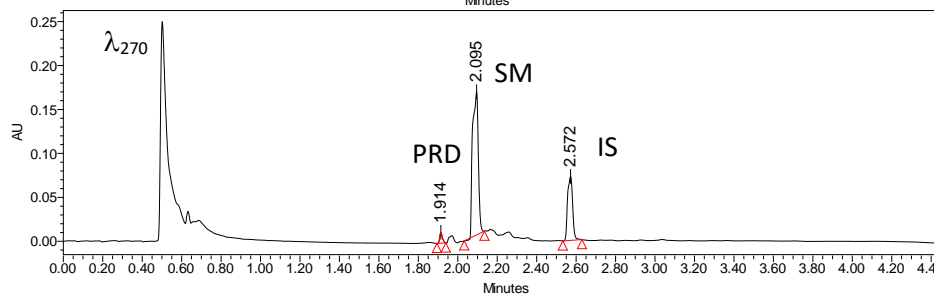
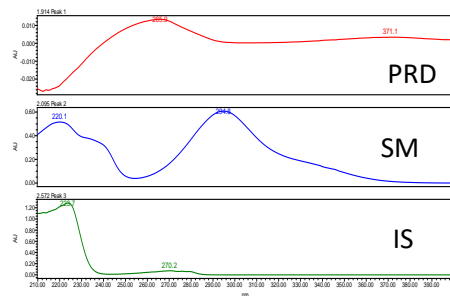
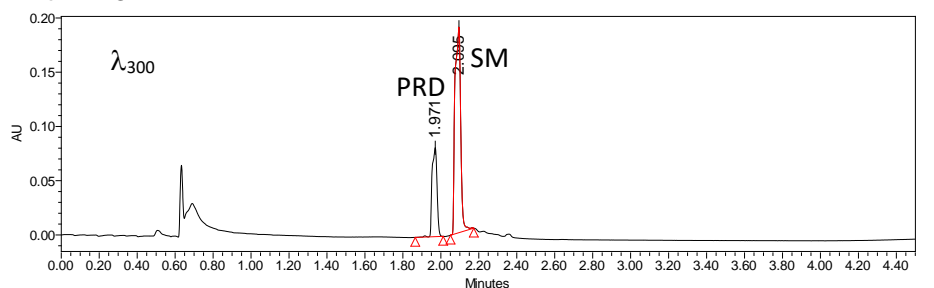


With AzaH



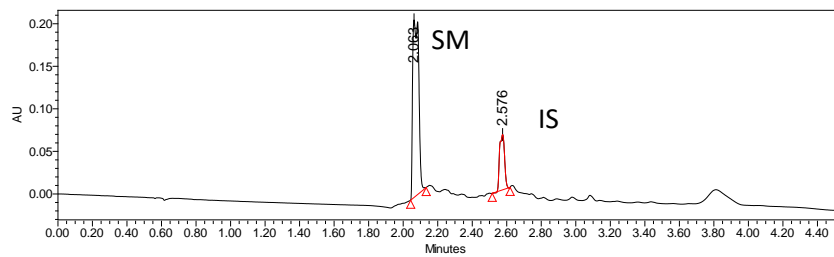
	Retention Time	Area	% Area	Height
1	1.946	59575	25.80	32920
2	2.074	40004	17.33	21701
3	2.567	131297	56.87	78806

With AfoD

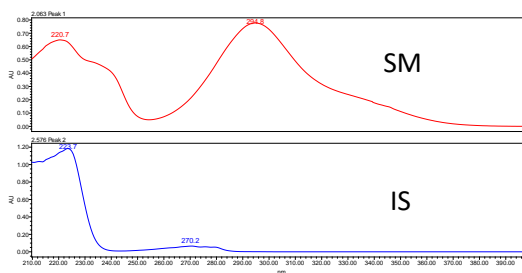


	Retention Time	Area	% Area	Height
1	1.946	59575	25.80	32920
2	2.074	40004	17.33	21701
3	2.567	131297	56.87	78806

NEC



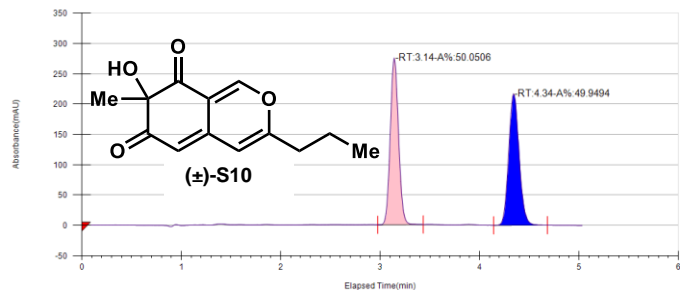
	Retention Time	Area	% Area	Height
1	2.063	507851	79.50	208715
2	2.576	130976	20.50	65081



Part IX. Determination of Enantiomeric Excess

Figure S16. PDA traces of racemic **S10** obtained from an IBX-mediated oxidative dearomatization, (*S*)-**S10** obtained from AfoD-mediated oxidative dearomatization, (*R*)-**S10** obtained from AzaH-mediated oxidative dearomatization, and **S10** obtained from AfoD Y118F mediated oxidative dearomatization (CHIRALPAK® AD-H, 30%, CO₂, 3.5 mL/min).

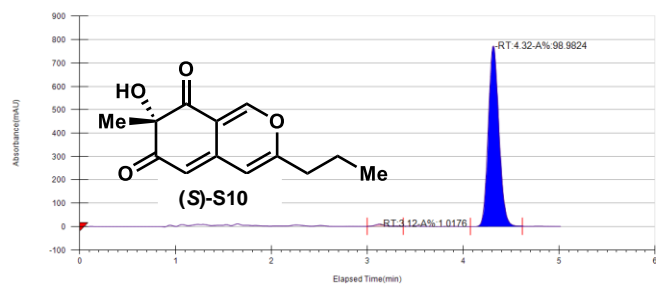
Racemic standard



Instrument method	Inj. Vol.	Solvent	Column	Sample	Temp.	Flow	% Modifier	Pressure
AD-H_30%_300-330	5	iPrOH	AD-H Chiral Analytical	sbdlV-087-rac	40	3.5	30	120

Peak No	% Area	Ret. Time	Cap Factor
1	50.0506	3.14 min	0
2	49.9494	4.34 min	0

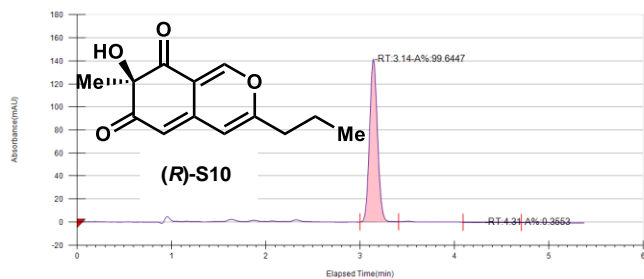
AfoD Reaction



Instrument method	Inj. Vol.	Solvent	Column	Sample	Temp.	Flow	% Modifier	Pressure
AD-H_30%_300-330	5	iPrOH	AD-H Chiral Analytical	sbdlV-087-AfoD	40	3.5	30	120

Peak No	% Area	Ret. Time	Cap Factor
1	1.0176	3.12 min	0
2	98.9824	4.32 min	0

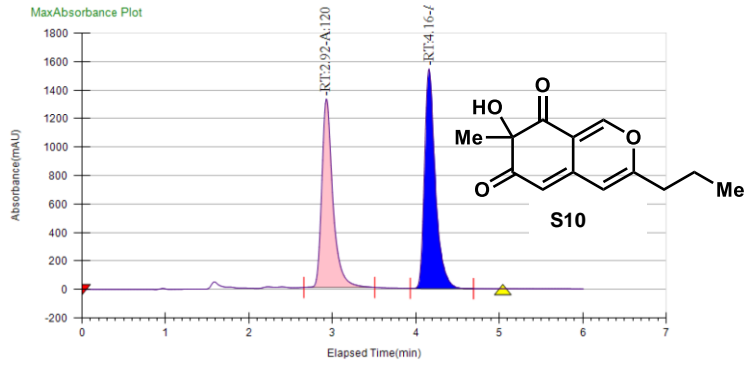
AzaH Reaction



Instrument method	Inj. Vol.	Solvent	Column	Sample	Temp.	Flow	% Modifier	Pressure
AD-H_30%_300-330	5	iPrOH	AD-H Chiral Analytical	sbdlV-087-rac	40	3.5	30	120

Peak No	% Area	Ret. Time	Cap Factor
1	99.6447	3.14 min	0
2	0.3553	4.31 min	0

AfoD Y118F reaction



Instrument Method	Inj. Vol.	Solvent	Column	Sample	Well Location	Temp. (C)	Flow (g/min)	% Modifier	Pressure (Bar)
AD-H_30%_300-330	6 uL	Isopropanol	AD-H	ARB-V-071 AfoD_1	12A	40	3.5	30	120

Peak No	% Area	Area	Ret. Time	Height	Cap. Factor
1	46.8333	12090.3845	2.92 min	1322.9644	0
2	53.1667	13725.3924	4.16 min	1541.5059	0

Figure S17. PDA traces of racemic **18** obtained from a 1:1 mixture of the compound generated using AzaH and AfoD, (*S*)-**18** obtained from AfoD-mediated oxidative dearomatization, (*R*)-**18** obtained from AzaH-mediated oxidative dearomatization (CHIRALPAK® AD-H, 30%, CO₂, 3.5 mL/min).

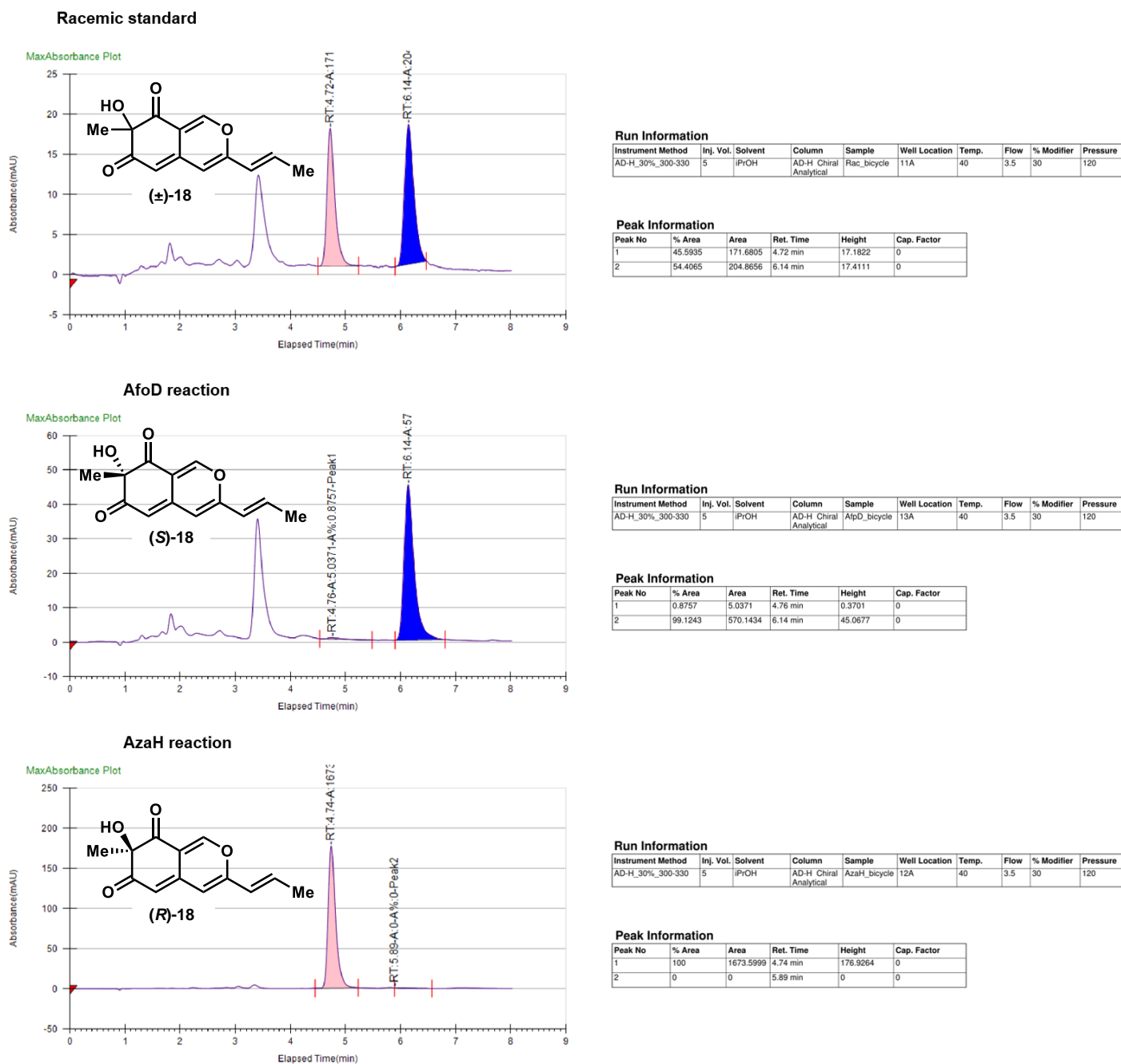
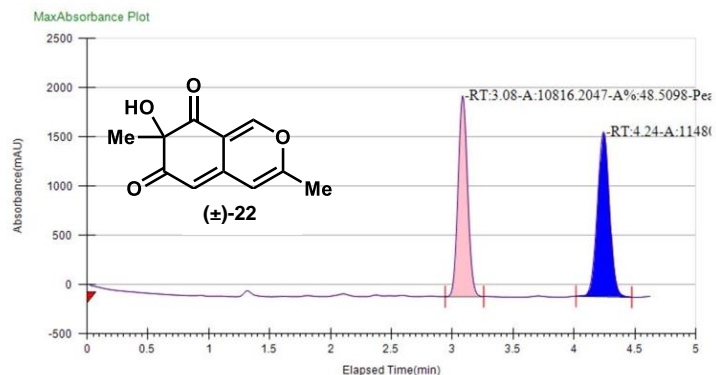


Figure S18. PDA traces of racemic **22** obtained from an IBX-mediated oxidative dearomatization, (*S*)-**22** obtained from AfoD-mediated oxidative dearomatization, (*R*)-**22** obtained from AzaH-mediated oxidative dearomatization (CHIRALPAK® AD-H, 30%, CO₂, 3.5 mL/min).

Racemic standard



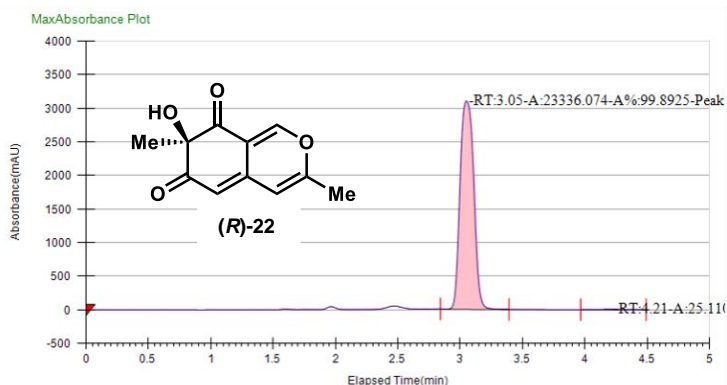
Run Information

Instrument Method	Inj. Vol.	Solvent	Column	Sample	Well Location	Temp.	Flow	% Modifier	Pressure
AD-H_30%-300-330	5	iPrOH	AD-H Chiral Analytical	sbdlV-174_30%	12A	40	3.5	30	120

Peak Information

Peak No	% Area	Area	Ret. Time	Height	Cap. Factor
1	48.5098	10816.2047	3.08 min	2038.3863	3082.3
2	51.4902	11480.7275	4.24 min	1675.0946	4240.6167

AzaH reaction



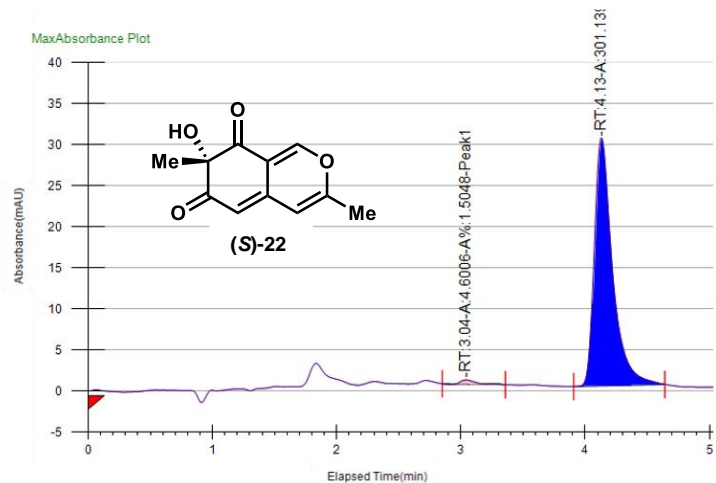
Run Information

Instrument Method	Inj. Vol.	Solvent	Column	Sample	Well Location	Temp.	Flow	% Modifier	Pressure
AD-H_30%-300-330	10	iPrOH	AD-H Chiral Analytical	sbdlV-108_30iPrOH	12A	40	3.5	30	120

Peak Information

Peak No	% Area	Area	Ret. Time	Height	Cap. Factor
1	99.8925	23336.074	3.05 min	3103.1264	3049.0167
2	0.1075	25.1102	4.21 min	2.823	4207.35

AfoD reaction



Run Information

Instrument Method	Inj. Vol.	Solvent	Column	Sample	Well Location	Temp.	Flow	% Modifier	Pressure
AD-H_30%-300-330	10	iPrOH	AD-H Chiral Analytical	JBP-3-169-AfoD	13A	40	3.5	30	120

Peak Information

Peak No	% Area	Area	Ret. Time	Height	Cap. Factor
1	1.5048	4.6006	3.04 min	0.51	0
2	98.4952	301.1399	4.13 min	30.1492	0

Run Information

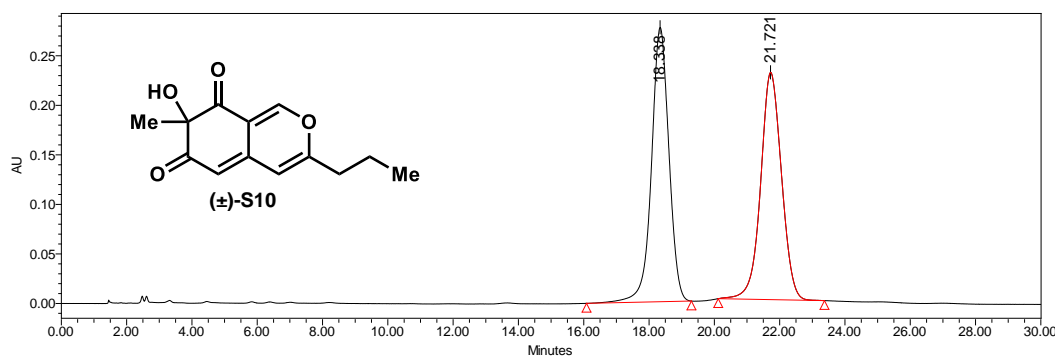
Instrument Method	Inj. Vol.	Solvent	Column	Sample	Well Location	Temp.	Flow	% Modifier	Pressure
AD-H_10%	1	iPrOH	AD-H Chiral Analytical	sbdVIII-120	11A	40	3.5	10	120

Peak Information

Peak No	% Area	Area	Ret. Time	Height	Cap. Factor
1	99.781	55.3487	1.54 min	12.5858	0
2	0.219	0.1215	1.99 min	0.0203	0

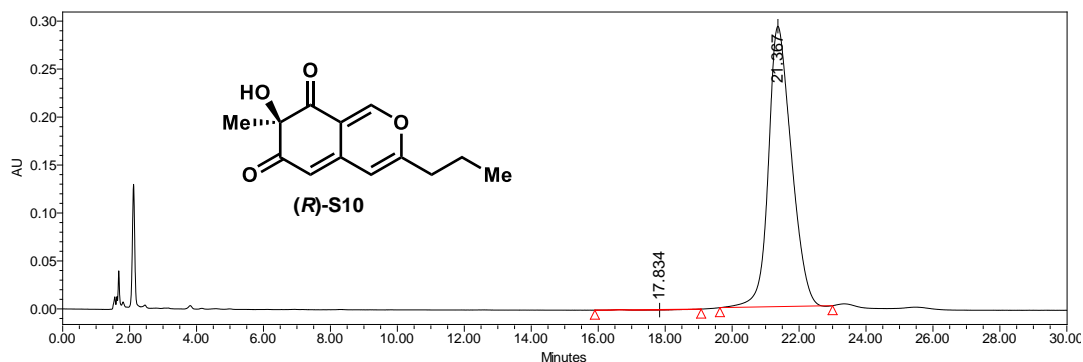
Figure S20. PDA traces of racemic **S10** obtained from an IBX-mediated oxidative dearomatization, (*R*)-**S10** obtained from FDMO-2 and FDMO-5-mediated oxidative dearomatization, and (*S*)-**S10** obtained from FDMO-6-mediated oxidative dearomatization (Phenomenex Lux Cellulose, 25% MeCN, 75% H₂O, 1 mL/min).

Racemic standard



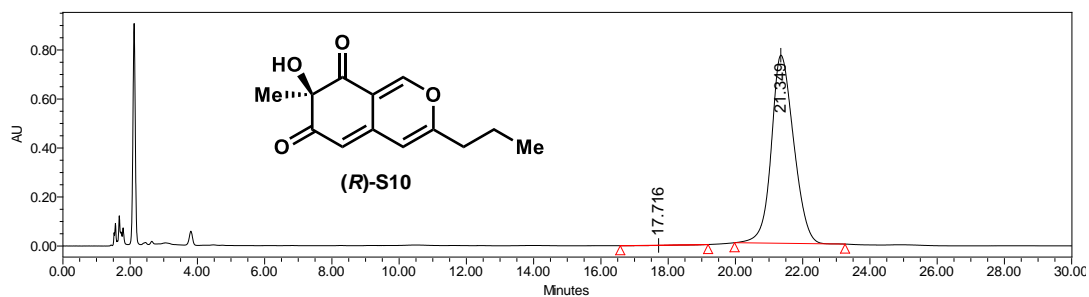
Name	Retention Time	Area	% Area	Height
1	18.341	13429370	50.10	362068
2	21.724	13377480	49.90	300570

FDMO-2 reaction



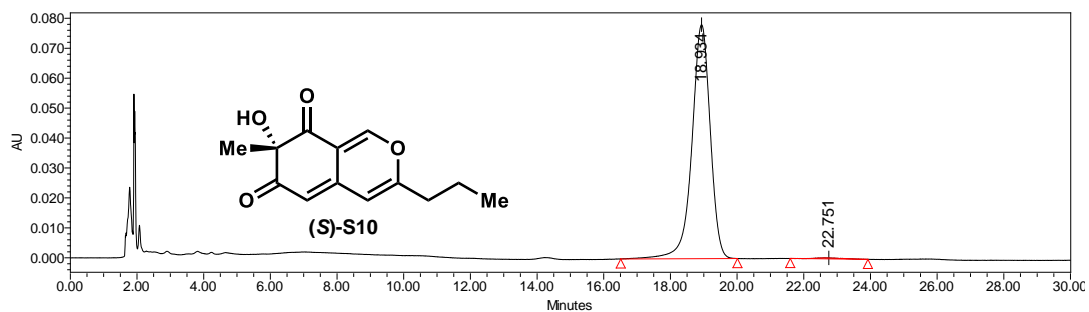
Name	Retention Time	Area	% Area	Height
1	17.860	229964	0.45	-2129
2	21.365	51102440	99.55	1059976

FDMO-5 reaction



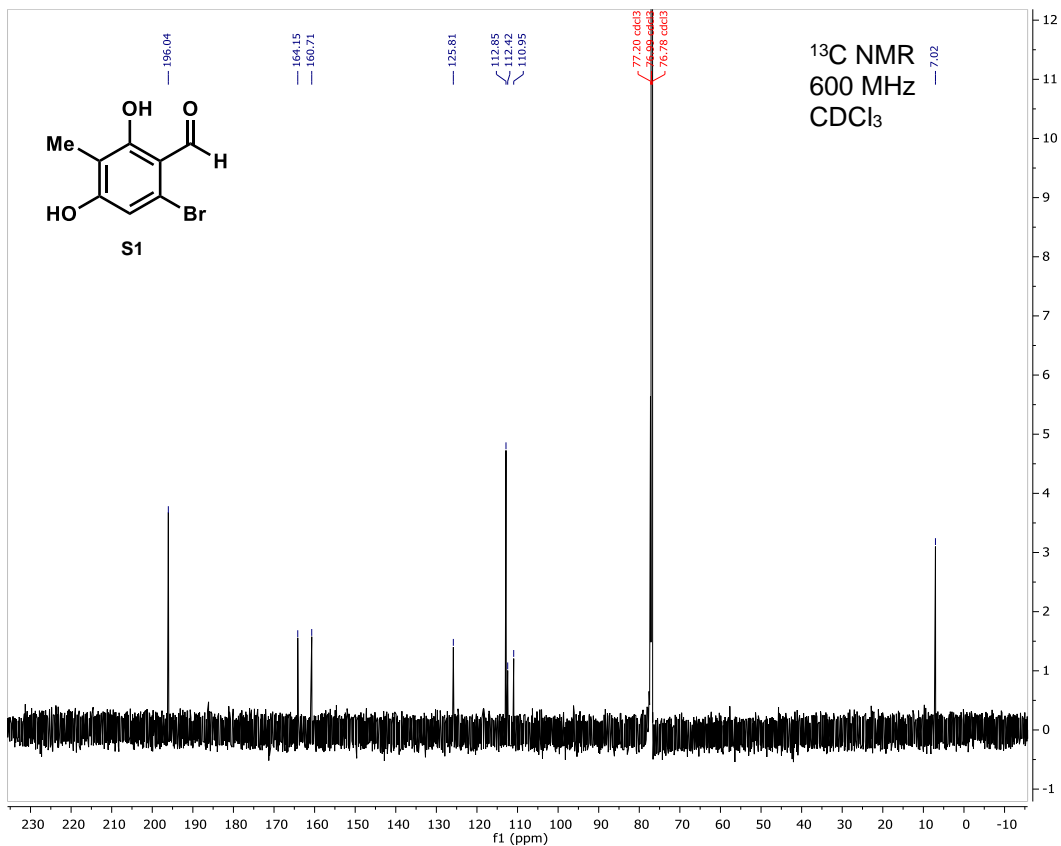
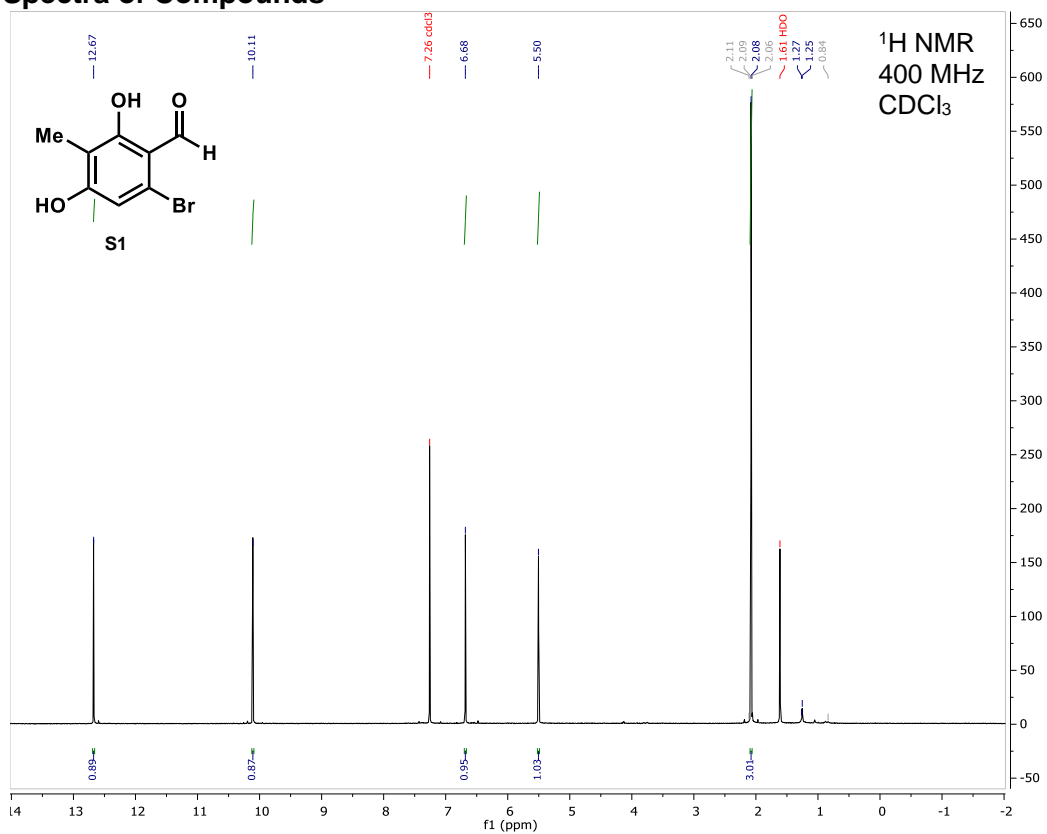
Name	Retention Time	Area	% Area	Height
1	18.829	149446	0.42	-2017
2	21.349	35753101	99.58	769344

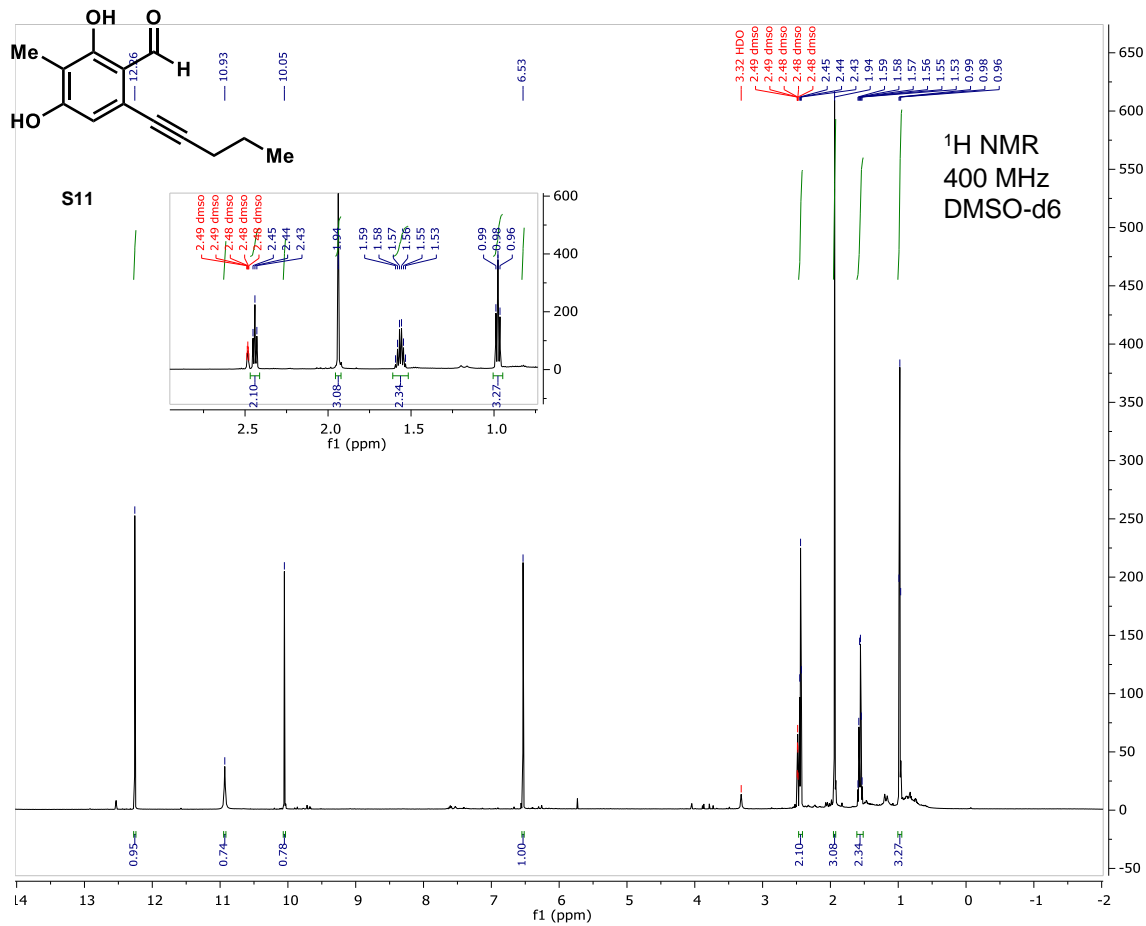
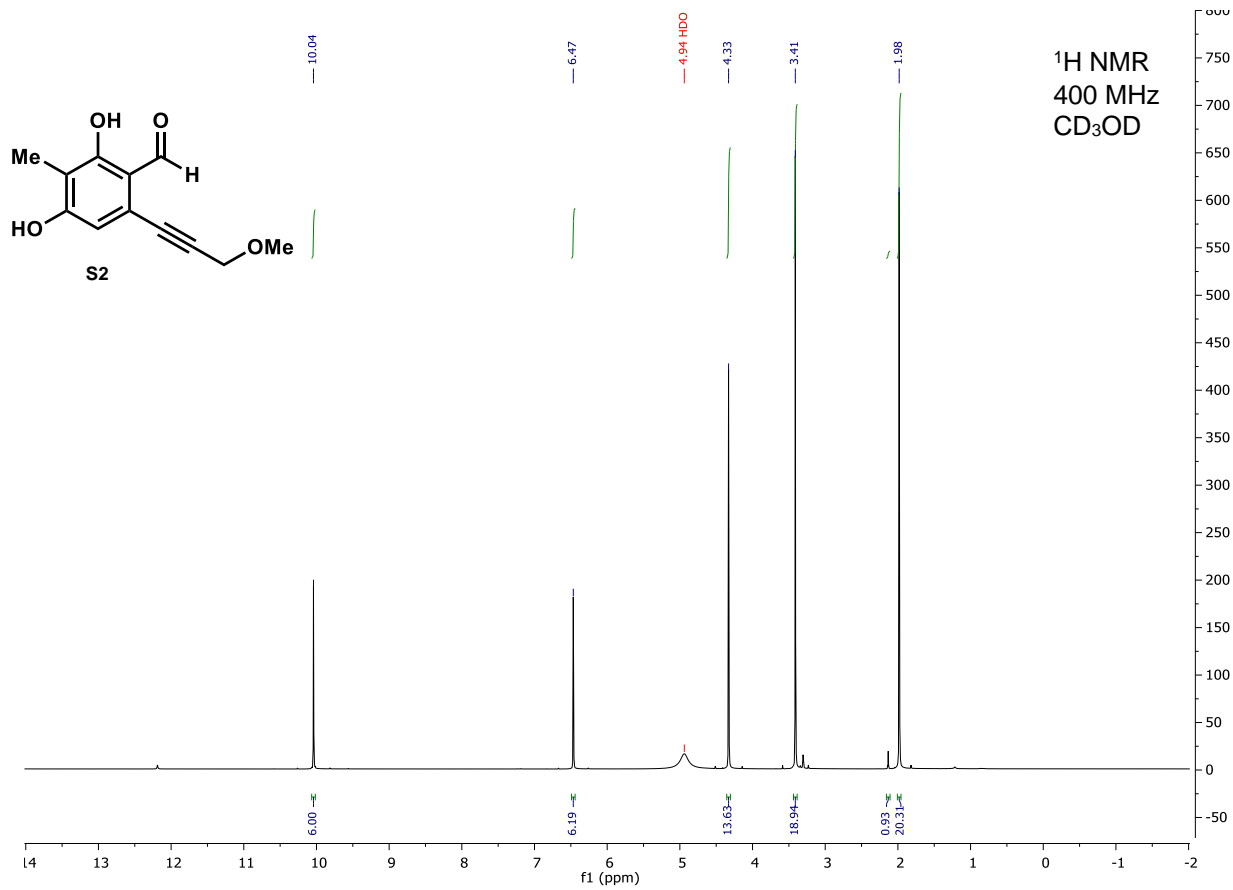
FDMO-6 reaction

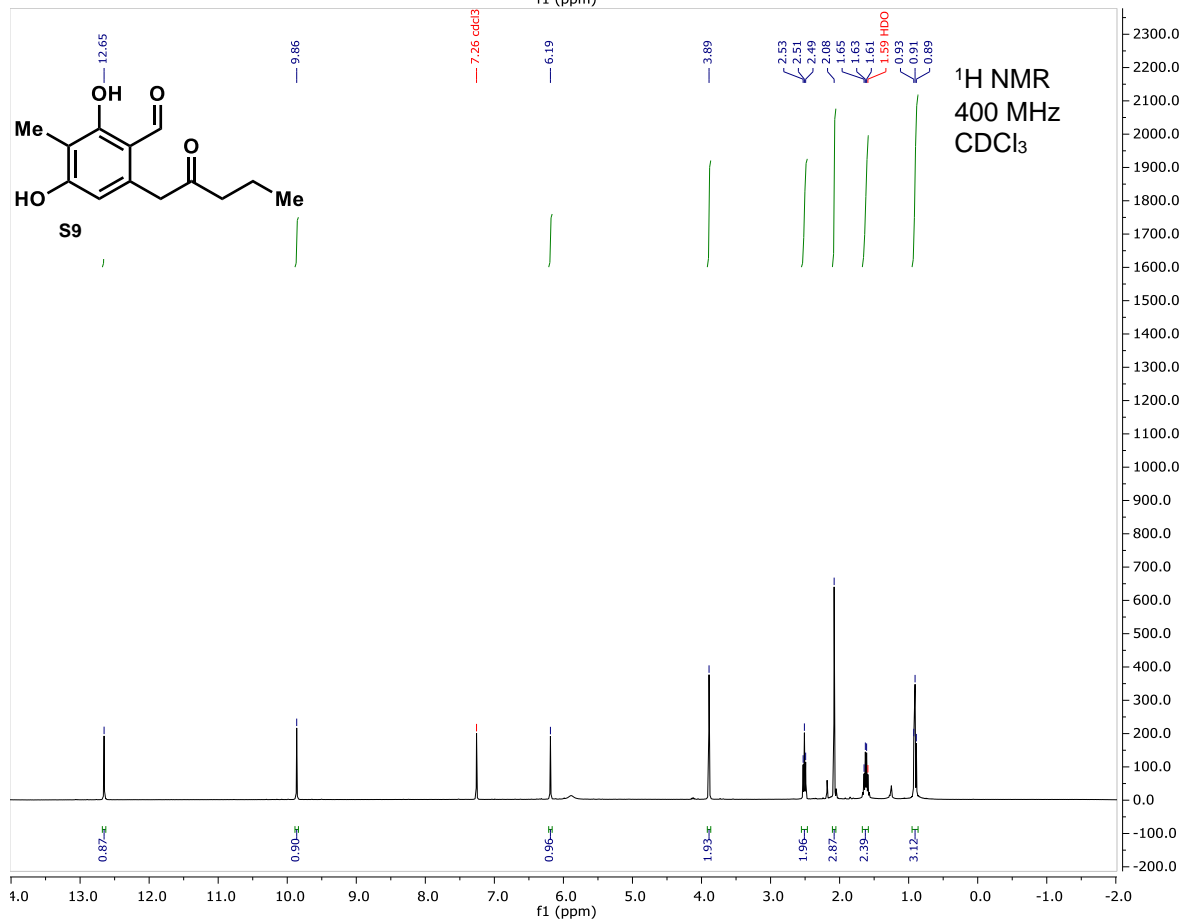
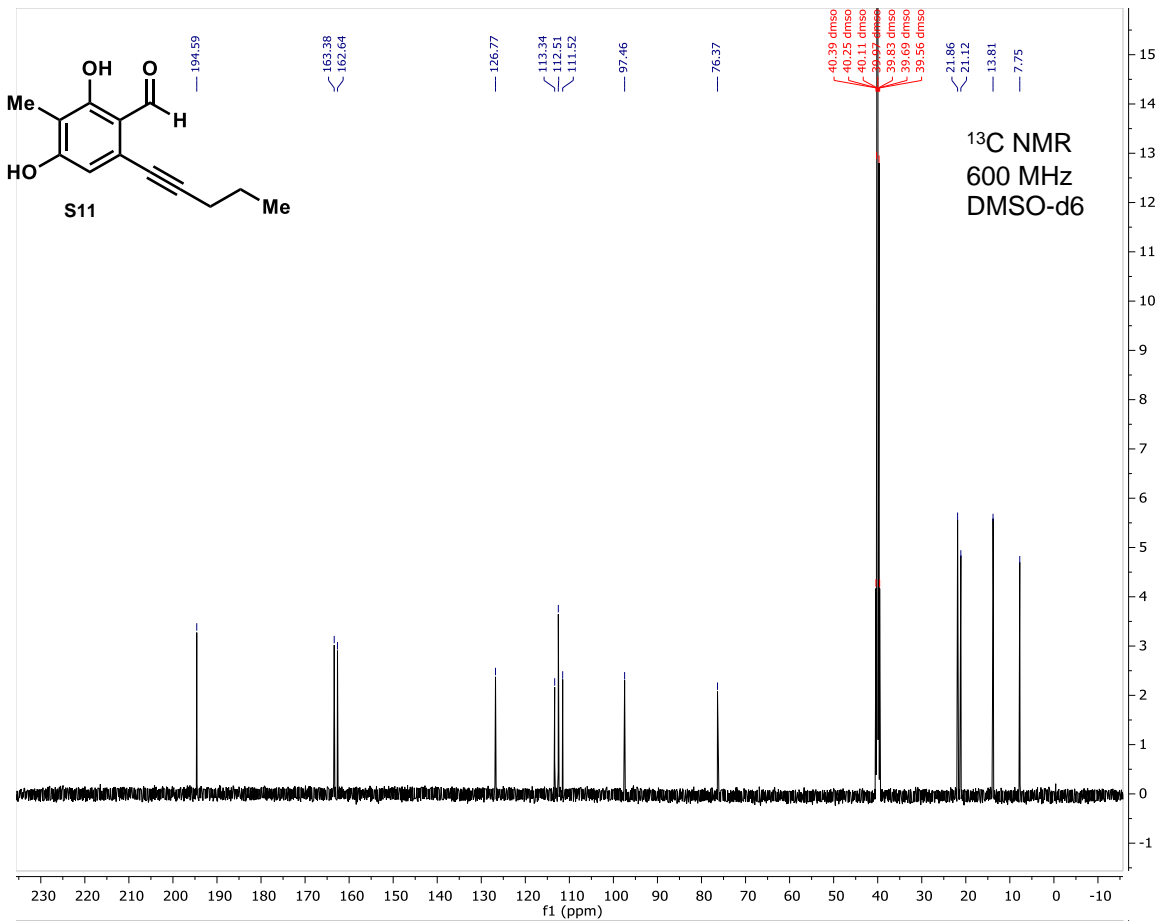


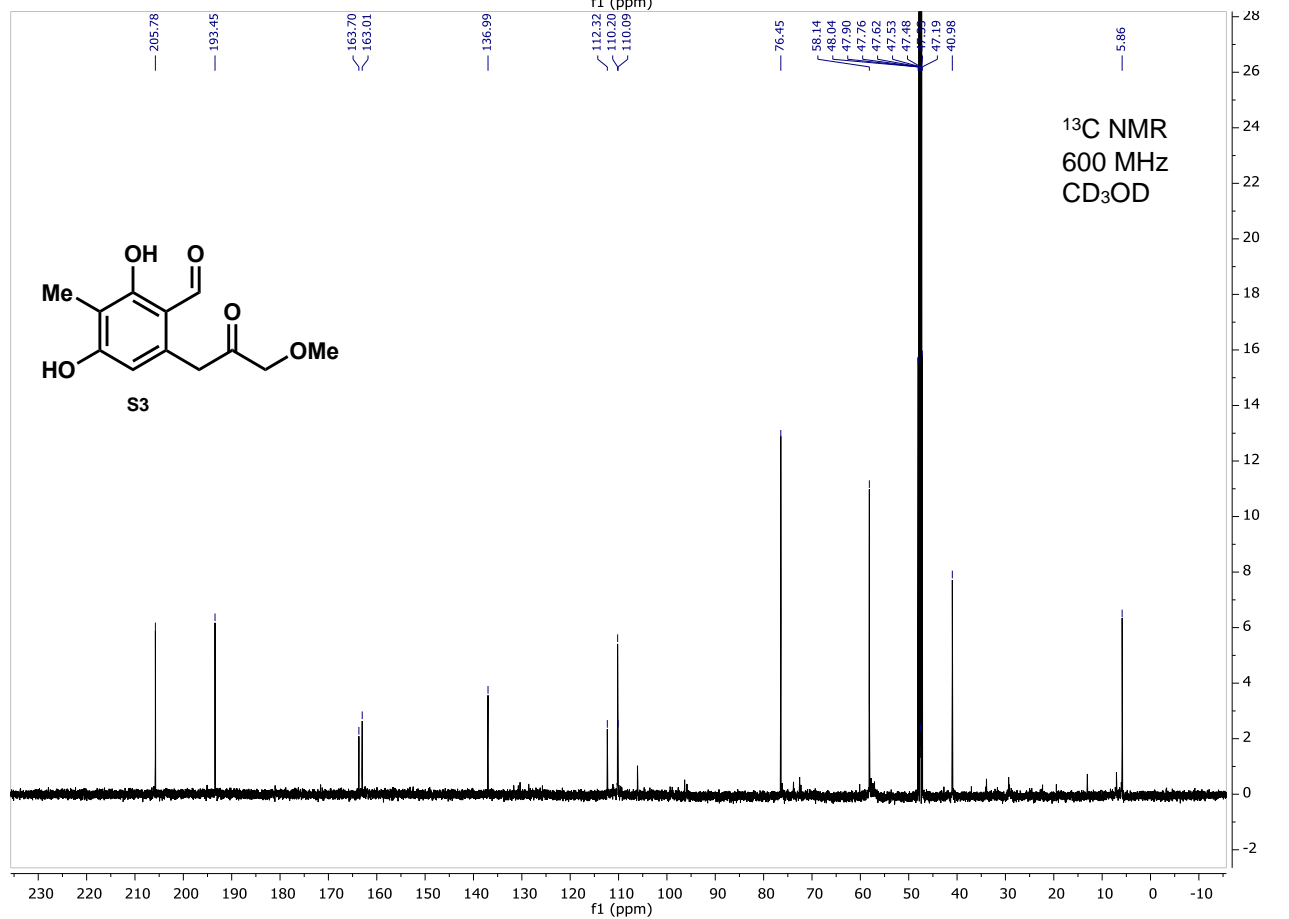
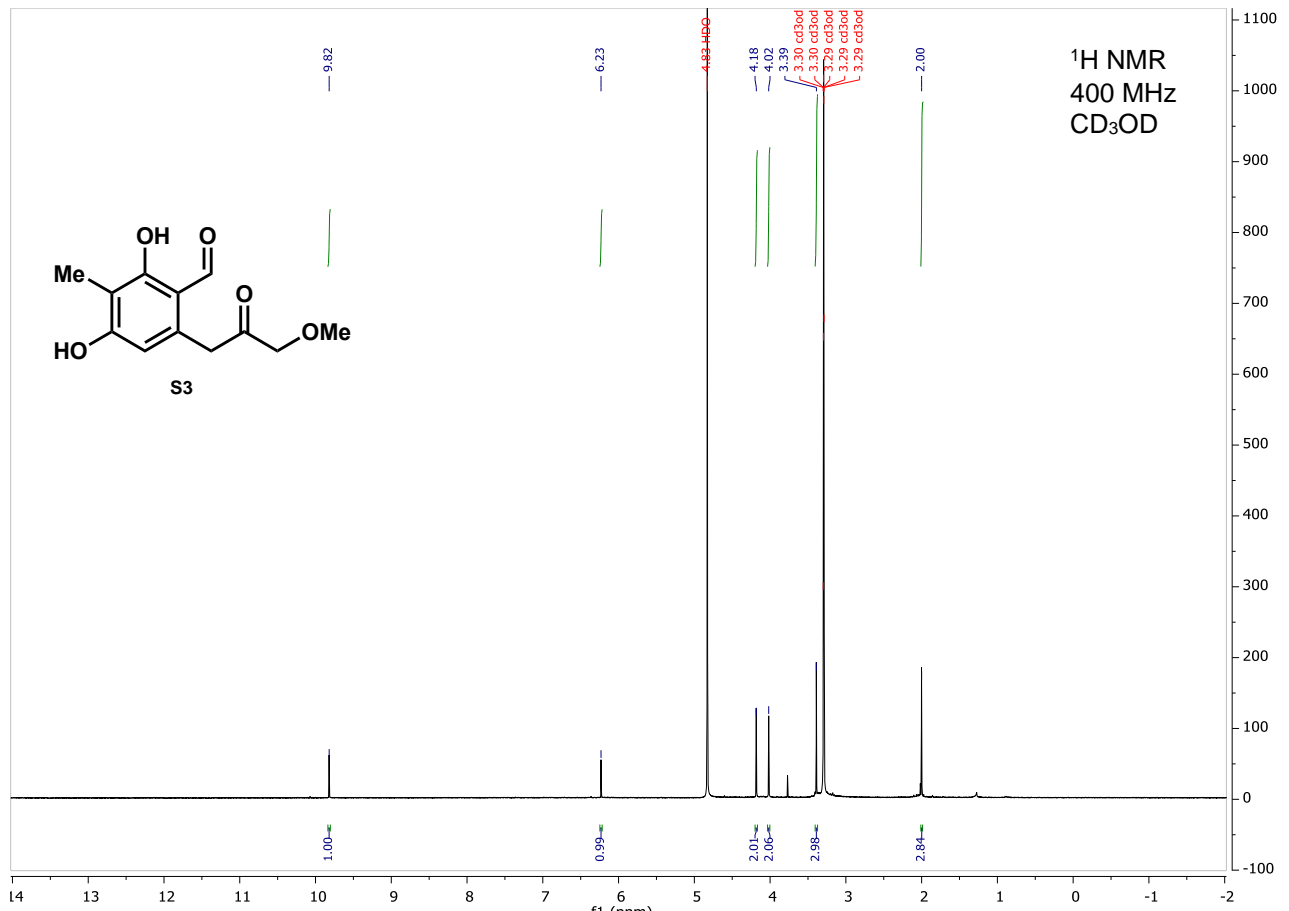
Name	Retention Time	Area	% Area	Height
1	18.934	3146288	99.83	83349
2	22.126	5282	0.17	-105

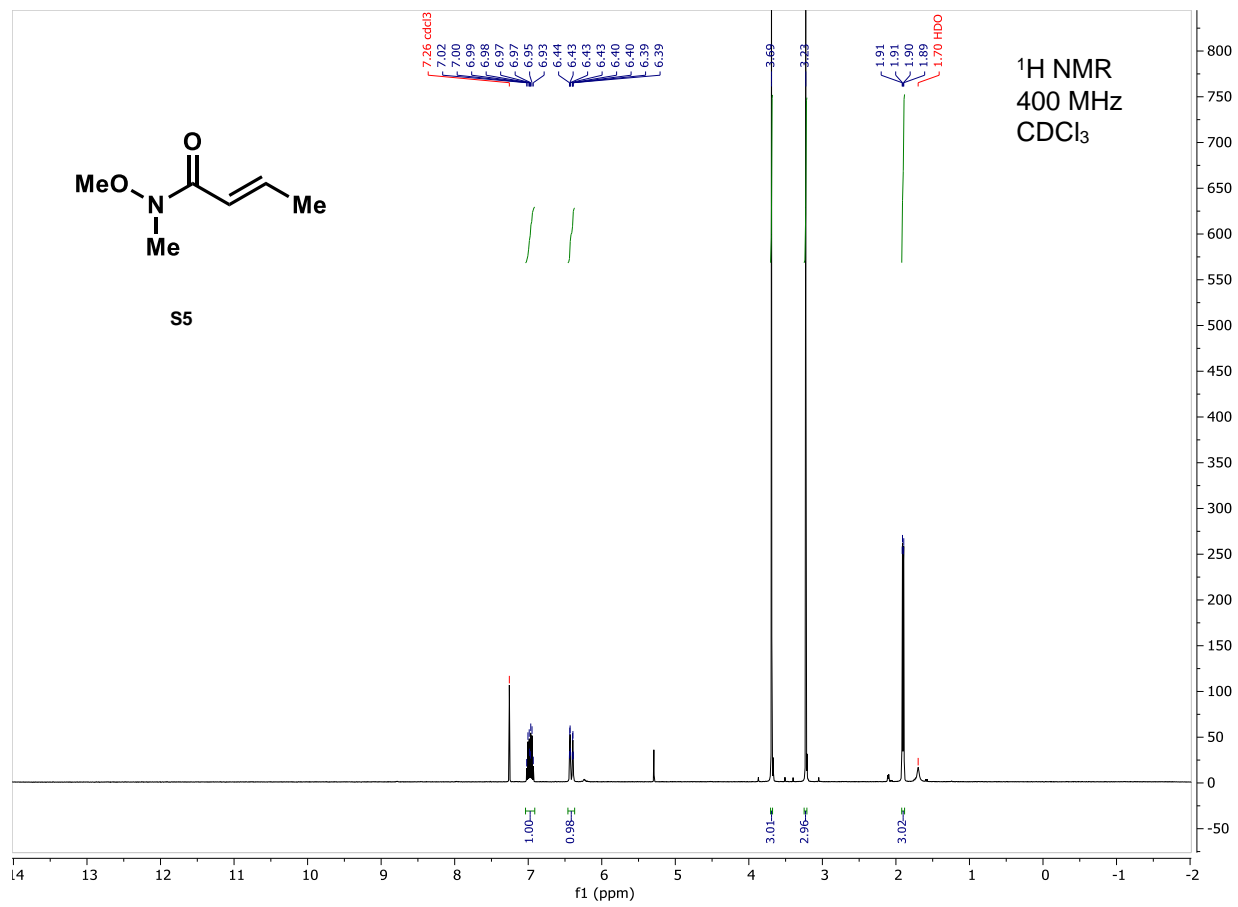
Part X. NMR Spectra of Compounds

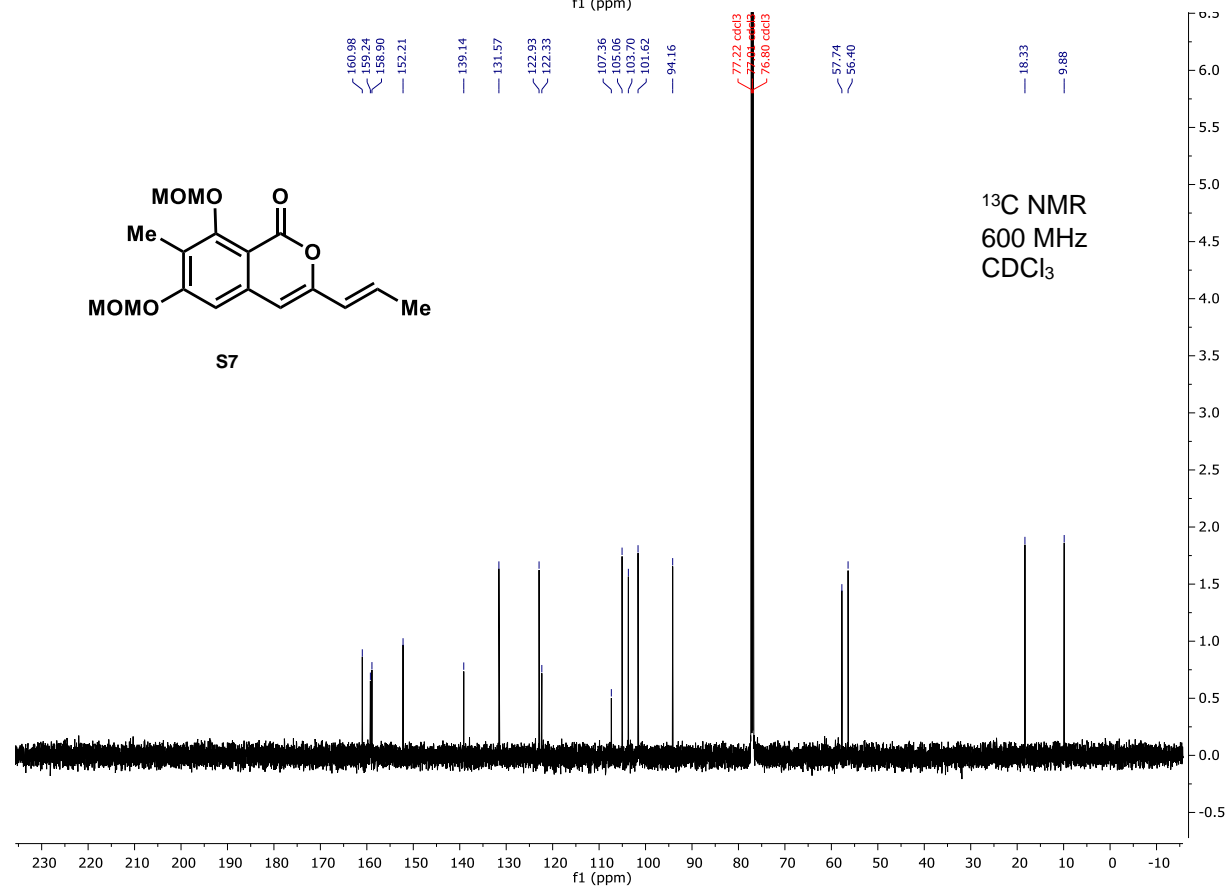
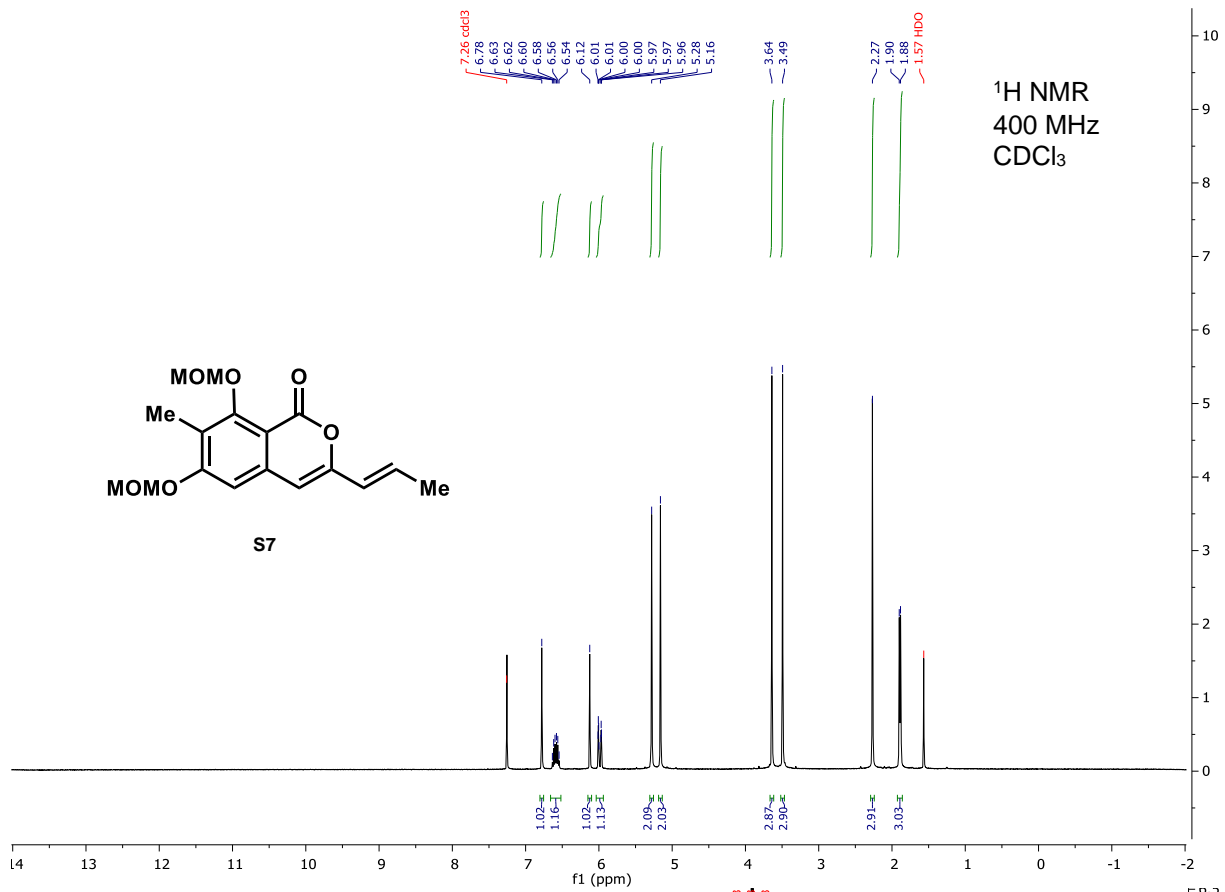


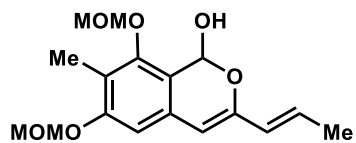




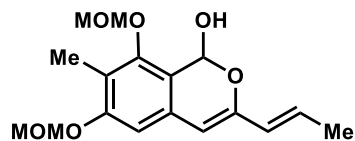
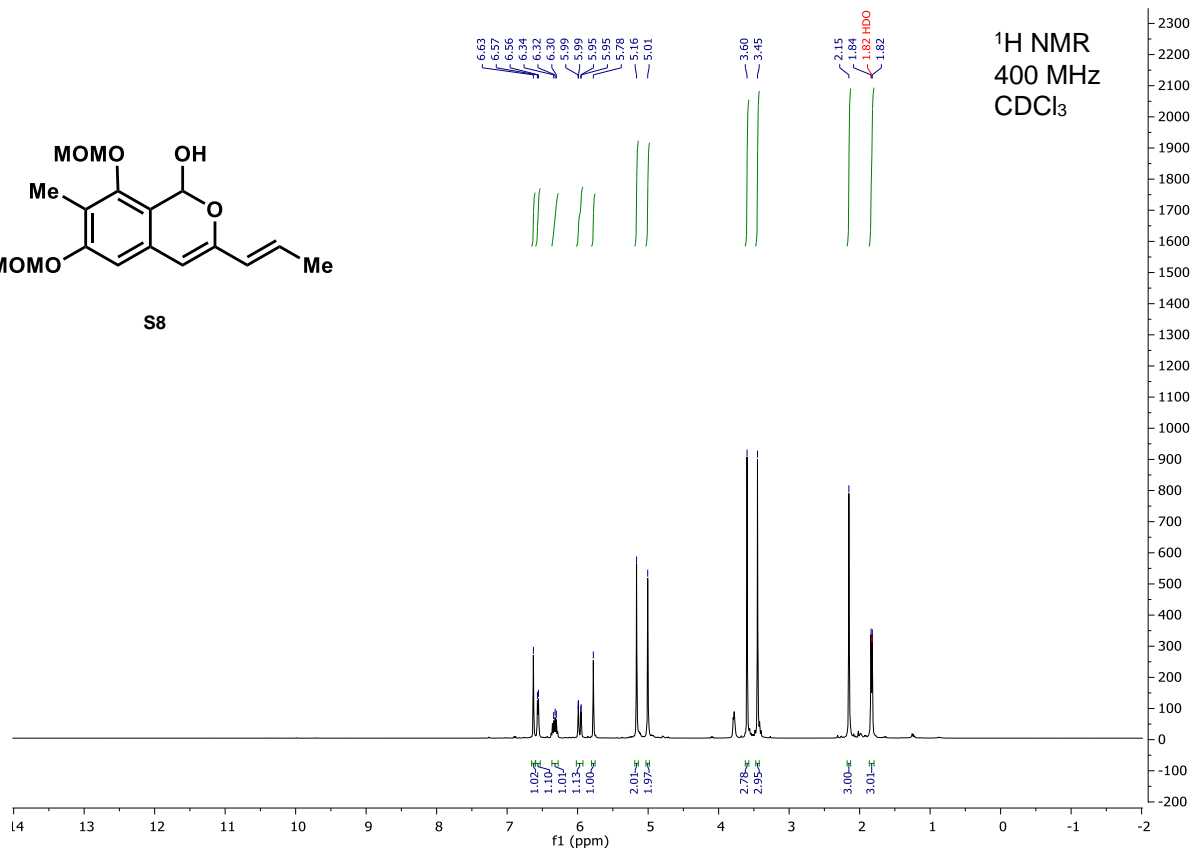




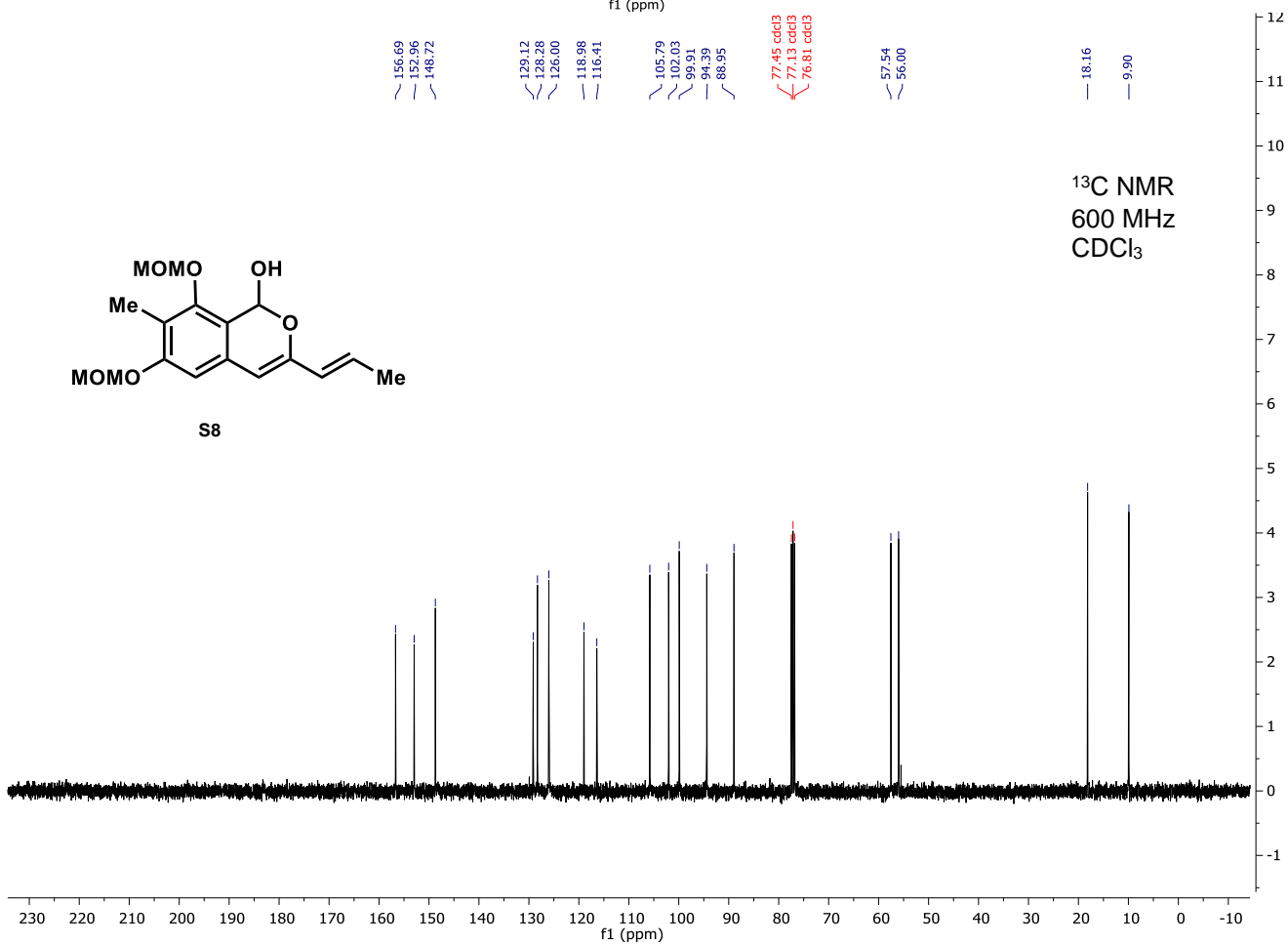


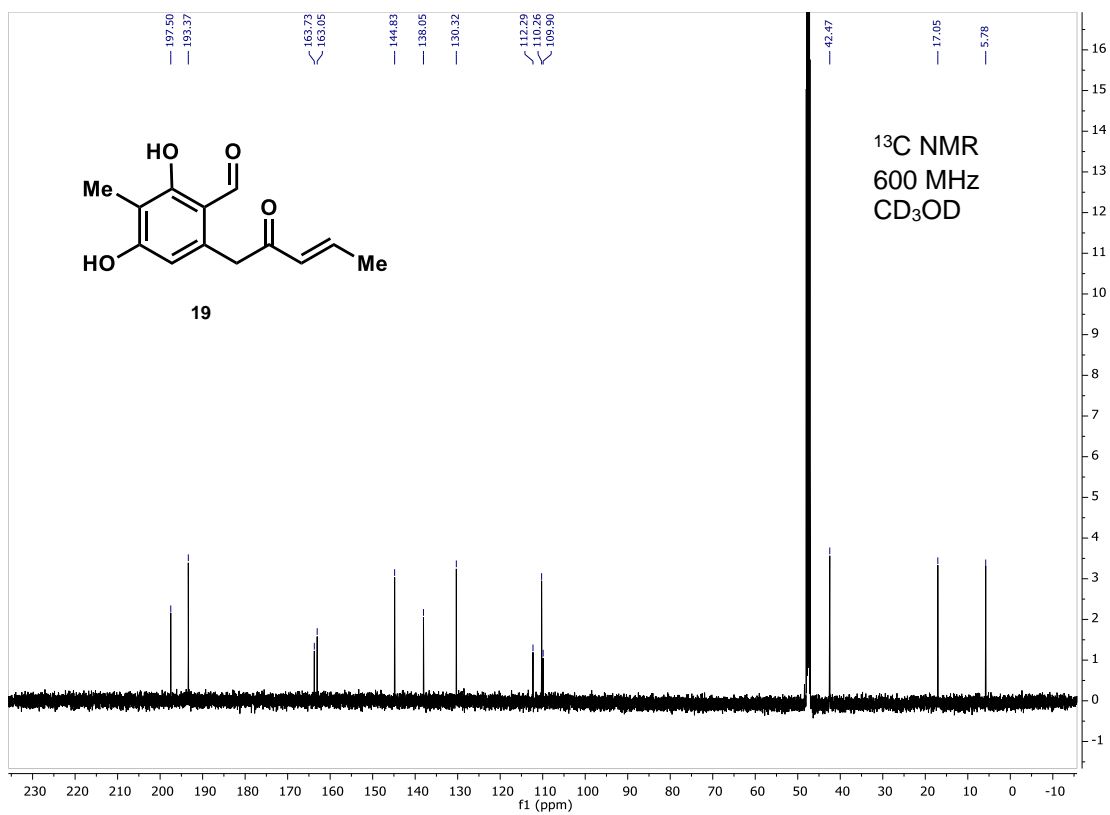
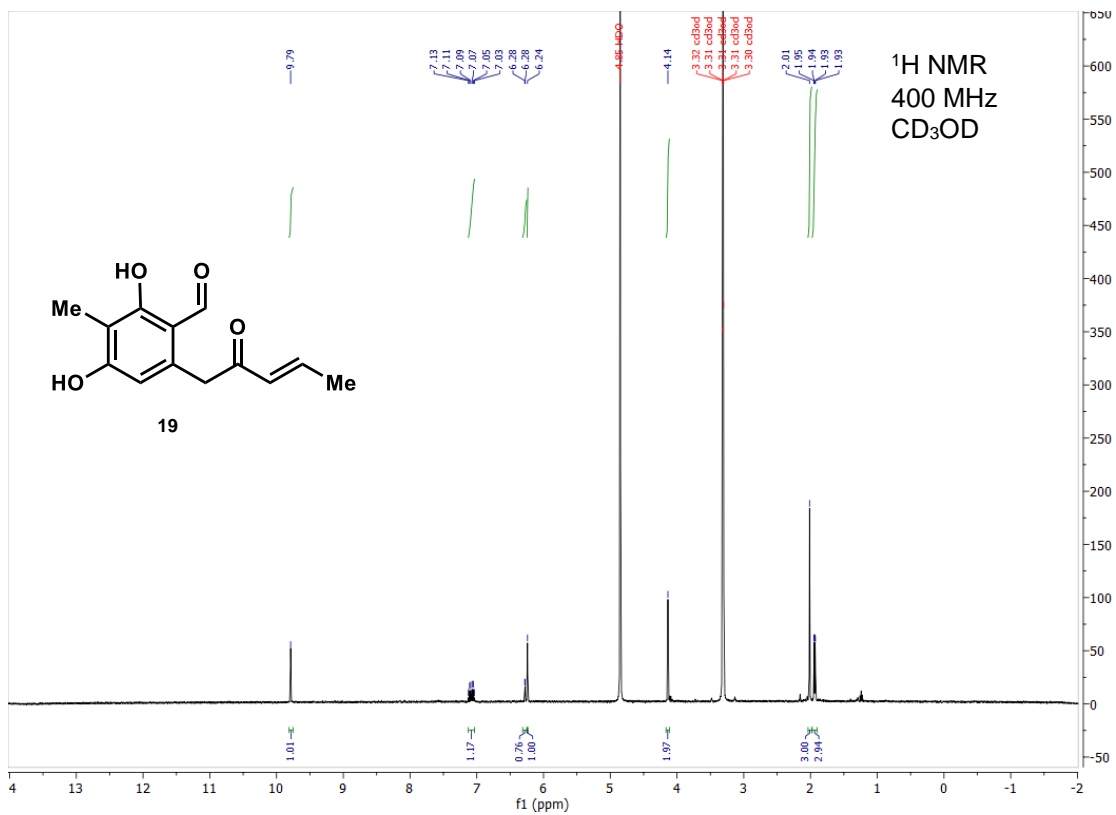


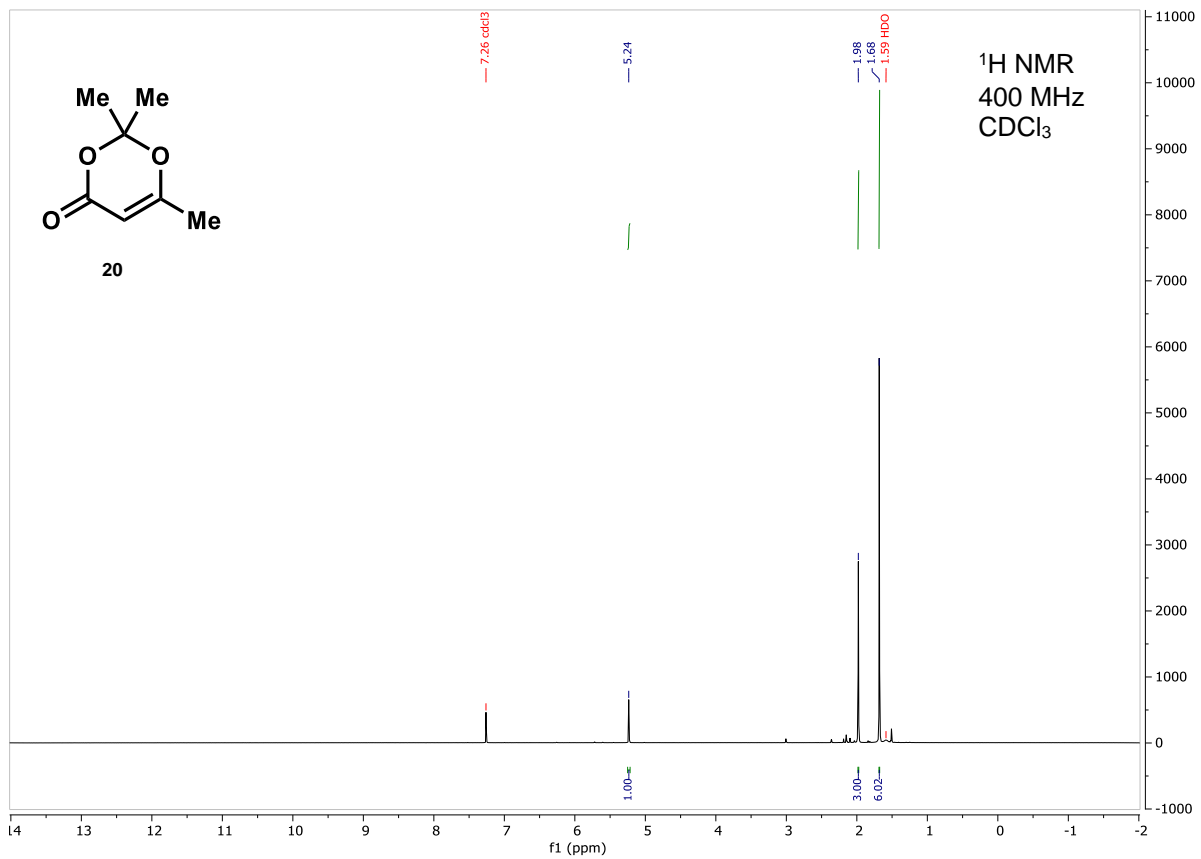
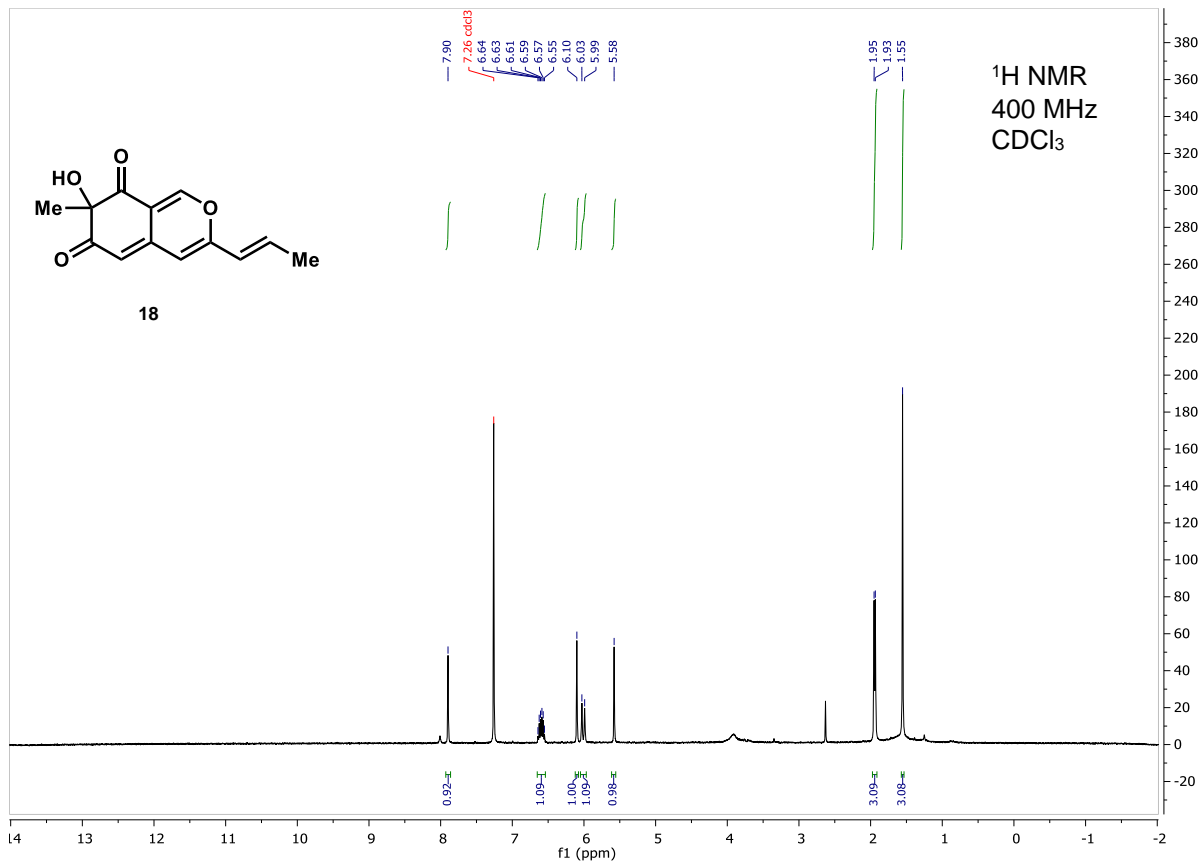
S8

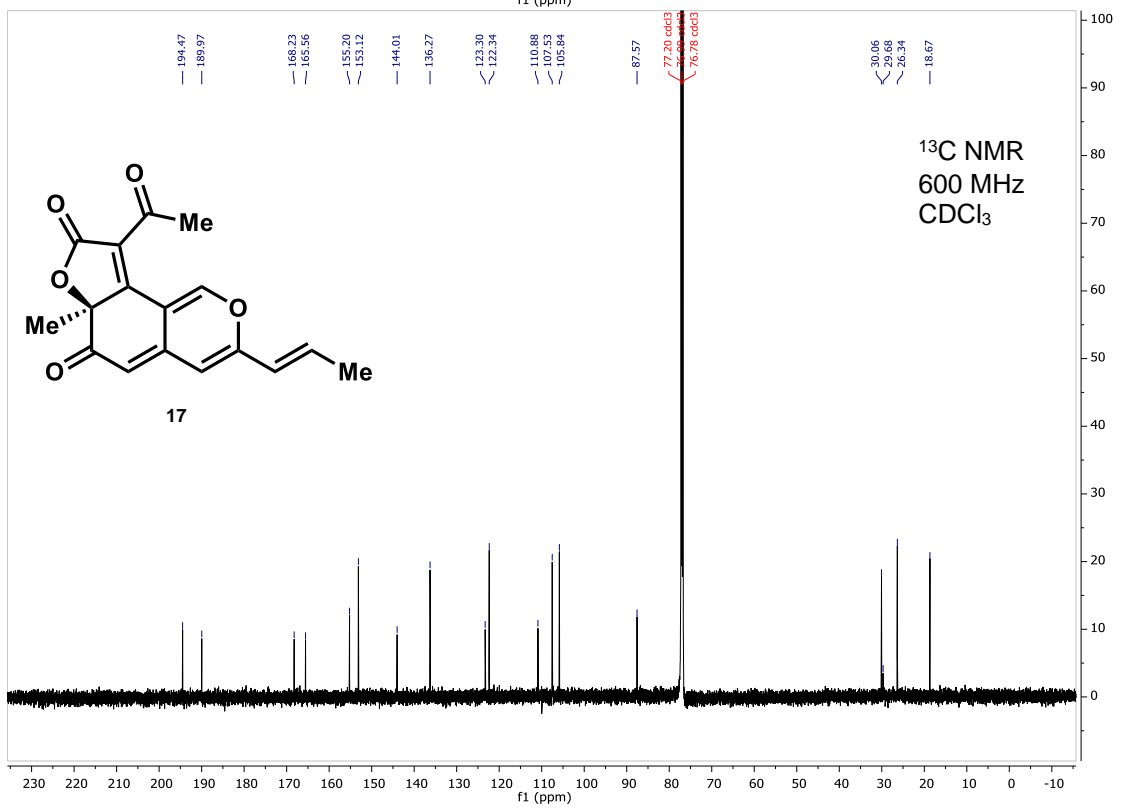


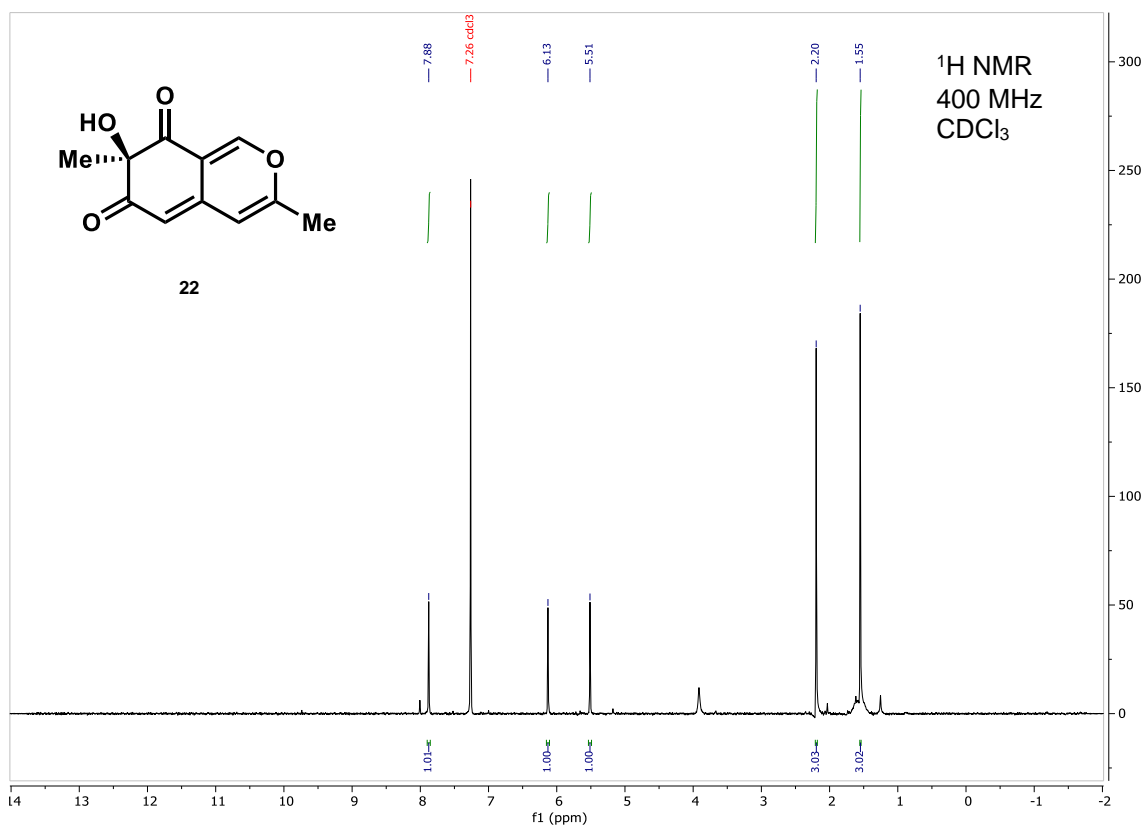
S8

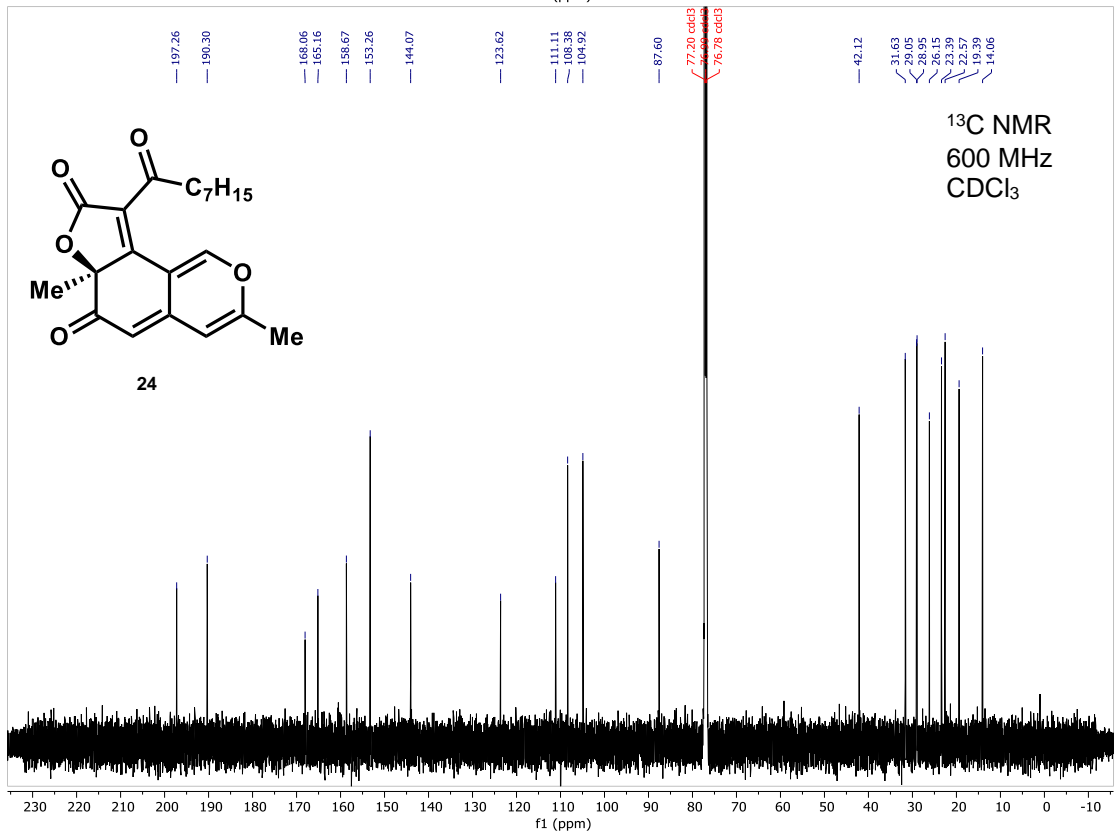
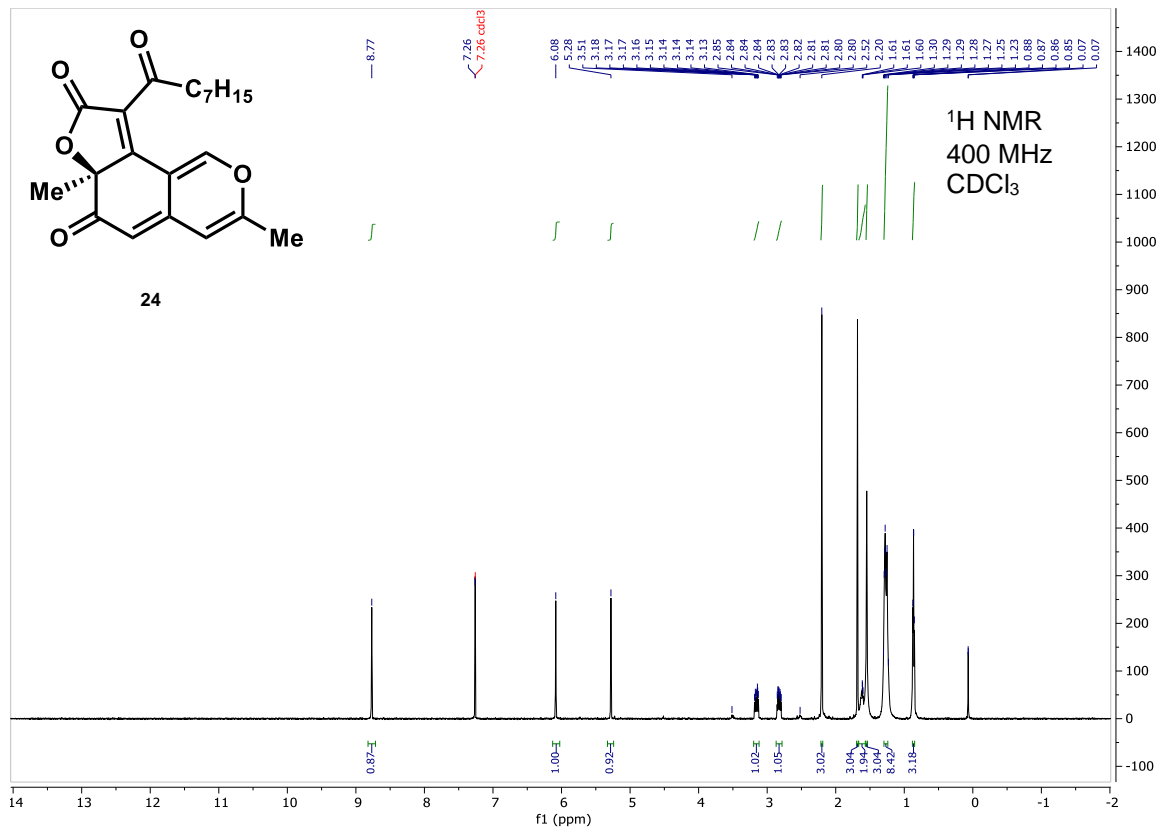


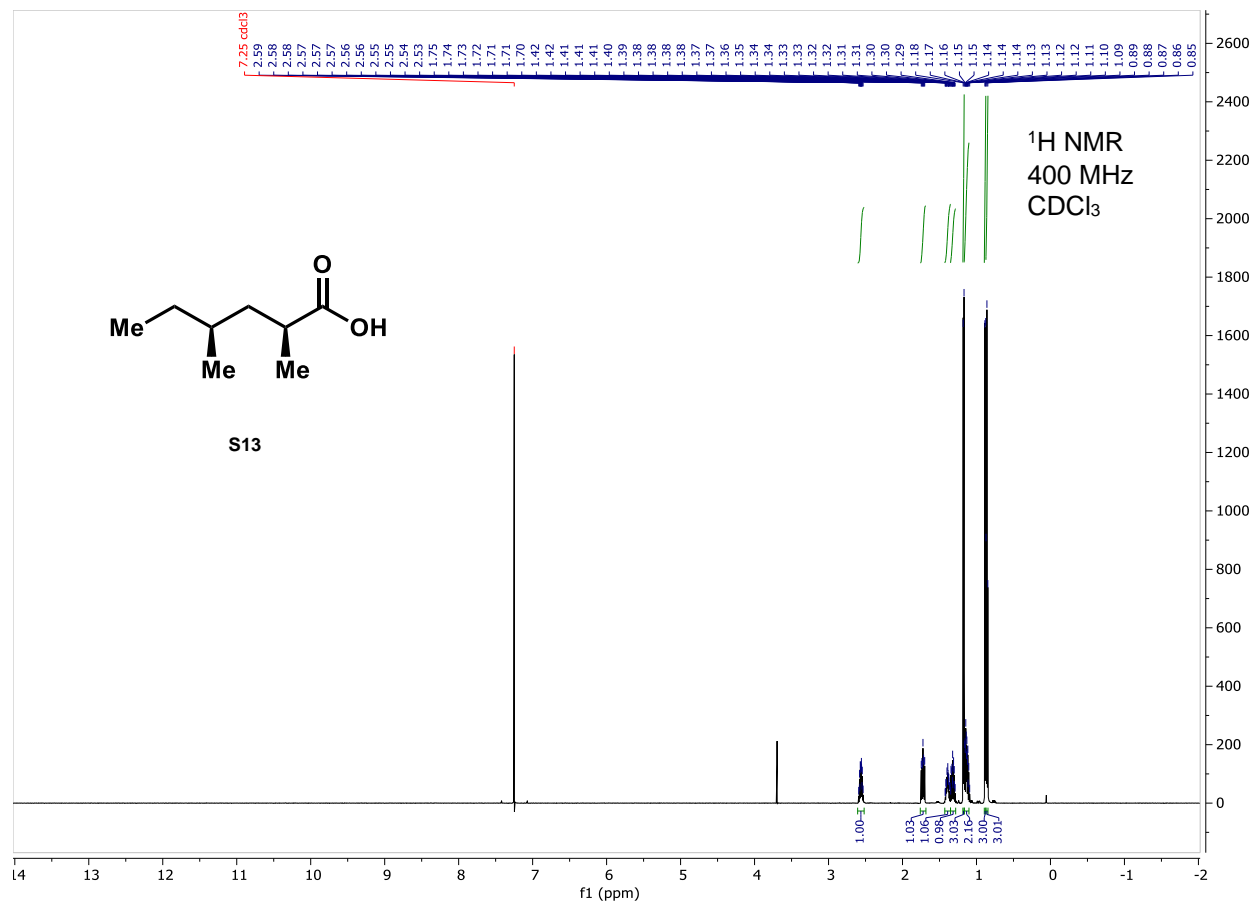


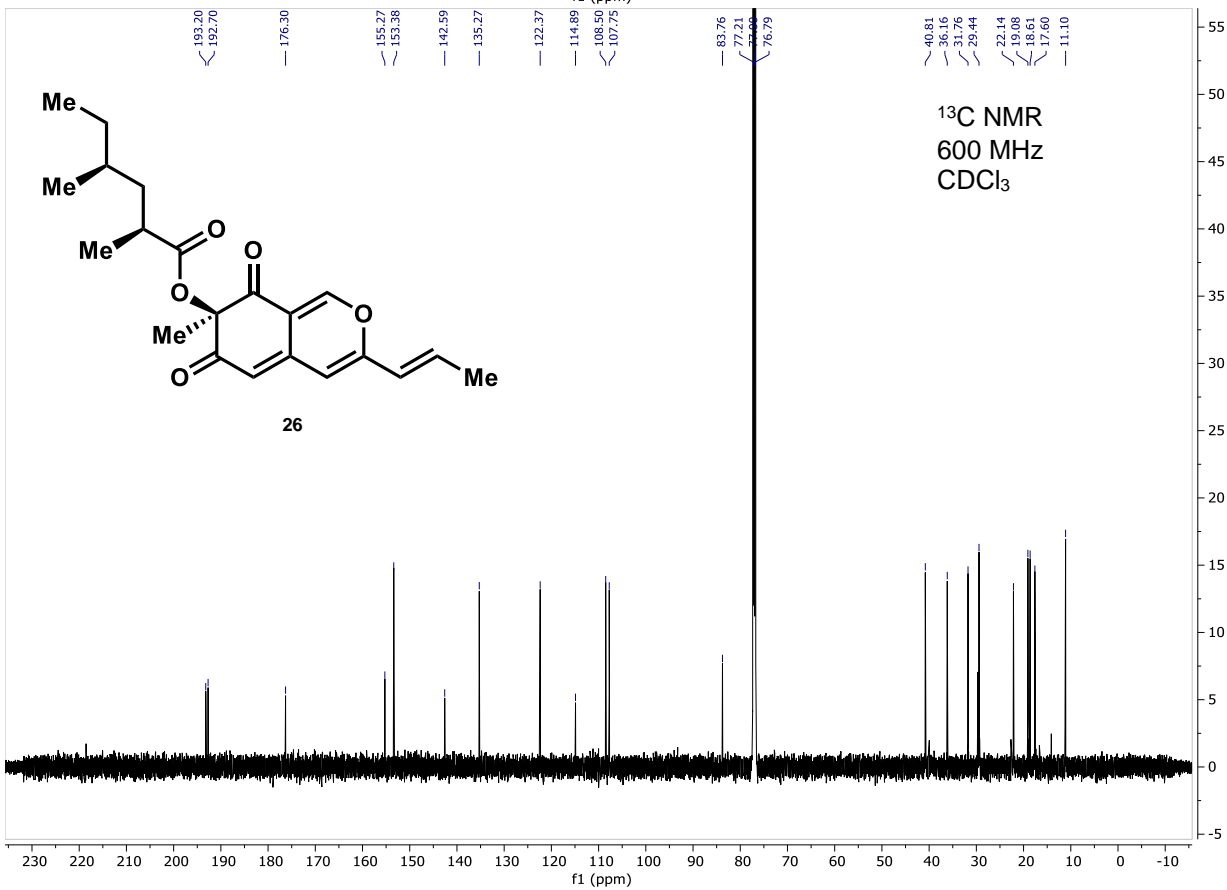
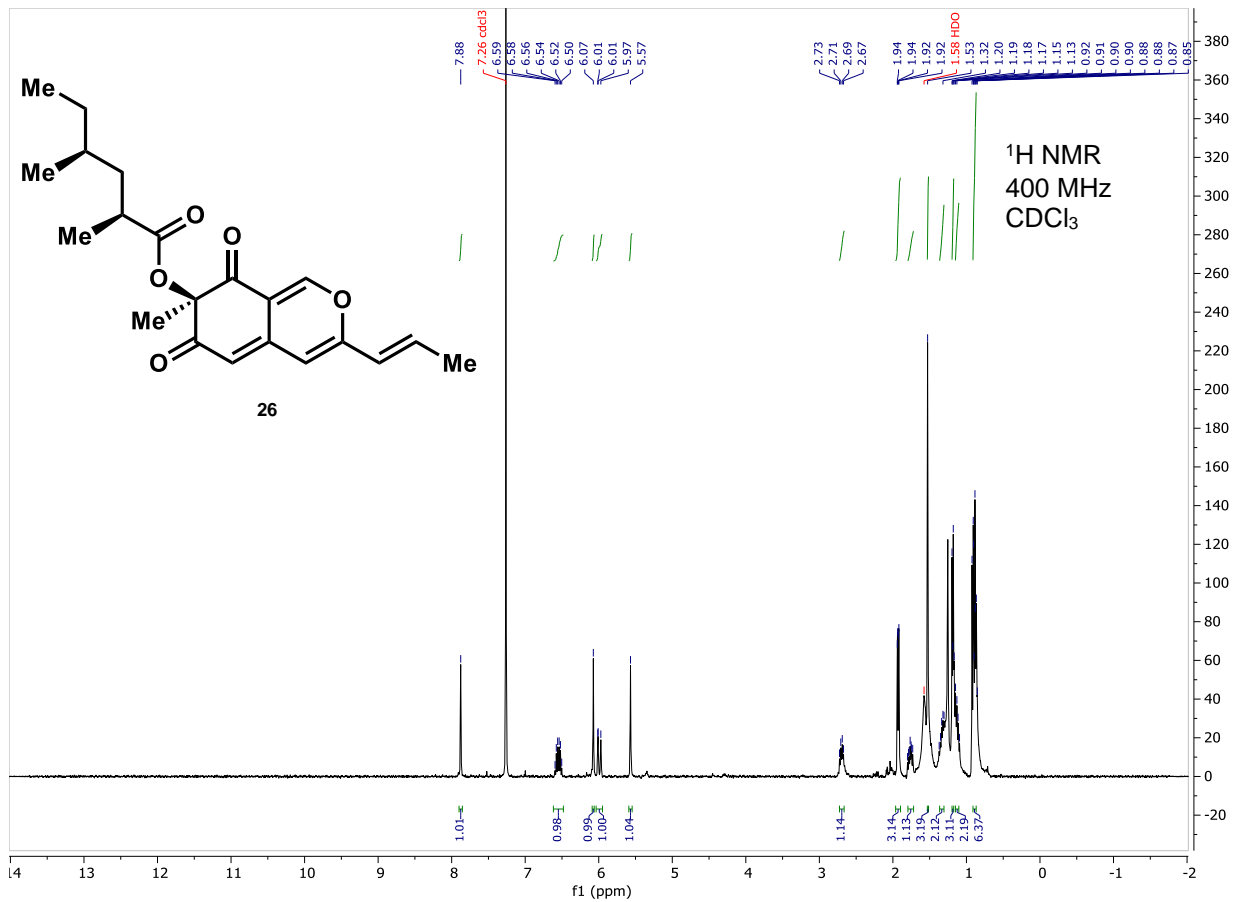


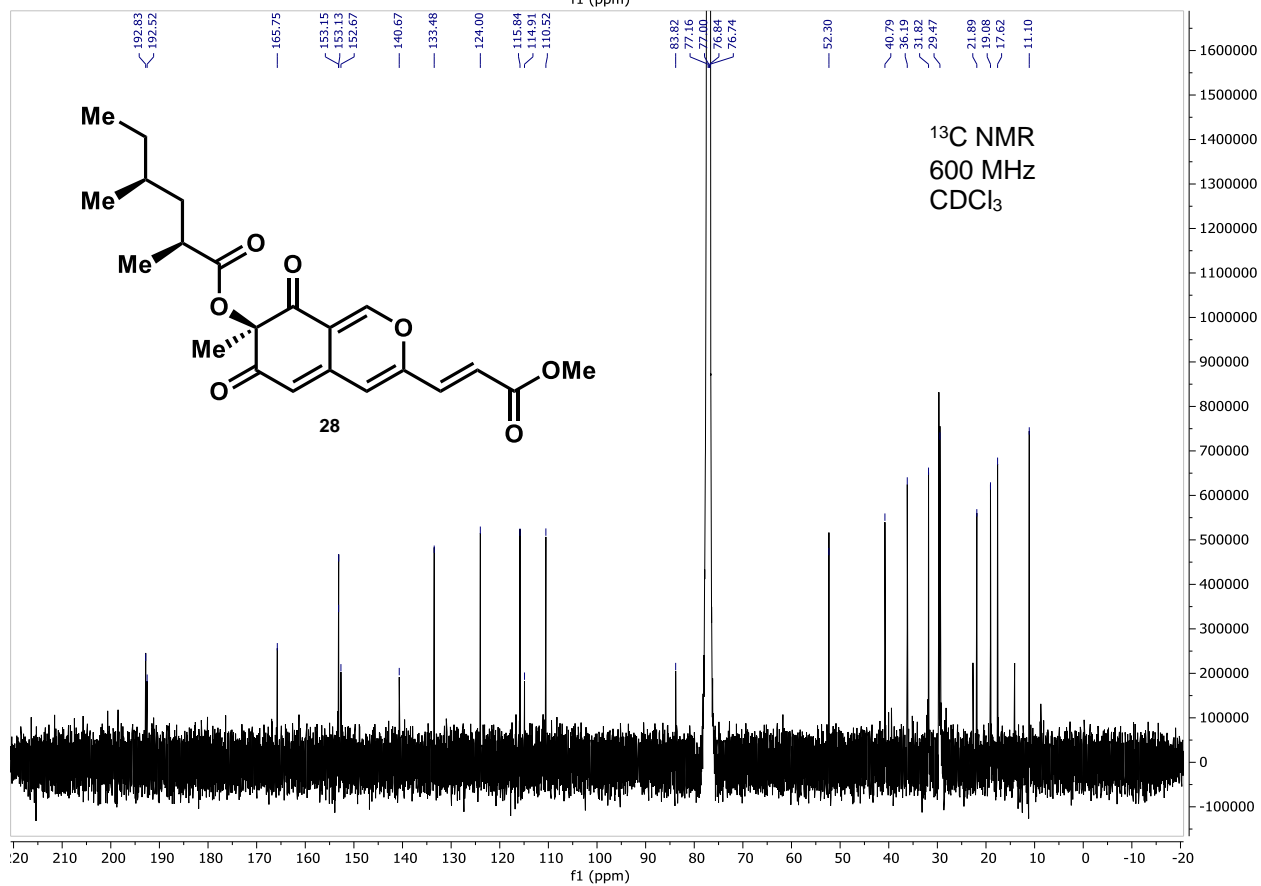
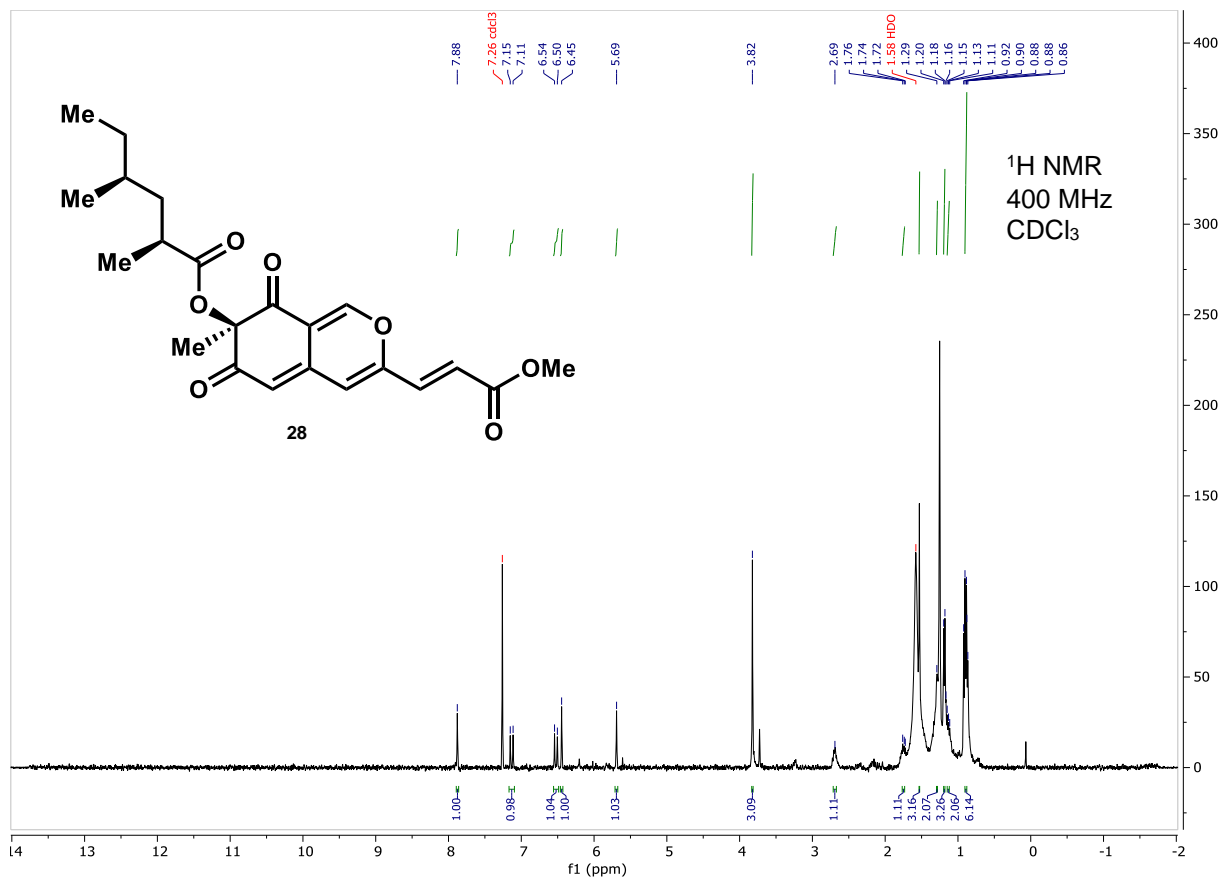










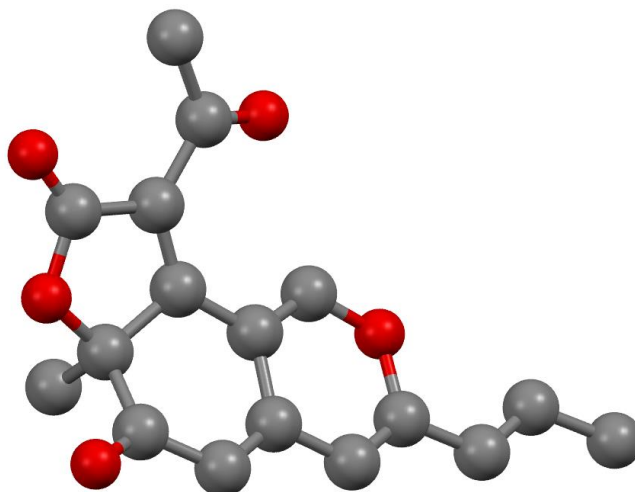


Part XI. Single-Crystal Structure Determination

Single-crystal X-ray diffraction data were collected using a Rigaku XtaLAB Synergy-S X-ray diffractometer configured in a kappa goniometer geometry. The diffractometer is equipped with a PhotonJet-S microfocus Cu source ($\lambda = 1.54187 \text{ \AA}$) set at a rough divergence of 9.5 and operated at 50 kV and 1 mA. X-ray intensities were measured at 298(1) K with the HyPix-6000HE detector placed 34.00 mm from the sample. The data were processed with CrysAlisPro v38.46 (Rigaku Oxford Diffraction) and corrected for absorption. The structures were solved in OLEX2¹⁷ using SHELXTL¹⁸ and refined using SHELXL.¹⁹ All non-hydrogen atoms were refined anisotropically with hydrogen atoms placed at idealized positions.

Table of Crystallographic Parameters

Material	exp_589
Space Group	P2 ₁ 2 ₁ 2 ₁
<i>a</i> Å	5.39440(6)
<i>b</i> Å	18.0328(2)
<i>c</i> Å	29.9372(4)
Volume (Å ³)	2912.18
Flack	0.00(6)
Temperature	298(1)
ρ_{calc} (g cm ⁻³)	1.361
R ₁ /wR ₂	3.00/8.46
GOF	1.052



ORTEP Diagram

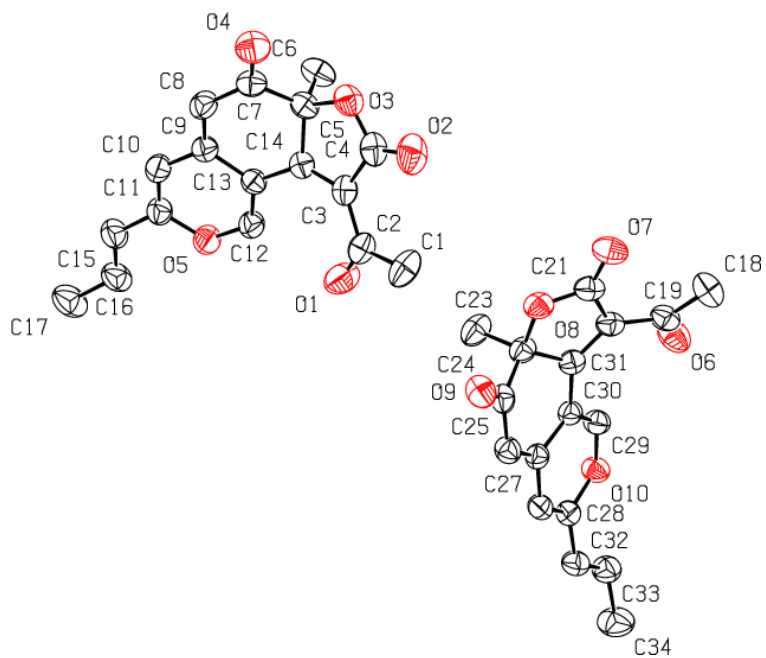


Figure S21. A view of exp_589 showing the atom labelling scheme. Thermal ellipsoids are drawn at the 50% probability level and H atoms are omitted for clarity.

Part XII. Circular Dichroism Spectroscopy of Azaphilones 18, 25, and 30

Instruments and methods

Circular dichroism (CD) spectra were collected on a J-1500 Circular Dichroism Spectrophotometer (Jasco). Samples were prepared in UPLC grade MeCN at a final concentration of 750 μM . Data points were collected at room temperature from 190 to 500 nm with a scan rate of 100 nm/min in a quartz cell with an optical path of 1 mm.

ECD Methodology

The general approach for absolute configuration assignment using ECD, including the detailed computational workflow, has been published elsewhere.²⁰⁻²² A subset of the details of the computational methodology is provided here. Conformers of each test structure were geometry optimized at the B3LYP/6-31G** level and stationary points were confirmed by performing frequency calculations.²³⁻³¹ All calculations were performed using Gaussian 09.³² Output conformers were ranked according to DFT energy and a clustering was performed in order to remove duplicates. Initial duplicate identification was performed solely on an electronic energy basis where two compounds were considered identical if the difference in Hartrees was less than 0.01. Rounding the differences led to inconsistencies in identification of duplicates. It became better to cluster the DFT minima by energy and then re-cluster each energy bucket by structure using an all atom RMS of 0.6 Å. This process removed just identical compounds. Two Boltzmann distributions were calculated based on the free energy (G) and the electronic energy (E).

To calculate UV and ECD spectra, B3LYP geometries were used as input. The spectra were then calculated using either the B3LYP or CAM-B3LYP³³ functionals, along with the 6-31++G** basis set^{34, 35} in vacuo. Only conformers which contributed more than 5.0% to the total in vacuo conformer distribution were selected for UV and ECD calculation. Time-dependent Density Functional Theory (TDDFT)³⁶ methodology was employed using the following keywords: TD=full,singlet, Nstates=100, and integral=ultrafinegrid. Spectral display, Boltzmann weighting, and curve fitting were carried out using SpecDis,^{37, 38} and were displayed with a wavelength shift and band broadening sigma values in order to best match the calculated and experimental UV spectra. This shift and band broadening were then applied to the ECD spectra, and the area under the curve fit was determined by SpecDis.

Trichoflectin (17)

Calculations of the ECD and UV spectra (CAM-B3LYP/6-31++G**) involved modeling the (*R*)- enantiomer of the natural product. Since no other stereoisomers were possible, it should be noted that the (*S*)-enantiomer is assumed to have a spectrum that will be equal and opposite at all wavelengths.

Figure S22 provides an overlay of the calculated and measured UV and ECD spectra using the theoretical spectrum of the (*R*)-enantiomer. The calculated spectrum has been shifted 30 nm and a band broadening of $\sigma=0.39$ eV applied in order to optimize the UV spectral match. A high degree of confidence is derived from the statistical and visual matching of the spectra, with the experimental spectrum matching the mirror image of the calculated (*R*)-enantiomer. Hence, the absolute configuration of trichoflectin can confidently be assigned as (*S*). Figure S23 shows the one conformer of the (*R*) enantiomer that contributed >5% to the Boltzmann weighted spectrum, and the coordinates of this conformer are shown with the electronic energy below. Assigned absolute configuration of the desired compounds is provided in Scheme S1.

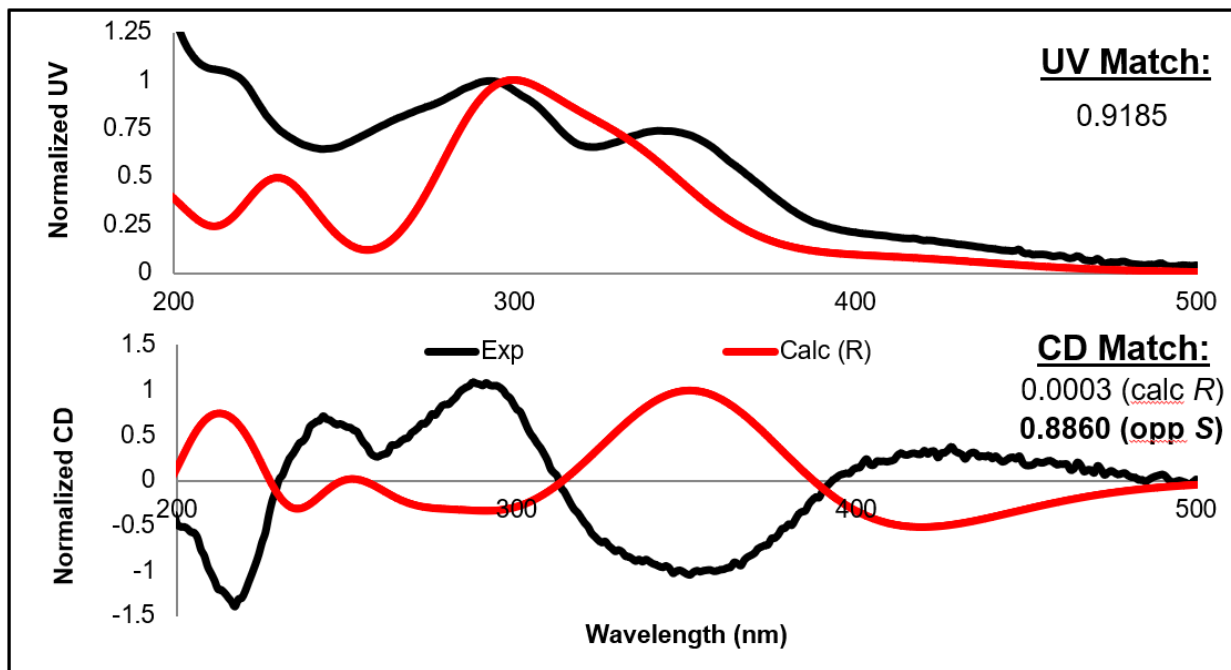
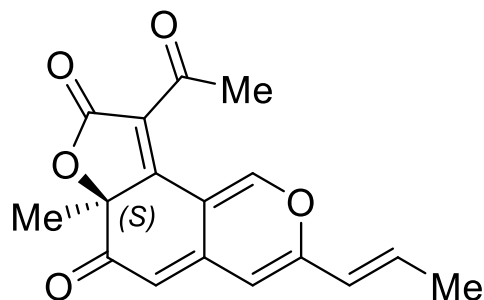
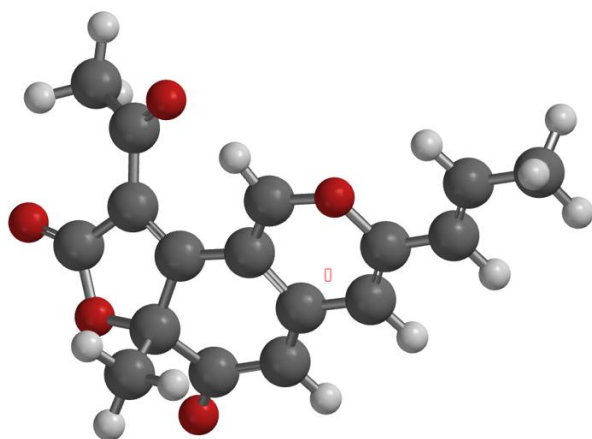


Figure S22. Comparison between experimental (black) and calculated (red) UV (top) and ECD (bottom) spectra. The calculated (R)-enantiomer is opposite of the experimental spectrum, with a large difference in fits ($\Delta=0.8857$) suggesting a confident assignment. The calculated spectrum has been shifted 30 nm, and a band broadening of 0.39 eV has been applied.



Scheme S1. Assigned absolute configuration of trichoflectin based on ECD analysis



Conformer 1: 93.3%

Figure S23. One conformer of the (*R*)-enantiomer of trichoflectin that contributes >5% to the Boltzmann distribution. Note the percentage shown above based is on *in vacuo* electronic energies.

Coordinates and electronic energies for B3LYP/6-31G conformational minima contributing >5% to the *in vacuo* Boltzmann distribution.**

Conformer 1: -1032.346471 hartrees

6	-1.92652	-1.24179	0.454749	8	-4.4906	0.97176	-0.14711
6	-1.43886	-2.36436	-0.50656	6	6.76245	0.716682	0.01421
6	-0.00398	-2.37628	-0.72861	6	-2.84313	3.30205	-0.90379
6	0.811717	-1.3366	-0.3621	6	-1.81538	-1.7794	1.89715
6	0.287916	-0.07181	0.177876	1	7.0976	1.54991	-0.61613
6	-1.16113	0.044932	0.262781	1	7.1483	-0.21358	-0.41144
6	1.15752	0.916672	0.51399	1	7.22791	0.866265	0.996514
6	2.24341	-1.37366	-0.51756	1	-2.48918	4.32822	-1.00616
8	-2.21691	-3.20925	-0.91931	1	-3.79449	3.26342	-0.3666
6	3.04043	-0.3412	-0.14027	1	-3.0406	2.8698	-1.89086
6	4.48685	-0.31902	-0.24494	1	-2.17304	-1.0227	2.60047
8	2.49748	0.804537	0.396205	1	-0.78389	-2.04131	2.14313
6	5.27154	0.705286	0.129229	1	-2.44014	-2.67163	1.98075
6	-2.0555	1.05447	0.067487	1	0.408491	-3.25877	-1.20725
6	-3.41789	0.444905	0.026975	1	0.849272	1.88074	0.892321
8	-3.29409	-0.90399	0.221383	1	2.70889	-2.25918	-0.93574
6	-1.79661	2.49736	-0.17149	1	4.92704	-1.22041	-0.66473
8	-0.75437	3.01999	0.214502	1	4.80462	1.59524	0.545569

Lunatoic Acid A Methyl Ester (28)

Calculations of the ECD and UV spectra (CAM-B3LYP/6-31++G**) involved modeling the (*R*) enantiomer of the natural product methyl ester. While the compound contains an ester chain with two stereocenters, the majority of the UV absorption and thus the ECD signal is expected to come from the stereocenter on the ring. Calculations of a hypothetical diastereomer with inversion at the stereocenter alpha to the ester carbonyl showed an analogous signal to that for the expected structure, indicating that this prior assumption is correct.

Figure S26 provides overlays of the calculated and measured UV and ECD spectra using the theoretical spectrum of the (*R*)-enantiomer. The calculated spectrum has been shifted -46 nm and a band broadening of $\sigma=0.28$ eV applied in order to optimize the UV spectral match. A high degree of confidence is derived from the statistical and visual matching of the spectra, with the experimental spectrum matching the calculated (*R*)-enantiomer. Hence, the absolute configuration of the methyl ester of Lunatoic Acid A can confidently be assigned as (*R*). Figure S27 shows the six conformers of the (*R*) enantiomer that contributed >5% to the Boltzmann weighted spectrum, and the coordinates of these conformers are shown with the electronic energies listed below. Assigned absolute configuration of the desired compounds is provided in Scheme S2.

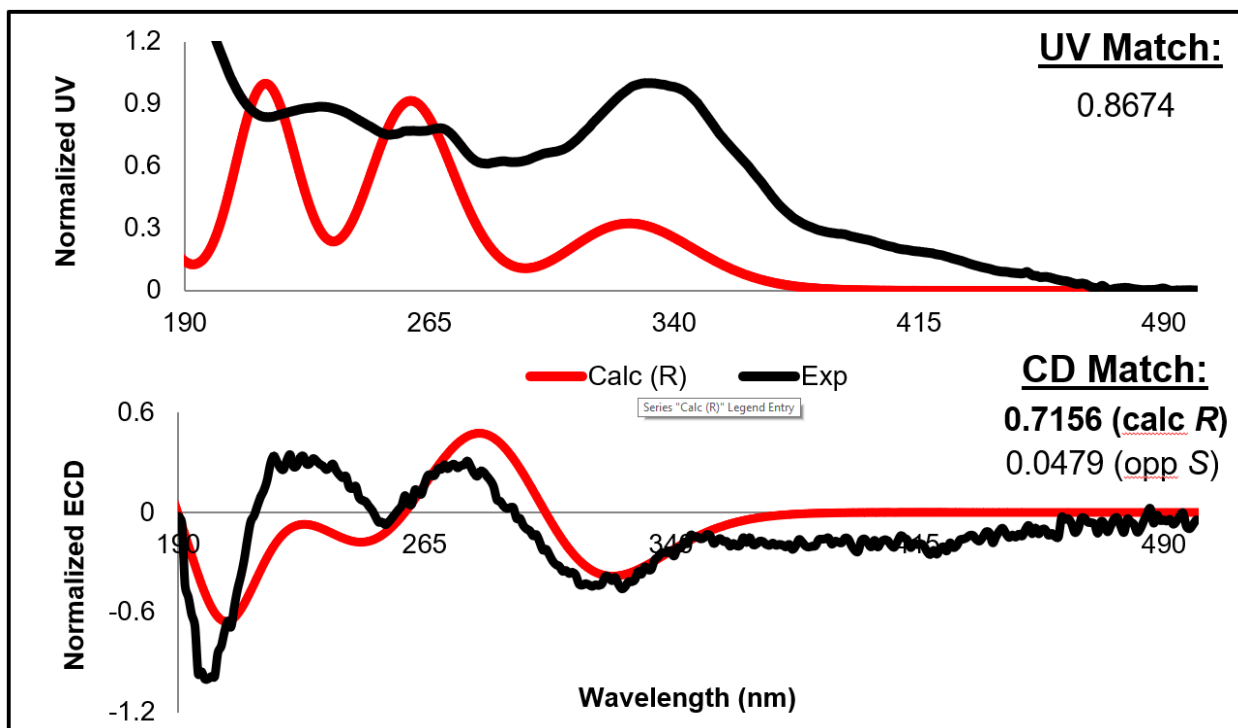
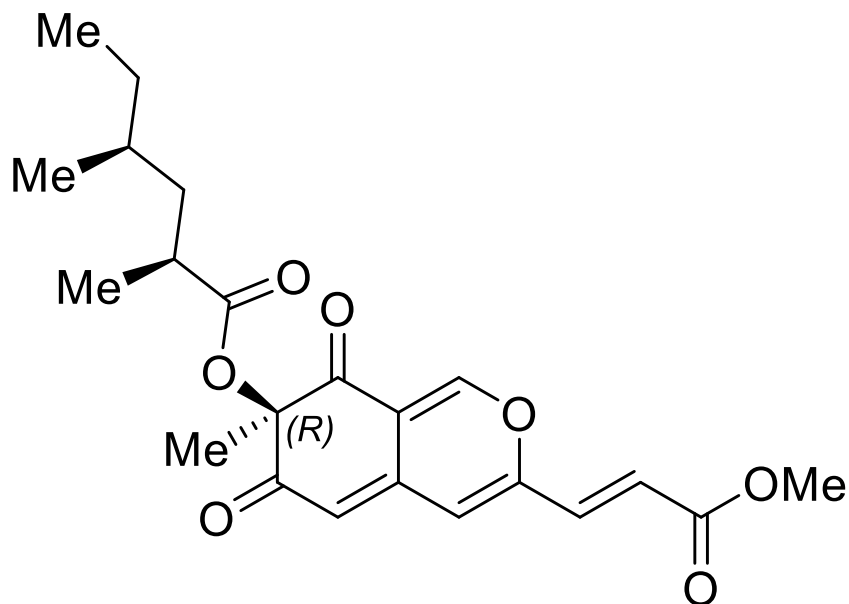


Figure S24. Comparison between experimental (black) and calculated (red) UV (top) and ECD (bottom) spectra. The calculated (*R*)-enantiomer is a good match to the experimental, with a large difference in fits ($\Delta=0.6677$) suggesting a confident assignment. The calculated spectrum has been shifted -46 nm, and a band broadening of 0.28 eV has been applied.



Scheme S2. Assigned absolute configuration of lunatoic acid A methyl ester based on ECD analysis.

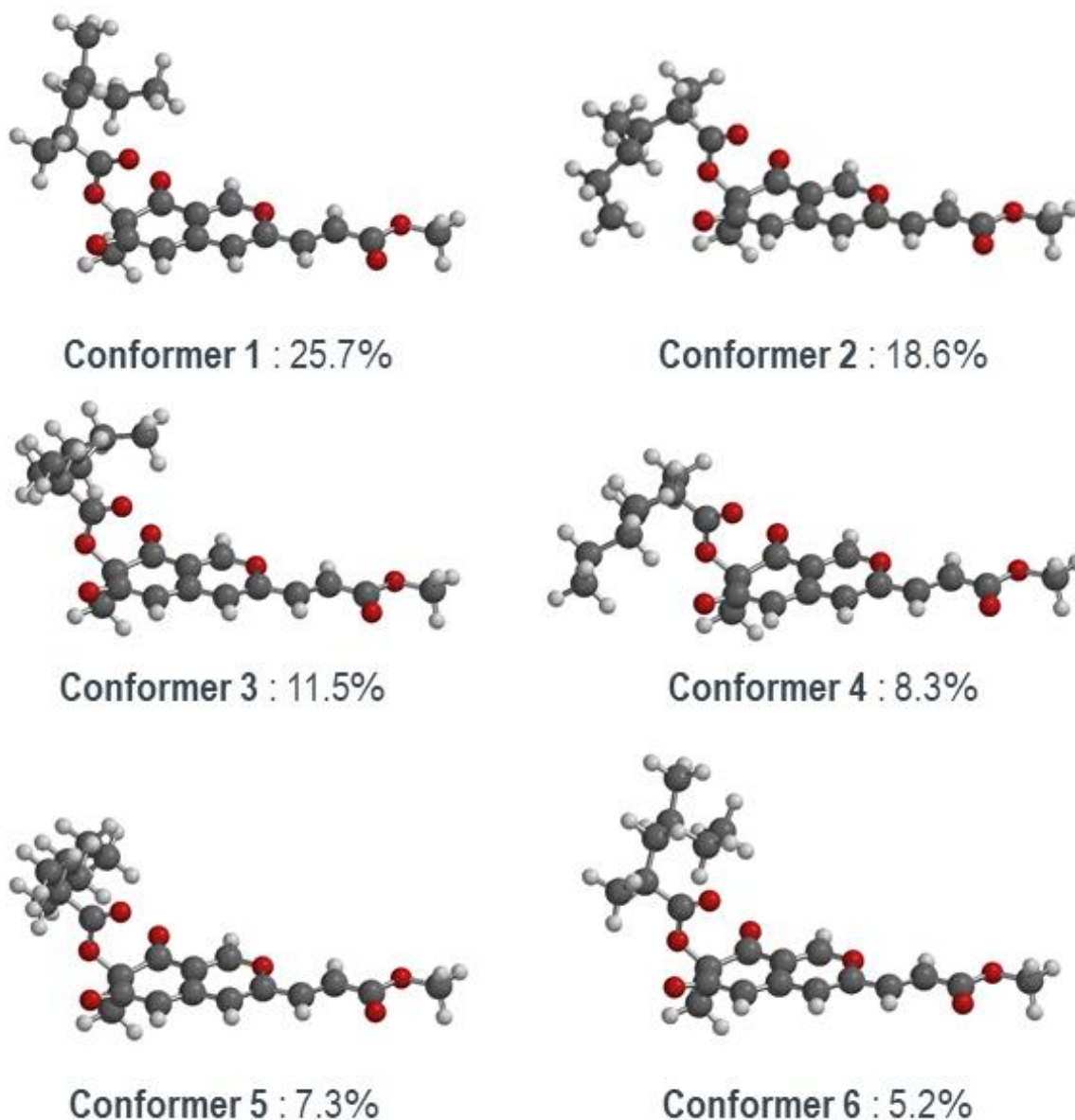


Figure S25. Six conformers of the (*R*)-enantiomer of lunatoic acid A methyl ester that contribute >5% to the Boltzmann distribution. Note the percentage shown above based is on *in vacuo* electronic energies.

Coordinates and electronic energies for B3LYP/6-31G conformational minima contributing >5% to the *in vacuo* Boltzmann distribution.**

<u>Conformer 1: -1380.662338 hartrees</u>				6	1.32039	-2.58496	-0.23991
6	1.78282	-1.68543	0.941074	6	-0.08437	-2.56709	-0.60377
				6	-0.9426	-1.60841	-0.14681

6	-0.5196	-0.5554	0.767273
6	0.874425	-0.48446	1.26383
6	-2.32929	-1.52556	-0.54115
6	-3.1488	-0.54276	-0.08739
8	-2.69057	0.431987	0.778282
6	-1.39911	0.390925	1.16506
6	-4.54266	-0.40614	-0.4433
6	-5.36122	0.565606	-0.00381
6	-6.77309	0.588333	-0.44821
8	-7.42645	1.63913	0.094655
8	-7.29006	-0.21849	-1.19745
6	-8.81115	1.75329	-0.27781
8	1.27673	0.428157	1.96608
8	2.14123	-3.32308	-0.7703
6	1.88912	-2.55832	2.19714
8	3.11592	-1.21925	0.681905
6	3.21769	-0.42005	-0.4067
6	4.65684	-0.13761	-0.77387
8	2.24322	-0.05119	-1.03495
6	4.86859	1.32854	-1.19008
6	5.00568	2.33153	-0.02596
6	3.77038	2.4135	0.898726
6	5.40257	3.71242	-0.57045
6	5.00231	-1.11961	-1.91571
6	2.48952	2.96521	0.26043
1	-9.18284	2.6388	0.236805
1	-9.36624	0.864184	0.032778
1	-8.90866	1.86616	-1.36077
1	2.26945	-1.95226	3.02238
1	2.57353	-3.38374	1.99027
1	0.910116	-2.96483	2.46741
1	5.50425	4.44226	0.240151
1	4.65198	4.09497	-1.27036
1	6.35778	3.66779	-1.10507
1	6.06683	-1.05241	-2.15839
1	4.42381	-0.8727	-2.81099
1	4.76711	-2.14983	-1.63287
1	1.67012	2.92449	0.983973
1	2.60967	4.00572	-0.05882
1	2.18371	2.37216	-0.60516
1	4.05069	1.6223	-1.85843
1	5.78692	1.37485	-1.78889
1	4.0386	3.04453	1.75683

1	3.55559	1.42696	1.32415
1	5.27726	-0.37544	0.096936
1	5.83819	1.97483	0.600279
1	-0.4089	-3.31549	-1.31925
1	-2.73808	-2.26244	-1.22363
1	-1.13259	1.20076	1.8328
1	-4.9434	-1.15583	-1.12031
1	-5.02585	1.34477	0.670543

Conformer 2: -1380.662034 hartrees

6	1.60301	-0.03006	1.10298
6	1.3789	-1.37343	0.355659
6	0.014003	-1.7783	0.076571
6	-1.04379	-0.9249	0.210908
6	-0.88031	0.452365	0.656243
6	0.458903	0.995158	0.987229
6	-2.40696	-1.28817	-0.0968
6	-3.43234	-0.40746	0.032594
8	-3.21705	0.887649	0.463061
6	-1.95435	1.26785	0.747312
6	-4.81605	-0.71065	-0.25362
6	-5.83805	0.154289	-0.13215
6	-7.21264	-0.28798	-0.45871
8	-8.09295	0.721015	-0.27846
8	-7.52427	-1.40097	-0.83766
6	-9.4627	0.393566	-0.57157
8	0.650022	2.17255	1.23702
8	2.3459	-2.0847	0.107215
6	1.81116	-0.3468	2.59071
8	2.82306	0.578009	0.669392
6	2.82824	0.976139	-0.62908
6	4.13858	1.63788	-1.00285
8	1.86405	0.836693	-1.35396
6	5.34521	0.822473	-0.50325
6	5.39588	-0.62932	-1.02382
6	6.2899	-1.51713	-0.1358
6	5.85781	-0.67645	-2.48719
6	4.13868	3.07093	-0.43476
6	5.70701	-1.793	1.25639
1	-10.0311	1.3026	-0.37759
1	-9.80742	-0.42213	0.069435

1	-9.56843	0.086968	-1.61553
1	2.01622	0.581948	3.12786
1	2.65955	-1.02784	2.68593
1	0.921112	-0.82186	3.01336
1	5.82731	-1.6996	-2.87624
1	6.88894	-0.31306	-2.58176
1	5.22695	-0.06024	-3.13642
1	5.05623	3.58945	-0.72908
1	4.0866	3.04841	0.657594
1	3.2833	3.64439	-0.80353
1	6.33759	-2.49318	1.81458
1	5.62542	-0.87924	1.85454
1	4.70273	-2.219	1.16926
1	5.31673	0.82973	0.590032
1	6.26441	1.34783	-0.79631
1	7.28637	-1.05919	-0.04828
1	6.44131	-2.47593	-0.64853
1	4.13371	1.68799	-2.09586
1	4.38433	-1.05266	-0.96904
1	-0.12316	-2.78673	-0.29964
1	-2.63015	-2.2909	-0.44405
1	-1.88497	2.30284	1.05848
1	-5.02839	-1.72114	-0.59244
1	-5.69587	1.17646	0.198431

Conformer 3: -1380.661580

hartrees

6	1.80645	-1.44169	0.96146
6	1.25025	-2.64964	0.155399
6	-0.17932	-2.70503	-0.09509
6	-0.9995	-1.63538	0.118238
6	-0.5044	-0.36532	0.63408
6	0.927277	-0.17683	0.961251
6	-2.41536	-1.64472	-0.16665
6	-3.19794	-0.55479	0.039268
8	-2.67158	0.624928	0.532123
6	-1.35133	0.67509	0.80152
6	-4.61807	-0.50162	-0.22184
6	-5.40103	0.573276	-0.02404
6	-6.84641	0.491423	-0.33301
8	-7.45656	1.66853	-0.07229
8	-7.42178	-0.4906	-0.76212

6	-8.86935	1.69464	-0.34157
8	1.38571	0.902317	1.30141
8	2.02181	-3.54237	-0.16765
6	2.00108	-1.88773	2.41606
8	3.1193	-1.11135	0.482608
6	3.14307	-0.63909	-0.78697
6	4.53741	-0.2664	-1.24181
8	2.13028	-0.48912	-1.44328
6	4.66904	1.27368	-1.1446
6	4.59209	1.85383	0.282993
6	4.31946	3.37107	0.257395
6	5.87038	1.54384	1.07516
6	4.76159	-0.76217	-2.67659
6	2.91313	3.7473	-0.22612
1	-9.20045	2.69967	-0.08196
1	-9.389	0.947829	0.264516
1	-9.06233	1.48472	-1.39691
1	2.44538	-1.06879	2.98614
1	2.66392	-2.75546	2.42639
1	1.04297	-2.16464	2.86562
1	5.79709	1.92248	2.1002
1	6.74457	2.01411	0.607319
1	6.06246	0.46803	1.13768
1	5.75721	-0.4714	-3.02445
1	4.01456	-0.32844	-3.34689
1	4.67943	-1.85142	-2.73795
1	2.74341	4.82575	-0.13886
1	2.75264	3.47711	-1.27494
1	2.15184	3.22853	0.365762
1	3.87972	1.70055	-1.77273
1	5.62504	1.56475	-1.60085
1	5.07915	3.86872	-0.36329
1	4.4569	3.76179	1.27411
1	5.25224	-0.74403	-0.56586
1	3.74888	1.38755	0.806291
1	-0.55972	-3.62808	-0.52008
1	-2.87746	-2.54332	-0.56017
1	-1.03229	1.64273	1.16855
1	-5.07182	-1.41047	-0.60798
1	-5.01289	1.51069	0.356631

Conformer 4: -1380.661272
hartrees

6	-1.55596	0.525882	-1.24688
6	-1.39326	-1.0005	-1.00539
6	-0.05116	-1.52379	-0.8291
6	1.02845	-0.71386	-0.622
6	0.913797	0.737612	-0.57223
6	-0.39731	1.40781	-0.74319
6	2.36829	-1.20795	-0.4078
6	3.41619	-0.37277	-0.18895
8	3.24754	0.998342	-0.15597
6	2.00729	1.49677	-0.33804
6	4.77861	-0.80378	0.026419
6	5.82249	0.014168	0.247073
6	7.1711	-0.5609	0.452202
8	8.07907	0.417463	0.662086
8	7.44234	-1.74653	0.437014
6	9.42675	-0.03819	0.875153
8	-0.55242	2.60508	-0.57627
8	-2.38406	-1.71879	-1.06503
6	-1.70204	0.748363	-2.75855
8	-2.78252	0.991689	-0.67293
6	-2.83081	0.930493	0.682381
6	-4.13767	1.4721	1.21872
8	-1.908	0.500183	1.34539
6	-5.34191	0.698497	0.642041
6	-5.24923	-0.83741	0.727787
6	-6.51003	-1.46636	0.103601
6	-5.01215	-1.3188	2.16701
6	-4.23525	2.97921	0.918661
6	-6.4124	-2.97899	-0.12288
1	10.0219	0.861883	1.02621
1	9.78444	-0.5968	0.006194
1	9.47759	-0.68702	1.75349
1	-1.86965	1.81069	-2.94948
1	-2.55413	0.164679	-3.11348
1	-0.80108	0.422162	-3.28621
1	-4.9906	-2.41061	2.22314
1	-5.8082	-0.96452	2.83488
1	-4.05431	-0.96166	2.55624
1	-5.1559	3.38547	1.34882
1	-4.2481	3.15507	-0.1603
1	-3.38633	3.52528	1.3407

1	-7.29867	-3.35722	-0.64326
1	-5.53364	-3.22271	-0.73012
1	-6.32747	-3.52973	0.819164
1	-5.46021	0.98631	-0.40951
1	-6.24213	1.04551	1.16859
1	-6.70048	-0.97928	-0.86224
1	-7.38038	-1.23849	0.736557
1	-4.08389	1.32562	2.30077
1	-4.39419	-1.15298	0.115844
1	0.047924	-2.60425	-0.81956
1	2.55469	-2.27614	-0.41827
1	1.97342	2.57747	-0.27647
1	4.9545	-1.87597	0.005158
1	5.71658	1.09205	0.282637

Conformer 5: -1380.661154
hartrees

6	-1.70828	-1.20718	-1.044
6	-1.12066	-2.5505	-0.52456
6	0.316767	-2.63888	-0.33668
6	1.12181	-1.53681	-0.34376
6	0.599747	-0.19309	-0.55821
6	-0.846	0.041816	-0.78461
6	2.54702	-1.58687	-0.11521
6	3.3148	-0.46736	-0.11168
8	2.76371	0.782449	-0.32434
6	1.43357	0.870572	-0.52933
6	4.74316	-0.45144	0.10636
6	5.51166	0.651664	0.116227
6	6.96763	0.525948	0.352105
8	7.56038	1.74003	0.329591
8	7.56432	-0.51695	0.541498
6	8.98158	1.72773	0.551402
8	-1.3222	1.16282	-0.85634
8	-1.87601	-3.50042	-0.37132
6	-1.91367	-1.33244	-2.55985
8	-3.0199	-1.01853	-0.49685
6	-3.04852	-0.83734	0.847156
6	-4.45833	-0.65166	1.36568
8	-2.03566	-0.79038	1.51714
6	-4.77348	0.863851	1.43291
6	-4.66903	1.65075	0.111329

6	-4.92025	3.14662	0.387374
6	-5.61908	1.09458	-0.95946
6	-4.59634	-1.31114	2.74352
6	-4.59509	4.06869	-0.79281
1	9.29665	2.76957	0.502455
1	9.48449	1.13527	-0.21748
1	9.21301	1.29956	1.53026
1	-2.38161	-0.4191	-2.93419
1	-2.56102	-2.19071	-2.75188
1	-0.95718	-1.48515	-3.06813
1	-5.57012	1.68249	-1.88047
1	-6.65876	1.11124	-0.6076
1	-5.3616	0.065677	-1.22357
1	-5.60462	-1.15335	3.13773
1	-3.87404	-0.88278	3.44345
1	-4.41277	-2.38806	2.68718
1	-4.71353	5.12105	-0.51411
1	-3.56092	3.92231	-1.12436
1	-5.2485	3.88323	-1.65103
1	-4.09515	1.31017	2.17161
1	-5.79004	0.969011	1.83696
1	-4.30819	3.45048	1.24707
1	-5.9671	3.28843	0.693539
1	-5.138	-1.13152	0.656004
1	-3.64387	1.55535	-0.2667
1	0.7176	-3.6258	-0.13015
1	3.02866	-2.54208	0.062222
1	1.09511	1.88971	-0.66938
1	5.21619	-1.41532	0.274219
1	5.10413	1.64318	-0.04225

Conformer 6: -1380.660826

hartrees

6	1.72315	-1.62726	1.01081
6	1.24166	-2.62238	-0.08242
6	-0.16608	-2.619	-0.43605
6	-1.00892	-1.61352	-0.05807
6	-0.56392	-0.48662	0.75176
6	0.838572	-0.38436	1.22068
6	-2.3998	-1.55165	-0.44166
6	-3.2047	-0.52476	-0.06623
8	-2.72664	0.518295	0.70386

6	-1.42978	0.499758	1.0748
6	-4.60218	-0.40712	-0.41468
6	-5.40691	0.606813	-0.05153
6	-6.82459	0.603336	-0.47743
8	-7.46216	1.70327	-0.01965
8	-7.35838	-0.26105	-1.14638
6	-8.85109	1.79673	-0.38191
8	1.26131	0.588955	1.82173
8	2.04829	-3.41738	-0.54816
6	1.80693	-2.38374	2.34257
8	3.06546	-1.2171	0.716302
6	3.19106	-0.52486	-0.44267
6	4.6419	-0.30463	-0.81074
8	2.23111	-0.19526	-1.11171
6	4.86933	1.08758	-1.42272
6	4.94597	2.25717	-0.4196
6	3.68055	2.36787	0.452821
6	5.23967	3.55856	-1.18128
6	5.00999	-1.43674	-1.79549
6	3.69924	3.51074	1.47278
1	-9.20878	2.72677	0.058749
1	-9.40842	0.942826	0.012222
1	-8.96316	1.81602	-1.46917
1	2.19988	-1.71345	3.11027
1	2.47304	-3.23965	2.2149
1	0.818603	-2.74182	2.64538
1	5.42632	4.39555	-0.50293
1	4.39167	3.82928	-1.82237
1	6.1209	3.45106	-1.82334
1	6.08112	-1.40892	-2.01595
1	4.45828	-1.31408	-2.73249
1	4.75794	-2.4165	-1.37973
1	2.8286	3.4425	2.13228
1	4.59742	3.46547	2.10064
1	3.67856	4.49506	0.994432
1	4.06901	1.27588	-2.14954
1	5.80757	1.0558	-1.99064
1	3.53263	1.43619	1.00763
1	2.80314	2.46653	-0.19955
1	5.23904	-0.42073	0.100448
1	5.79589	2.06093	0.254076
1	-0.50645	-3.42507	-1.07773
1	-2.82413	-2.34211	-1.05077

1 -1.14669 1.36374 1.6632 1 -5.05606 1.43894 0.547458
 1 -5.01815 -1.20969 -1.01787

Deflectin-1a (24)

Calculations of the ECD and UV spectra (B3LYP/6-31++G**) involved modeling the truncated (*R*) enantiomer of the natural product, shortening the exocyclic alkyl chain to a propyl group. This way there was still some conformational flexibility, but at a reduced computational cost. Since no other stereoisomers were possible, it should be noted that the (*S*)-enantiomer is assumed to have a spectrum that will be equal and opposite at all wavelengths.

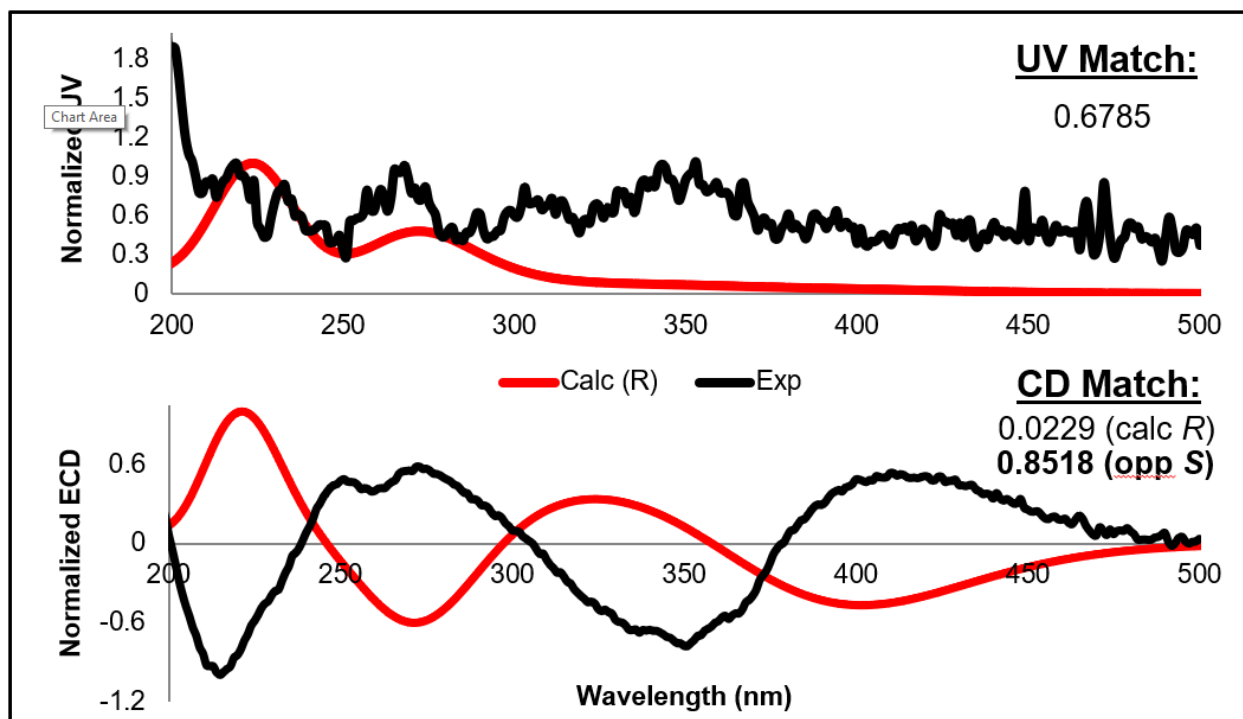
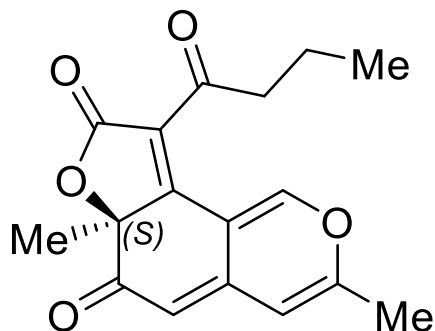


Figure S26. Comparison between experimental (black) and calculated (red) UV (top) and ECD (bottom) spectra. The calculated (*R*)-enantiomer is opposite of the experimental spectrum, with a large difference in fits ($\Delta=0.8289$) suggesting a confident assignment. The calculated spectrum has been shifted -34 nm, and a band broadening of 0.3 eV has been applied.



Scheme S3. Assigned absolute configuration of truncated deflectin based on ECD analysis.

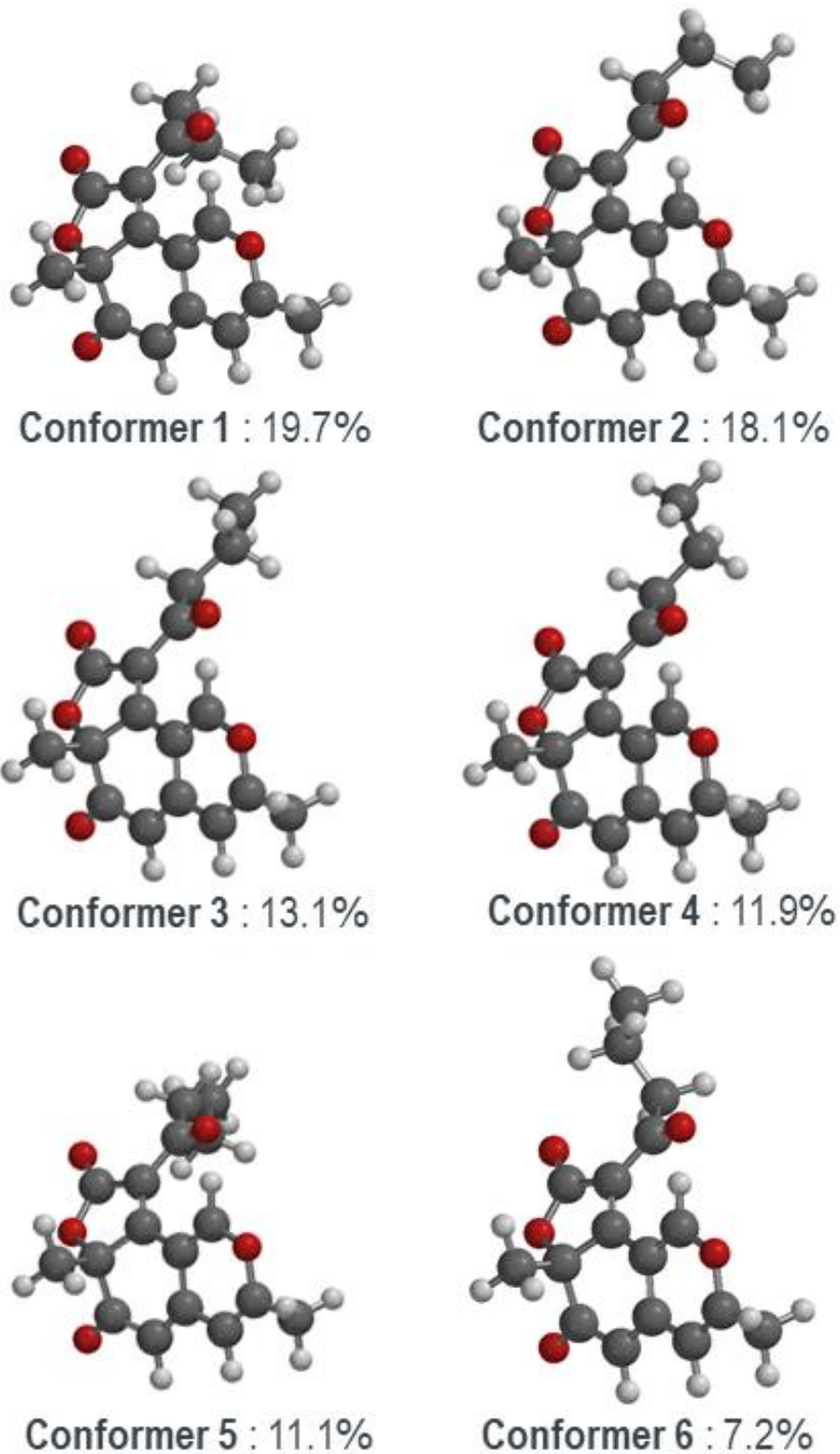


Figure S27. Six conformers of the (*R*)-enantiomer of truncated deflectin-1a that contribute >5% to the Boltzmann distribution. Note the percentage shown above based is on *in vacuo* electronic energies.

Coordinates and electronic energies for B3LYP/6-31G conformational minima contributing >5% to the *in vacuo* Boltzmann distribution.**

<u>Conformer 1: -1033.613962 hartrees</u>							
6	1.12532	-0.04345	-0.39212	6	-3.0367	-2.1407	-0.16933
6	1.99275	0.732157	0.506105	6	-3.06518	-1.968	1.36533
6	3.30798	0.164545	0.702653	6	-1.88548	-2.64397	2.07088
6	3.70807	-0.95125	0.058724	6	0.047576	2.71521	-1.59817
8	2.8718	-1.61446	-0.80807	1	4.91526	-2.65373	0.503621
6	1.61067	-1.16264	-0.98929	1	5.69066	-1.08748	0.843001
6	-0.24074	0.436799	-0.53748	1	5.51202	-1.66536	-0.83119
6	-0.45225	1.9203	-0.3767	1	-1.96232	-2.53676	3.1572
6	0.276203	2.47925	0.879938	1	-1.84539	-3.71359	1.8375
6	1.57228	1.87365	1.13487	1	-0.92928	-2.20641	1.76156
6	5.0355	-1.62273	0.154105	1	-0.18359	3.77097	-1.44072
8	-0.18568	3.42614	1.49476	1	-0.46423	2.36183	-2.49698
6	-1.45471	-0.16625	-0.63897	1	1.12617	2.59644	-1.7238
6	-2.49589	0.888061	-0.45779	1	-3.10279	-3.19773	-0.44239
8	-1.86713	2.0917	-0.28838	1	-3.88139	-1.59557	-0.60229
8	-3.69893	0.782672	-0.43922	1	-4.00926	-2.38602	1.73215
6	-1.75682	-1.61382	-0.78063	1	-3.09299	-0.90045	1.60707
8	-0.96298	-2.36216	-1.34426	1	4.00284	0.655146	1.37472
				1	1.02743	-1.78942	-1.64834
				1	2.20866	2.37403	1.8575
				6	2.28943	1.45998	-1.06108
				6	4.35993	-3.00144	-0.06963
6	1.12455	-0.26641	0.307283	8	1.15626	3.51001	-1.44011
				6	1.37198	0.449204	0.391607
6	2.26771	0.221135	-0.47835	6	1.99964	1.79257	0.218404
				8	1.00322	2.72868	0.145072
6	3.34533	-0.7326	-0.62018	8	3.16773	2.08818	0.142914
				6	2.14281	-0.81834	0.425308
6	3.31263	-1.94174	-0.02342	8	1.66299	-1.82714	0.93665
				6	3.53106	-0.82161	-0.18453
8	2.23687	-2.33275	0.738887	6	4.14405	-2.21836	-0.30714
				6	3.46052	-3.08584	-1.36975
6	1.17513	-1.50542	0.861629				
6	0.02309	0.624155	0.393856	6	0.89721	2.64077	1.61047
6	0.26797	2.1012	0.310862	1	3.94811	-3.92427	-0.492
6	1.23803	2.44194	-0.8567				

-
 1 5.20818 -2.68012 -0.67588
 -
 1 4.71146 -3.23342 0.941464
 1 3.94002 -4.06679 -1.44702
 1 2.40785 -3.24503 -1.12034
 1 3.51058 -2.61139 -2.35686
 1 -1.0324 3.71945 1.5056
 -
 1 0.22707 2.43922 2.4501
 -
 1 1.86575 2.17166 1.79764

Conformer 3: -1033.613578 hartrees

6 -1.23669 0.367215 -0.25506
 6 -2.39903 -0.12519 0.498848
 6 -3.45192 0.849675 0.677926
 6 -3.38244 2.08379 0.13827
 8 -2.29045 2.48058 -0.59741
 6 -1.2499 1.63178 -0.7509
 6 -0.11296 -0.54982 -0.37714
 6 -0.44715 -2.02001 -0.36658
 6 -1.4339 -2.38875 0.778195
 6 -2.45933 -1.38886 1.02254
 6 -4.40172 3.16789 0.226283
 8 -1.38534 -3.48506 1.31077
 6 1.24071 -0.41422 -0.36279
 6 1.82764 -1.78285 -0.25038
 8 0.804028 -2.69148 -0.22508
 8 2.98556 -2.11847 -0.18343
 6 2.04843 0.831619 -0.33746
 8 1.59408 1.88107 -0.78567

Conformer 4: -1033.613481 hartrees

-
 6 1.16263 -0.38101 0.220523
 -
 6 2.40001 0.133099 -0.38523
 -
 6 3.44651 -0.85331 -0.53626
 -
 6 3.30464 -2.1192 -0.09307
 8 -2.1423 -2.53751 0.51102

1 4.14471 -0.15612 0.43636
 1 3.49183 -0.31005 -1.15492
 1 4.08734 -2.71781 0.665863
 1 5.20723 -2.10655 -0.54866
 -
 1 4.21514 -0.46655 -1.20995
 -
 1 0.36813 -1.93743 1.43516
 -
 1 3.11123 1.75434 -1.70571

6 3.43612 0.767733 0.264145
 6 4.12596 2.12836 0.346454
 6 5.53042 2.02448 0.946302
 6 -1.08342 -2.47786 -1.69396
 1 -3.96898 4.05911 0.693254
 1 -5.26285 2.84194 0.811555
 1 -4.73918 3.45517 -0.77537
 1 6.01292 3.00558 0.997751
 1 5.49985 1.6137 1.96193
 1 6.17009 1.36781 0.346005
 1 -1.25056 -3.55592 -1.64194
 1 -0.40215 -2.25596 -2.5194
 1 -2.03663 -1.97206 -1.86332
 1 4.01855 0.049544 -0.32738
 1 3.36471 0.290609 1.25149
 1 3.50852 2.81195 0.940619
 1 4.17124 2.56697 -0.65634
 1 -4.33325 0.579987 1.24865
 1 -0.42639 2.06877 -1.29639
 1 -3.29392 -1.69019 1.64721

-
 6 1.10736 -1.67595 0.626863
 -
 6 0.04957 0.55392 0.301997
 -
 6 0.41246 2.01128 0.432348
 -
 6 1.51029 2.43529 -0.58532
 -
 6 2.53386 1.42861 -0.80765
 -
 6 4.30737 -3.21985 -0.16391

-
8 1.53384 3.56825 -1.03667
6 1.29868 0.455493 0.146455
6 1.84474 1.84502 0.081729
8 0.80578 2.72429 0.224366
8 2.98285 2.21887 -0.06994
6 2.11868 -0.76834 -0.04675
8 1.72595 -1.85224 0.377492
6 3.42359 -0.63768 -0.80651
6 4.20384 -1.94904 -0.92925
6 4.84226 -2.39582 0.390592
-
6 0.92807 2.35529 1.84364
-
1 3.90327 -4.06598 -0.72992
-
1 5.22487 -2.87623 -0.64395
-
1 4.54526 -3.58327 0.841596
1 5.41245 -3.32099 0.258882
1 5.52894 -1.63143 0.772205
1 4.07651 -2.57643 1.14925
-
1 1.12083 3.42941 1.88756
-
1 0.16683 2.09296 2.58284
1 -1.8505 1.81319 2.06358
1 4.01663 0.149602 -0.32628
1 3.17871 -0.22008 -1.79379
1 4.98355 -1.81297 -1.68758
1 3.53375 -2.73376 -1.29737
-
1 4.38175 -0.5671 -1.00381
-
1 0.22974 -2.12859 1.06416
-
1 3.42927 1.75158 -1.32867

Conformer 5: -1033.613417 hartrees

6 -1.28767 0.218168 -0.29924
6 -2.21665 -0.5007 0.585253
6 -3.45445 0.199085 0.84786
6 -3.74166 1.38401 0.271162
8 -2.8556 1.99399 -0.58535
6 -1.65796 1.41507 -0.82441

6 0.010014 -0.40554 -0.5129
6 0.047735 -1.9102 -0.42909
6 -0.70447 -2.44705 0.822674
6 -1.91543 -1.71289 1.14633
6 -4.98261 2.19305 0.436761
8 -0.33731 -3.47014 1.37615
6 1.28483 0.053474 -0.64059
6 2.19597 -1.1267 -0.54633
8 1.43292 -2.25264 -0.40061
8 3.40297 -1.17042 -0.57187
6 1.75903 1.45745 -0.75213
8 1.01665 2.33155 -1.19275
6 3.16063 1.78466 -0.28827
6 3.34581 1.5836 1.23018
6 4.76986 1.9244 1.67516
6 -0.57977 -2.57506 -1.67001
1 -4.7392 3.18535 0.831304
1 -5.6774 1.69967 1.11806
1 -5.47437 2.33802 -0.53116
1 4.88825 1.7911 2.75506
1 5.49623 1.2759 1.17413
1 5.02313 2.96293 1.4345
1 -0.4718 -3.6575 -1.57239
1 -0.05535 -2.23779 -2.56775
1 -1.63953 -2.32352 -1.75203
1 3.35205 2.82513 -0.56546
1 3.86638 1.13206 -0.81272
1 3.12583 0.542541 1.48743
1 2.62291 2.2093 1.76876
1 -4.18405 -0.24573 1.51496
1 -1.02206 2.00861 -1.46489
1 -2.58722 -2.17362 1.86324

Conformer 6: -1033.613007 hartrees

6 -1.33004 -0.33625 0.191808
6 -2.46505 0.40933 -0.37277
6 -3.67628 -0.36659 -0.52076
6 -3.75735 -1.64969 -0.11357
8 -2.67727 -2.28908 0.448706
6 -1.50175 -1.63261 0.561122
6 -0.06485 0.378031 0.271432
6 -0.15474 1.8741 0.43505

6	-1.17503	2.515	-0.54881	1	-5.79421	-2.0308	-0.63283
6	-2.36977	1.71762	-0.7651	1	-5.22243	-2.89313	0.815677
6	-4.94413	-2.5486	-0.1861	1	6.46885	-1.68168	0.384072
8	-0.99925	3.64314	-0.97797	1	5.75537	-2.49987	-1.01506
6	1.24305	0.040367	0.096574	1	5.90155	-0.73386	-0.99846
6	2.0288	1.30911	0.044704	1	-0.5682	3.36281	1.93305
8	1.16892	2.35948	0.216565	1	0.138091	1.85931	2.58141
8	3.21456	1.47291	-0.11853	1	-1.57714	1.90262	2.09278
6	1.83025	-1.30289	-0.13255	1	3.37509	-0.5662	-1.46007
8	1.2409	-2.31551	0.238784	1	3.1723	-2.33988	-1.38505
6	3.18478	-1.41488	-0.79951	1	4.10728	-2.35242	0.914763
6	4.30321	-1.49201	0.263832	1	4.26382	-0.59047	0.882688
6	5.68656	-1.61045	-0.37837	1	-4.55345	0.097571	-0.95702
6	-0.57534	2.27283	1.86396	1	-0.7104	-2.24947	0.96088
1	-4.71207	-3.43639	-0.78408	1	-3.20125	2.20988	-1.25887

Part XIII. Bibliography

1. Frigerio, M.; Santagostino, M.; Sputore, S., A User-Friendly Entry to 2-Iodoxybenzoic Acid (IBX). *J. Org. Chem.* **1999**, *64*, 4537-4538.
2. Baker Dockrey, S. A.; Lukowski, A. L.; Becker, M. R.; Narayan, A. R. H., Biocatalytic site- and enantioselective oxidative dearomatization of phenols. *Nat. Chem.* **2018**, *10*, 119-125.
3. Zhu, J.; Germain, A. R.; Porco Jr., J. A., Synthesis of Azaphilones and Related Molecules by Employing Cycloisomerization of o-Alkynylbenzaldehydes. *Angew. Chem. Int. Ed.* **2004**, *43*, 1239-1243.
4. MichaelChong, J.; Shen, L., Preparation of Chloromethyl Methyl Ether Revisited. *Synth. Commun.* **1998**, *28*, 2801-2806.
5. Peixoto, P. A.; Boulangé, A.; Ball, M.; Naudin, B.; Alle, T.; Cosette, P.; Karuso, P.; Franck, X., Design and Synthesis of Epicocconone Analogues with Improved Fluorescence Properties. *J. Am. Chem. Soc.* **2014**, *136*, 15248-15256.
6. Evans, D. A.; Fandrick, K. R.; Song, H.-J., Enantioselective Friedel–Crafts Alkylations of α,β -Unsaturated 2-Acyl Imidazoles Catalyzed by Bis(oxazoliny)pyridine–Scandium(III) Triflate Complexes. *J. Am. Chem. Soc.* **2005**, *127*, 8942-8943.
7. Zhu, J.; Porco, J. A., Asymmetric Syntheses of (–)-Mitorubrin and Related Azaphilone Natural Products. *Org. Lett.* **2006**, *8*, 5169-5171.
8. Fuse, S.; Yoshida, H.; Oosumi, K.; Takahashi, T., Rapid and Structurally Diverse Synthesis of Multi-Substituted β -Keto Amide Derivatives Based on a Dioxinone Scaffold. *Eur. J. Org. Chem.* **2014**, *2014*, 4854-4860.
9. Thines, E.; Anke, H.; Sterner, O., Trichoflectin, a Bioactive Azaphilone from the Ascomycete *Trichopezizella nidulus*. *J. Nat. Prod.* **1998**, *61*, 306-308.
10. Anke, H.; Kemmer, T.; Höfle, G., Deflectins, new antimicrobial azaphilones from *Aspergillus deflectus*. *J. Antibiot.* **1981**, *34*, 923-928.
11. Myers, A. G.; Yang, B. H.; Chen, H.; McKinstry, L.; Kopecky, D. J.; Gleason, J. L., Pseudoephedrine as a Practical Chiral Auxiliary for the Synthesis of Highly Enantiomerically Enriched Carboxylic Acids, Alcohols, Aldehydes, and Ketones. *J. Am. Chem. Soc.* **1997**, *119*, 6496-6511.
12. Nukina, M.; Marumo, S., Lunatoic acid A and B, aversion factor and its related metabolite of *cochliobolus lunata*. *Tetrahedron Lett.* **1977**, *18*, 2603-2606.
13. Marsini, M. A.; Gowin, K. M.; Pettus, T. R. R., Total Synthesis of (\pm)-Mitorubrinic Acid. *Org. Lett.* **2006**, *8*, 3481-3483.
14. Zallot, R.; Oberg, N. O.; Gerlt, J. A., 'Democratized' genomic enzymology web tools for functional assignment. *Curr. Opin. Chem. Biol.* **2018**, *47*, 77-85.
15. Gerlt, J. A., Genomic Enzymology: Web Tools for Leveraging Protein Family Sequence–Function Space and Genome Context to Discover Novel Functions. *Biochemistry* **2017**, *56*, 4293-4308.
16. Gerlt, J. A.; Bouvier, J. T.; Davidson, D. B.; Imker, H. J.; Sadkhin, B.; Slater, D. R.; Whalen, K. L., Enzyme Function Initiative-Enzyme Similarity Tool (EFI-EST): A web tool for generating protein sequence similarity networks. *Biochim. Biophys. Acta. Proteins Proteom.* **2015**, *1854*, 1019-1037.
17. Dolomanov, O. V.; Bourhis, L. J.; Gildea, R. J.; Howard, J. A. K.; Puschmann, H., OLEX2: a complete structure solution, refinement and analysis program. *J. Appl. Crystallogr.* **2009**, *42*, 339-341.
18. Sheldrick, G. M., SHELXT - integrated space-group and crystal-structure determination. *Acta Crystallogr. A* **2015**, *71*, 3-8.
19. Sheldrick, G. M., Crystal structure refinement with SHELXL. *Acta Crystallogr. C* **2015**, *71*, 3-8.
20. Sherer, E. C.; Lee, C. H.; Shpungin, J.; Cuff, J. F.; Da, C.; Ball, R.; Bach, R.; Crespo, A.; Gong, X.; Welch, C. J., Systematic approach to conformational sampling for assigning absolute configuration using vibrational circular dichroism. *J. Med. Chem.* **2014**, *57*, 477-94.
21. Liu, Z.; Shultz, C. S.; Sherwood, C. A.; Krska, S.; Dormer, P. G.; Desmond, R.; Lee, C.; Sherer, E. C.; Shpungin, J.; Cuff, J.; Xu, F., Highly enantioselective synthesis of anti aryl β -hydroxy α -amino esters via DKR transfer hydrogenation. *Tetrahedron Lett.* **2011**, *52*, 1685-1688.
22. Joyce, L. A.; Nawrat, C. C.; Sherer, E. C.; Biba, M.; Brunskill, A.; Martin, G. E.; Cohen, R. D.; Davies, I. W., Beyond optical rotation: what's left is not always right in total synthesis. *Chem. Sci.* **2018**, *9*, 415-424.
23. Petersson, G. A.; Al-Laham, M. A., A complete basis set model chemistry. II. Open-shell systems and the total energies of the first-row atoms. *J. Chem. Phys.* **1991**, *94*, 6081-6090.

24. Petersson, G. A.; Bennett, A.; Tensfeldt, T. G.; Al-Laham, M. A.; Shirley, W. A.; Mantzaris, J., A complete basis set model chemistry. I. The total energies of closed-shell atoms and hydrides of the first-row elements. *J. Chem. Phys.* **1988**, *89*, 2193-2218.
25. Rassolov, V. A.; Pople, J. A.; Ratner, M. A.; Windus, T. L., 6-31G* basis set for atoms K through Zn. *J. Chem. Phys.* **1998**, *109*, 1223-1229.
26. Rassolov, V. A.; Ratner, M. A.; Pople, J. A.; Redfern, P. C.; Curtiss, L. A., 6-31G* basis set for third-row atoms. *J. Comput. Chem.* **2001**, *22* (9), 976-984.
27. Francl, M. M.; Pietro, W. J.; Hehre, W. J.; Binkley, J. S.; Gordon, M. S.; DeFrees, D. J.; Pople, J. A., Self-consistent molecular orbital methods. XXIII. A polarization-type basis set for second-row elements. *J. Chem. Phys.* **1982**, *77*, 3654-3665.
28. Hehre, W. J.; Ditchfield, R.; Pople, J. A., Self—Consistent Molecular Orbital Methods. XII. Further Extensions of Gaussian—Type Basis Sets for Use in Molecular Orbital Studies of Organic Molecules. *J. Chem. Phys.* **1972**, *56*, 2257-2261.
29. Becke, A. D., Density-functional thermochemistry. III. The role of exact exchange. *J. Chem. Phys.* **1993**, *98*, 5648-5652.
30. Lee, C.; Yang, W.; Parr, R. G., Development of the Colle-Salvetti correlation-energy formula into a functional of the electron density. *Phys. Rev. B* **1988**, *37*, 785-789.
31. Miehlich, B.; Savin, A.; Stoll, H.; Preuss, H., Results obtained with the correlation energy density functionals of becke and Lee, Yang and Parr. *Chem. Phys. Lett.* **1989**, *157*, 200-206.
32. M. J. Frisch, G. W. T., H. B. Schlegel, G. E. Scuseria, M. A. Robb, J. R. Cheeseman, G. Scalmani, V. Barone, B. Mennucci, G. A. Petersson, H. Nakatsuji, M. Caricato, X. Li, H. P. Hratchian, A. F. Izmaylov, J. Bloino, G. Zheng, J. L. Sonnenberg, M. Hada, M. Ehara, K. Toyota, R. Fukuda, J. Hasegawa, M. Ishida, T. Nakajima, Y. Honda, O. Kitao, H. Nakai, T. Vreven, J. A. Montgomery, Jr., J. E. Peralta, F. Ogliaro, M. Bearpark, J. J. Heyd, E. Brothers, K. N. Kudin, V. N. Staroverov, R. Kobayashi, J. Normand, K. Raghavachari, A. Rendell, J. C. Burant, S. S. Iyengar, J. Tomasi, M. Cossi, N. Rega, J. M. Millam, M. Klene, J. E. Knox, J. B. Cross, V. Bakken, C. Adamo, J. Jaramillo, R. Gomperts, R. E. Stratmann, O. Yazyev, A. J. Austin, R. Cammi, C. Pomelli, J. W. Ochterski, R. L. Martin, K. Morokuma, V. G. Zakrzewski, G. A. Voth, P. Salvador, J. J. Dannenberg, S. Dapprich, A. D. Daniels, Ö. Farkas, J. B. Foresman, J. V. Ortiz, J. Cioslowski, and D. J. Fox.
33. Yanai, T.; Tew, D. P.; Handy, N. C., A new hybrid exchange–correlation functional using the Coulomb-attenuating method (CAM-B3LYP). *Chem. Phys. Lett.* **2004**, *393*, 51-57.
34. Marenich, A. V.; Cramer, C. J.; Truhlar, D. G., Universal Solvation Model Based on Solute Electron Density and on a Continuum Model of the Solvent Defined by the Bulk Dielectric Constant and Atomic Surface Tensions. *J. Phys. Chem. B* **2009**, *113*, 6378-6396.
35. Clark, T.; Chandrasekhar, J.; Spitznagel, G. W.; Schleyer, P. V. R., Efficient diffuse function-augmented basis sets for anion calculations. III. The 3-21+G basis set for first-row elements, Li–F. *J. Comput. Chem.* **1983**, *4*, 294-301.
36. Bauernschmitt, R.; Ahlrichs, R., Treatment of electronic excitations within the adiabatic approximation of time dependent density functional theory. *Chem. Phys. Lett.* **1996**, *256*, 454-464.
37. Bruhn, T.; Schaumlöffel, A.; Hemberger, Y.; Bringmann, G., SpecDis: Quantifying the Comparison of Calculated and Experimental Electronic Circular Dichroism Spectra. *Chirality* **2013**, *25*, 243-249.
38. Mazzeo, G.; Santoro, E.; Andolfi, A.; Cimmino, A.; Troselj, P.; Petrovic, A. G.; Superchi, S.; Evidente, A.; Berova, N., Absolute Configurations of Fungal and Plant Metabolites by Chiroptical Methods. ORD, ECD, and VCD Studies on Phyllostin, Scytolide, and Oxysporone. *J. Nat. Prod.* **2013**, *76*, 588-599.